

Catalytic dehydration of ethanol with different loading of WO_3 supported on
activated carbon and clay catalysts



A Thesis Submitted in Partial Fulfillment of the Requirements
for the Degree of Master of Engineering in Chemical Engineering

Department of Chemical Engineering

FACULTY OF ENGINEERING

Chulalongkorn University

Academic Year 2019

Copyright of Chulalongkorn University

การเร่งปฏิกิริยาดีไฮเดรชันของเอทานอลด้วยตัวเร่งปฏิกิริยาทั้งสแตนออกไซด์ที่มีปริมาณต่างกันบน
ถ่านกัมมันต์และเคลย์



วิทยานิพนธ์นี้เป็นส่วนหนึ่งของการศึกษาตามหลักสูตรปริญญาวิศวกรรมศาสตรมหาบัณฑิต
สาขาวิชาวิศวกรรมเคมี ภาควิชาวิศวกรรมเคมี
คณะวิศวกรรมศาสตร์ จุฬาลงกรณ์มหาวิทยาลัย
ปีการศึกษา 2562
ลิขสิทธิ์ของจุฬาลงกรณ์มหาวิทยาลัย

Thesis Title	Catalytic dehydration of ethanol with different loading of WO_3 supported on activated carbon and clay catalysts
By	Mr. Jirayu Liewchalermwong
Field of Study	Chemical Engineering
Thesis Advisor	Professor BUNJERD JONGSOMJIT, Ph.D.

Accepted by the FACULTY OF ENGINEERING, Chulalongkorn University in
Partial Fulfillment of the Requirement for the Master of Engineering

----- Dean of the FACULTY OF
ENGINEERING
(Professor SUPOT TEACHAVORASINSKUN, D.Eng.)

THESIS COMMITTEE

----- Chairman
(Professor ARTIWAN SHOTIPRUK, Ph.D.)

----- Thesis Advisor
(Professor BUNJERD JONGSOMJIT, Ph.D.)

----- Examiner
(Professor MUENDUEN PHISALAPHONG, Ph.D.)

----- External Examiner
(Assistant Professor Sasiradee Jantasee, Ph.D.)

จรรยา ลีวเฉลิมวงศ์ : การเร่งปฏิกิริยาดีไฮเดรชันของเอทานอลด้วยตัวเร่งปฏิกิริยา
 ทั้งสแตนออกไซด์ที่มีปริมาณต่างกันบนถ่านกัมมันต์และเคลย์. (Catalytic dehydration
 of ethanol with different loading of WO_3 supported on activated carbon
 and clay catalysts) อ.ที่ปรึกษาหลัก : ศ. ดร.บรรเจิด จงสมจิตร

งานวิจัย นี้ศึกษาการเร่งปฏิกิริยาการคายน้ำของเอทานอล ซึ่งเป็นการเพิ่มมูลค่าของเอทานอล โดยการผลิต ไดเอทิลอีเทอร์ หรือเอทิลีน ด้วยตัวเร่งปฏิกิริยาทั้งสแตนออกไซด์ ที่มีปริมาณต่างกันบนถ่านกัมมันต์ และเคลย์ โดยการโหลดปริมาณทั้งสแตน ที่แตกต่างกันระหว่าง 2-13.5 เปอร์เซ็นต์ โดยน้ำหนัก โดยตัวเร่งปฏิกิริยา ถูกทดสอบเร่งปฏิกิริยา ในเครื่องปฏิกรณ์ชนิดเบดนิ่ง ในช่วงอุณหภูมิของปฏิกิริยา 200 ถึง 400 องศาเซลเซียส จากผลการศึกษาพบว่า ทั้งสแตนปริมาณน้อยบนตัวเร่งปฏิกิริยา นั้นลดความเป็นกรดของตัวเร่งปฏิกิริยา แต่ส่งเสริมอัตราการคายไฮโดรเจนของเอทานอลเป็นอะซีตัลดีไฮด์ แต่เมื่อเพิ่มปริมาณทั้งสแตน นั้นช่วยเพิ่มความเป็นกรดของตัวเร่งปฏิกิริยา และยังส่งเสริมปฏิกิริยาการคายน้ำของเอทานอล ในขณะที่ไดเอทิลอีเทอร์ไม่ถูกพบเมื่อใช้ตัวเร่งปฏิกิริยาถ่านกัมมันต์ เว้นแต่ถ่านกัมมันต์ ซึ่งมีทั้งสแตนร้อยละ 13.5 โดยน้ำหนัก นอกจากนี้พบว่าตัวเร่งปฏิกิริยาถ่านกัมมันต์จากบริษัท ทีพีไอ เมื่อใส่ทั้งสแตนในปริมาณ 2 เปอร์เซ็นต์โดยน้ำหนัก มีอัตราการเกิดปฏิกิริยาของอะซีตัลดีไฮด์สูงสุดคือ 4.7 ไมโครโมลต่อกรัมตัวเร่งปฏิกิริยาต่อวินาที ที่อุณหภูมิ 400 องศาเซลเซียส ปริมาณทั้งสแตน 13.5 เปอร์เซ็นต์โดยน้ำหนักบนตัวเร่งปฏิกิริยาเคลย์ มีอัตราการเกิดปฏิกิริยาของเอทิลีน และไดเอทิลอีเทอร์สูงสุด คือ 64.07 และ 14.7 ไมโครโมลต่อกรัมตัวเร่งปฏิกิริยาต่อวินาที ที่ 250 องศาเซลเซียส ตามลำดับ

จุฬาลงกรณ์มหาวิทยาลัย
 CHULALONGKORN UNIVERSITY

สาขาวิชา วิศวกรรมเคมี
 ปีการศึกษา 2562

ลายมือชื่อนิสิต
 ลายมือชื่อ อ.ที่ปรึกษาหลัก

6070437821 : MAJOR CHEMICAL ENGINEERING

KEYWORD: ETHANOL DEHYDRATION, DIETHYL ETHER, ETHYLENE, ACTIVATED
CARBON, MONTMORILLONITE, TUNGSTEN TRIOXIDE

Jirayu Liewchalermwong : Catalytic dehydration of ethanol with different
loading of WO_3 supported on activated carbon and clay catalysts .

Advisor: Prof. BUNJERD JONGSOMJIT, Ph.D.

The catalytic ethanol dehydration is a reaction, which increases the value of ethanol by producing diethyl ether (DEE) or ethylene. The catalysts which have been used for this reaction were tungsten catalysts supported on activated carbon and montmorillonite catalysts, by varying W loading between 2-13.5 wt.%. The catalysts were tested in a fixed bed microreactor under atmospheric pressure and temperature range of 200 to 400°C. The results showed that Low tungsten on catalyst decreased the total surface acidity. Besides, additional tungsten loading increased the total surface acidity. Low tungsten loading enhanced ethanol dehydrogenation to acetaldehyde. The high content of tungsten in catalysts was able to promote dehydration reaction of ethanol, whereas diethyl ether did not occur on activated carbon catalysts except 13.5wt% of tungsten on activated carbon catalyst. The 2 wt% of tungsten over activated carbon catalyst from TPI performed the highest reaction rate of acetaldehyde which reached $4.7 \mu\text{mol}\cdot\text{s}^{-1}\cdot\text{g}_{\text{cat}}^{-1}$ at 400°C. The 13.5 wt% of tungsten on montmorillonite catalyst performed the highest reaction rate of ethylene and diethyl ether which reached $64.07 \mu\text{mol}\cdot\text{s}^{-1}\cdot\text{g}_{\text{cat}}^{-1}$ at 400°C and $14.7 \mu\text{mol}\cdot\text{s}^{-1}\cdot\text{g}_{\text{cat}}^{-1}$ at 250°C, respectively.

Field of Study: Chemical Engineering

Student's Signature

Academic Year: 2019

Advisor's Signature

ACKNOWLEDGEMENTS

I would like to gratefully thank my advisor Prof. Bunjerd Jongsomjit, Ph.D. for immense knowledge, invaluable suggestion, research guideline and help at each point in all the time of research. This research cannot be achieved without his advice. Moreover, I am also sincerely thanks to the thesis committee, Prof. Artiwan Shotipruk, Ph.D as a chairman, Muenduen Phisalaphong, Ph.D. as an examiner and Asst. Prof. Sasiradee Jantasee, Ph.D. as an external examiner for suggestions to improve thesis research.

The author thanks the Chulalongkorn University and Cat-React industrial project for the financial support of this project.

Finally, I am grateful to my parents for continuous support and encouragement during research in my master's degree. I am also thankful to my friends, senior and laboratory's scientists in the Center of Excellence on Catalysis and Catalytic Reaction Engineering for continued support, help and encouragement.

Jirayu Liewchalermwong



จุฬาลงกรณ์มหาวิทยาลัย
CHULALONGKORN UNIVERSITY

TABLE OF CONTENTS

	Page
.....	iii
ABSTRACT (THAI)	iii
.....	iv
ABSTRACT (ENGLISH)	iv
ACKNOWLEDGEMENTS	v
TABLE OF CONTENTS	vi
LIST OF TABLES	x
LIST OF FIGURES.....	xii
CHAPTER 1	1
1.1 INTRODUCTION.....	1
1.2 OBJECTIVE	2
1.3 RESEARCH SCOPE	2
1.4 RESEARCH METHODOLOGY.....	3
Chapter 2	5
2.1 ACTIVATED CARBON (AC CATALYST).....	5
2.2 MONTMORILLONITE (MMT CATALYST)	7
2.2 AMMONIUM METATUNGSTATE (AMT).....	7
2.3 TUNGSTEN TRIOXIDE.....	8
2.4 ETHYLENE	10
2.5 DIETHYL ETHER (DEE).....	10
2.6 ACETALDEHYDE	11

2.7 ETHANOL DEHYDRATION REACTION.....	12
2.8 LITERATURE REVIEW.....	15
2.8.1 Activated carbon catalyst.....	15
2.8.2 Montmorillonite catalyst.....	15
2.8.3 Tungsten oxide.....	15
2.8.4 Tungsten supported over activated carbon catalyst.....	16
2.8.5 Tungsten supported over catalyst.....	16
CHAPTER 3.....	17
3.1 Materials.....	17
3.2 CATALYST PREPARATION.....	17
3.2.1 Synthesis Tungsten supported on activated carbon catalyst.....	17
3.2.2 Synthesis Tungsten supported on montmorillonite catalyst.....	18
3.3 CATALYST CHARACTERIZATION.....	18
3.3.1 X-ray diffraction (XRD).....	18
3.3.2 Ammonia temperature-programmed desorption (NH ₃ -TPD).....	18
3.3.3 Scanning electron microscope (SEM) and Energy dispersive X-ray spectroscopy (EDX).....	19
3.3.4 N ₂ physisorption (BET).....	19
3.4 Catalytic Ethanol dehydration reaction.....	19
3.5 Analysis and calculation.....	21
3.5 Research plan.....	23
CHAPTER 4.....	24
4.1 W supported on AC catalysts.....	24
4.1.1 Catalyst characterization.....	24

4.1.1.1 Scanning electron microscope (SEM) and Energy dispersive X-ray spectroscopy (EDX)	24
4.1.1.2 X-ray Powder Diffraction (XRD)	29
4.1.1.3 N ₂ physisorption (BET).....	31
4.1.1.4 Ammonia temperature-programmed desorption (NH ₃ -TPD).....	38
4.1.2 Catalytic ethanol dehydration reaction	41
4.1.3 stability test.....	49
4.1.4 Summary.....	50
4.2 W supported on MMT catalysts.....	51
4.2.1 Catalyst characterization.....	51
4.2.1.1 Scanning electron microscope (SEM) and Energy dispersive X-ray spectroscopy (EDX)	51
4.2.1.2 X-ray Powder Diffraction (XRD)	53
4.2.1.3 N ₂ physisorption (BET).....	54
4.2.1.4 Ammonia temperature-programmed desorption (NH ₃ -TPD).....	59
4.2.2 Catalytic ethanol dehydration reaction	61
4.1.3 stability test.....	65
4.2.4 Summary.....	66
4.3 Comparison and discussion of W supported on AC catalysts and W supported on MMT catalysts.....	66
CHAPTER 5	66
5.1 Conclusions.....	68
5.2 Recommendations	70
REFERENCES.....	71
VITA	98

APPENDIX A78

APPENDIX B.....83

APPENDIX C.....86



LIST OF TABLES

	Page
Table 1 Ammonium metatungstate properties	8
Table 2 Tungsten trioxide properties	9
Table 3 Ethylene properties	10
Table 4 Diethyl ether properties	11
Table 5 Acetaldehyde properties.....	12
Table 6 The chemical used in ethanol dehydration reaction.....	20
Table 7 The operating conditions in gas chromatograph.....	20
Table 8 Schedule of the research plan.....	23
Table 9 Chemical composition obtained by EDX of W supported on AC catalysts....	27
Table 10 Textural properties of AC, 13.5WAC, ACG, and 13.5WACG.....	32
Table 11 Specific surface area of various W supported on AC catalysts (TPI).....	32
Table 12 Properties of various W supported on AC catalysts.....	38
Table 13 Product distribution of W supported on AC catalysts (Sigma-Aldrich) (WHSV=3.13 $\text{g}_{\text{ethanol}} \cdot \text{g}_{\text{cat}}^{-1} \cdot \text{h}^{-1}$)	42
Table 14 Product distribution of W supported on AC catalysts (TPI) (WHSV=3.13 $\text{g}_{\text{ethanol}} \cdot \text{g}_{\text{cat}}^{-1} \cdot \text{h}^{-1}$)	43
Table 15 Product distribution of W supported on AC catalysts (Sigma-Aldrich) (WHSV=11.44 $\text{g}_{\text{ethanol}} \cdot \text{g}_{\text{cat}}^{-1} \cdot \text{h}^{-1}$)	44
Table 16 Product distribution of W supported on AC catalysts (TPI) (WHSV=11.44 $\text{g}_{\text{ethanol}} \cdot \text{g}_{\text{cat}}^{-1} \cdot \text{h}^{-1}$)	45
Table 17 Textural properties of MMT and 13.5WMMT	54
Table 18 Specific surface area of various W supported on MMT catalysts	55

Table 19 Properties of various W supported on MMT catalysts.....59

Table 20 Product distribution of W supported on MMT catalysts.....62



LIST OF FIGURES

	Page
Figure 1 Acidic and basic surface functionalities on a carbon basal plane [18].....	5
Figure 2 Types of nitrogen surface functional groups: (a) pyrrole, (b) primary amine, (c) secondary amine, (d) pyridine, (e) imine, (f) tertiary amine, (g) nitro, (h) nitroso, (i) .	6
<i>Figure 3 Surface oxygen containing groups on carbon and their decomposition by TPD [20].....</i>	<i>6</i>
Figure 4 Montmorillonite structure [21].....	7
Figure 5 Schematic of the gas phase ethanol dehydration reaction.....	21
Figure 6 The morphologies of various W supported on AC catalysts (TPI) measured by SEM at mag. X650	25
Figure 7 The morphologies of various W supported on AC catalysts (TPI) measured by SEM at mag. X3,000.....	26
Figure 8 The morphologies of W supported on AC catalysts (Sigma-Aldrich) measured by SEM at mag. X650	27
Figure 9 The morphologies of W supported on AC catalysts (Sigma-Aldrich) measured by SEM at mag. X3,000.....	27
Figure 10 SEM-EDX mapping of various W supported on AC catalysts.....	28
Figure 11 X-ray Powder diffraction patterns of various W supported on AC catalysts (TPI).....	30
Figure 12 X-ray Powder diffraction patterns of W supported on AC catalysts (Sigma-Aldrich).....	30
Figure 13 N ₂ adsorption–desorption isotherms of AC	33
Figure 14 N ₂ adsorption–desorption isotherms of 13.5WAC	33
Figure 15 N ₂ adsorption–desorption isotherms of ACG.....	34

Figure 16 N ₂ adsorption–desorption isotherms of 13.5WACG	34
Figure 17 N ₂ adsorption–desorption isotherms of AC, 13.5WAC, ACG, and 13.5WACG	35
Figure 18 Pore size distribution of AC.....	35
Figure 19 Pore size distribution of 13.5WAC	36
Figure 20 Pore size distribution of ACG.....	36
Figure 21 Pore size distribution of 13.5WACG.....	37
Figure 22 Pore size distribution of AC, 13.5WAC, ACG, and 13.5WACG.....	37
Figure 23 NH ₃ -TPD profile of various W supported on AC catalysts (TPI).....	39
Figure 24 NH ₃ -TPD profile of ACG and 13.5WACG	39
Figure 25 NH ₃ -TPD profile of W loading on different manufacturer of AC catalyst	40
Figure 26 Total acidity of various W supported on AC catalysts (TPI).....	40
Figure 27 Ethanol conversion of various W supported on AC catalysts for ethanol dehydration at various operating temperature (WHSV=3.13 g _{ethanol} ·g _{cat} ⁻¹ ·h ⁻¹).....	42
Figure 28 Ethanol conversion of various W supported on AC catalysts for ethanol dehydration at various operating temperature (WHSV=11.44 g _{ethanol} ·g _{cat} ⁻¹ ·h ⁻¹)	44
Figure 29 Acetaldehyde reaction rate of various W supported on AC catalysts for ethanol dehydration at various operating temperature (WHSV=3.13 g _{ethanol} ·g _{cat} ⁻¹ ·h ⁻¹)..	46
Figure 30 Acetaldehyde reaction rate of various W supported on AC catalysts for ethanol dehydration at various operating temperature (WHSV=11.44 g _{ethanol} ·g _{cat} ⁻¹ ·h ⁻¹)	46
Figure 31 Ethylene reaction rate of various W supported on AC catalysts for ethanol dehydration at various operating temperature (WHSV=3.13 g _{ethanol} ·g _{cat} ⁻¹ ·h ⁻¹).....	47
Figure 32 Ethylene reaction rate of various W supported on AC catalysts for ethanol dehydration at various operating temperature (WHSV=11.44 g _{ethanol} ·g _{cat} ⁻¹ ·h ⁻¹)	47
Figure 33 Diethyl ether reaction rate of various W supported on AC catalysts for ethanol dehydration at various operating temperature (WHSV=3.13 g _{ethanol} ·g _{cat} ⁻¹ ·h ⁻¹)..	48

Figure 34 Diethyl ether reaction rate of various W supported on AC catalysts for ethanol dehydration at various operating temperature (WHSV=11.44 $\text{g}_{\text{ethanol}} \cdot \text{g}_{\text{cat}}^{-1} \cdot \text{h}^{-1}$)	48
Figure 35 Ethanol conversion of AC and 13.5WAC in stability test of catalytic ethanol dehydration reaction (the reaction condition: T= 400°C and WHSV= 3.13 h^{-1})	49
Figure 36 Ethanol conversion of 13.5WAC in stability test of catalytic ethanol dehydration reaction (the reaction condition: T = 400°C and WHSV= 11.44 h^{-1})	50
Figure 37 The morphologies of various W supported on MMT catalysts measured by SEM at mag. X650	51
Figure 38 The morphologies of various W supported on MMT catalysts measured by SEM at mag. X3,000	52
Figure 39 X-ray Powder Diffraction patterns of various W supported on MMT catalysts	53
Figure 40 N_2 adsorption–desorption isotherms of MMT	55
Figure 41 N_2 adsorption–desorption isotherms of 13.5WMMT	56
Figure 42 N_2 adsorption–desorption isotherms of MMT and 13.5WMMT	56
Figure 43 Pore size distribution of MMT	57
Figure 44 Pore size distribution of 13.5WMMT	57
Figure 45 Pore size distribution of MMT and 13.5WMMT	58
Figure 46 NH_3 -TPD profile of various W supported on MMT catalysts	60
Figure 47 Total acidity of various W supported on MMT catalysts	60
Figure 48 Ethanol conversion of various W supported on MMT catalysts for ethanol dehydration at various operating temperature (WHSV=11.44 $\text{g}_{\text{ethanol}} \cdot \text{g}_{\text{cat}}^{-1} \cdot \text{h}^{-1}$)	61
Figure 49 Acetaldehyde reaction rate of various W supported on MMT catalysts for ethanol dehydration at various operating temperature (WHSV=11.44 $\text{g}_{\text{ethanol}} \cdot \text{g}_{\text{cat}}^{-1} \cdot \text{h}^{-1}$)	63
Figure 50 Ethylene reaction rate of various W supported on MMT catalysts for ethanol dehydration at various operating temperature (WHSV=11.44 $\text{g}_{\text{ethanol}} \cdot \text{g}_{\text{cat}}^{-1} \cdot \text{h}^{-1}$)	63

Figure 51 Diethyl ether reaction rate of various W supported on MMT catalysts for ethanol dehydration at various operating temperature (WHSV=11.44 $\text{g}_{\text{ethanol}} \cdot \text{g}_{\text{cat}}^{-1} \cdot \text{h}^{-1}$) 64

Figure 52 Ethanol conversion of 13.5WMMT in stability test of catalytic ethanol dehydration reaction with various operating temperature (the reaction condition: WHSV= 11.44 $\text{g}_{\text{ethanol}} \cdot \text{g}_{\text{cat}}^{-1} \cdot \text{h}^{-1}$) 65



CHAPTER 1

INTRODUCTION

1.1 INTRODUCTION

Ethanol is a renewable fuel made from corn, rice, cassava, sugarcane, and other plant materials through fermentation process. At present, the demand for ethanol for energy and the substance used in various industries is continuously increasing. However, due to the increase in the amount of ethanol production that exceeds the demand, the price of ethanol is continuously falling. Therefore, the ethanol processing to add value is interesting[1, 2]. The dehydration of ethanol produces ethylene and diethyl ether. Dehydration of ethanol produces ethylene at high temperature, but diethyl ether is produced at lower temperature. Ethylene is one of common products in the world industry, and important feedstock for the petrochemical industry. Product of ethylene as the petrochemical such as acetic acid, ethylene oxide, ethylene glycol, ethylbenzene, etc. It is also used as a polymerization raw material to produce polyethylene [3]. Diethyl ether is one of important commercial ethers. It is often used as a solvent in the chemical such as oil, fat, latex, micro cellulose and alkaloid solvent[4]. Another important reaction of ethanol is dehydrogenation which is a reaction producing acetaldehyde. Acetaldehyde is mainly used as an intermediate in the synthesis of other chemicals and is used in the production of perfumes, polyester resins and basic dyes[5]. Acid catalysts are commonly used for dehydration and dehydrogenation of ethanol such as sulfuric acid, zeolites, silica-alumina and alumina[6]. Activated carbon is one of acid catalysts, and it is also studied on ethanol conversion. It has low price and high specific surface area. However, activated carbon catalyst (AC catalyst) has a lower ethanol conversion than other common acid catalysts [7]. Montmorillonite clay (MMT) is acid catalyst. It has moderate specific surface area and high acidity. Moreover, montmorillonite catalyst is usually found in nature. In this study, AC catalyst is represented of micropore catalyst and MMT catalyst is represented of mesopore catalyst. Acid catalyst is often loaded with metal oxide for modifying acid

properties such as TiO_2 , ZrO_2 , SiO_2 , Nb_2O_5 and WO_3 . The interesting of tungsten (W) metal was found since it promotes Brønsted acid site and increases the catalyst stability and activity[8-10]. The study of ethanol dehydration over WO_3/TiO_2 catalysts is reported that WO_3 enhances ethanol conversion and dehydration reaction[11]. Therefore, adding tungsten onto the catalytic activated carbon for enhance ethanol conversion is interesting.

In present study, the effects of tungsten loading over activated carbon catalyst and montmorillonite catalyst were investigated. In the study, different amounts of WO_3 loading were varied from 2-13.5 wt%. The catalysts were characterized using various characterization techniques. Then, the WO_3 supported on activated carbon and montmorillonite catalysts were studied in ethanol dehydration.

1.2 OBJECTIVE

1. To investigate the effect of different between tungsten(VI) oxide loading on commercial activated carbon catalysts and montmorillonite catalysts in ethanol dehydration reaction.

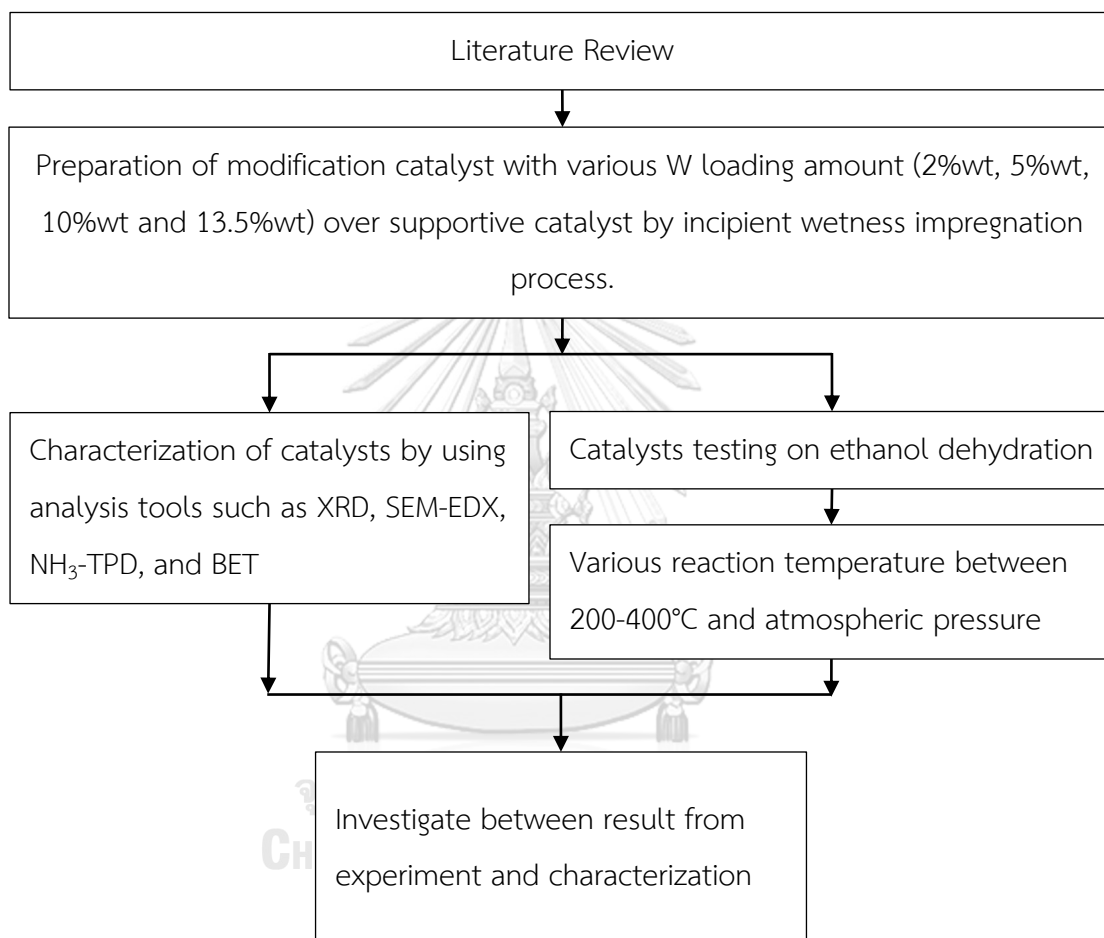
1.3 RESEARCH SCOPE

1. Four percent by mass of tungsten to activated carbon catalysts and montmorillonite catalysts (2, 5, 10 and 13.5) were prepared by incipient wetness impregnation process.
2. Characterize the modified catalysts with Scanning electron microscope (SEM) and Energy dispersive X-ray spectroscopy (EDX), Ammonia temperature programmed desorption (NH_3 -TPD), X-ray diffraction (XRD) and N_2 physisorption (BET).
3. Modified catalysts were tested in ethanol dehydration at operating temperature 200-400 °C and atmospheric pressure.

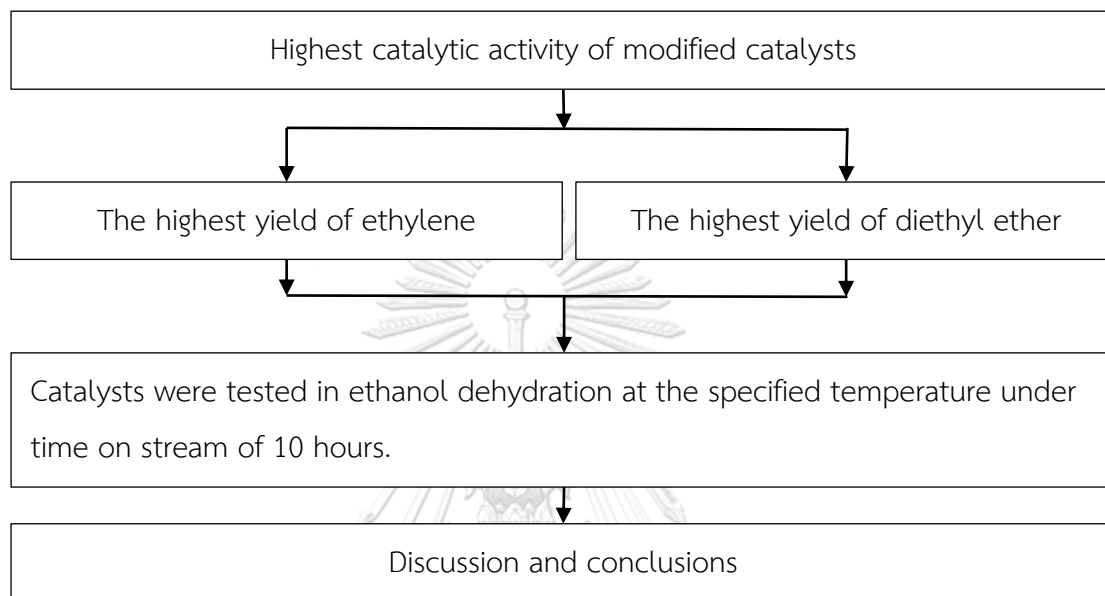
4. To determine which of the tungsten loading on activated carbon and tungsten loading on montmorillonite are most suitable to give the best activity and to yield in ethanol dehydration.

1.4 RESEARCH METHODOLOGY

Part I: Effect of WO_3 loading was investigated.



Part II: The best catalyst in part I was chosen based on the highest yield of ethylene (at high temperature) and the highest yield of diethyl ether (at low temperature). The chosen catalyst was tested on ethanol dehydration at the specified temperature under time on stream of 10 hours. The stability of catalyst and cause of deactivation was evaluated further.



CHAPTER 2

BACKGROUND AND LITERATURE REVIEW

2.1 ACTIVATED CARBON (AC CATALYST)

Activated carbon is produced from almost all carbon-containing organic materials, mainly wood, nutshells, sawdust, peat, fruit stones, coal, lignite, petroleum coke, etc.[12] The main purpose of making activated carbon is to have a high surface area [13, 14] available for adsorption or chemical reactions. Because of its high degree of micro porosity, activated carbon has a surface area in excess of 3,000 m²/g [13-15] as determined by nitrogen and carbon dioxide adsorption[16].

Activated carbon is a non-graphitizable carbon. It means cannot be transformed into graphite solely by high heat treatment. Carbon structure of activated carbon after carbonization is same as precursor because fusion cannot take place. This means that the precursor must produce a non-graphitizable char[17].

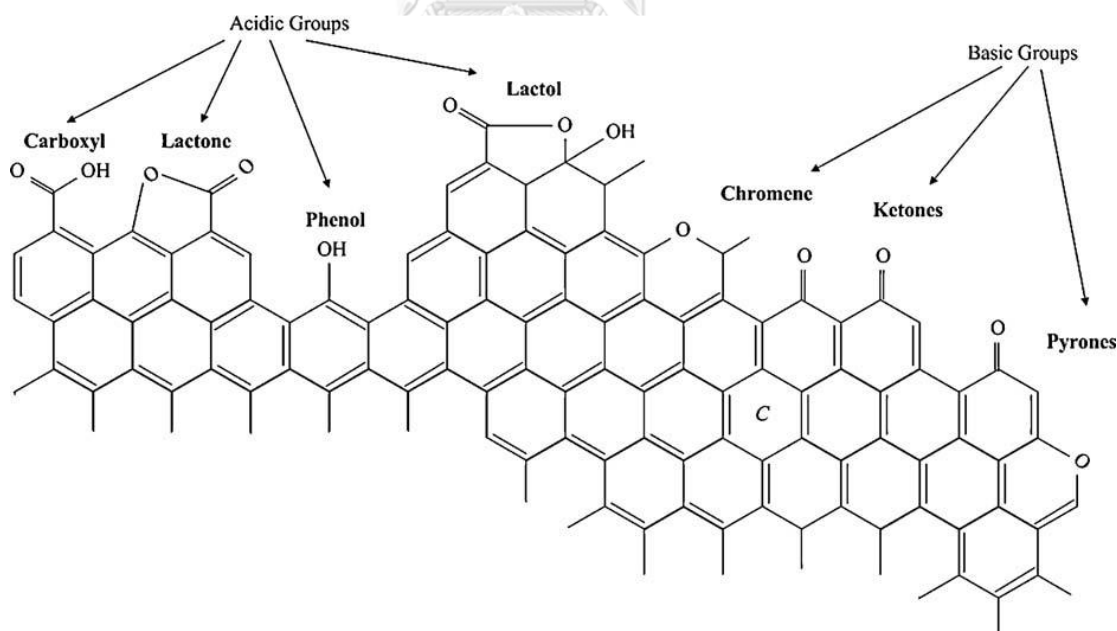


Figure 1 Acidic and basic surface functionalities on a carbon basal plane [18]

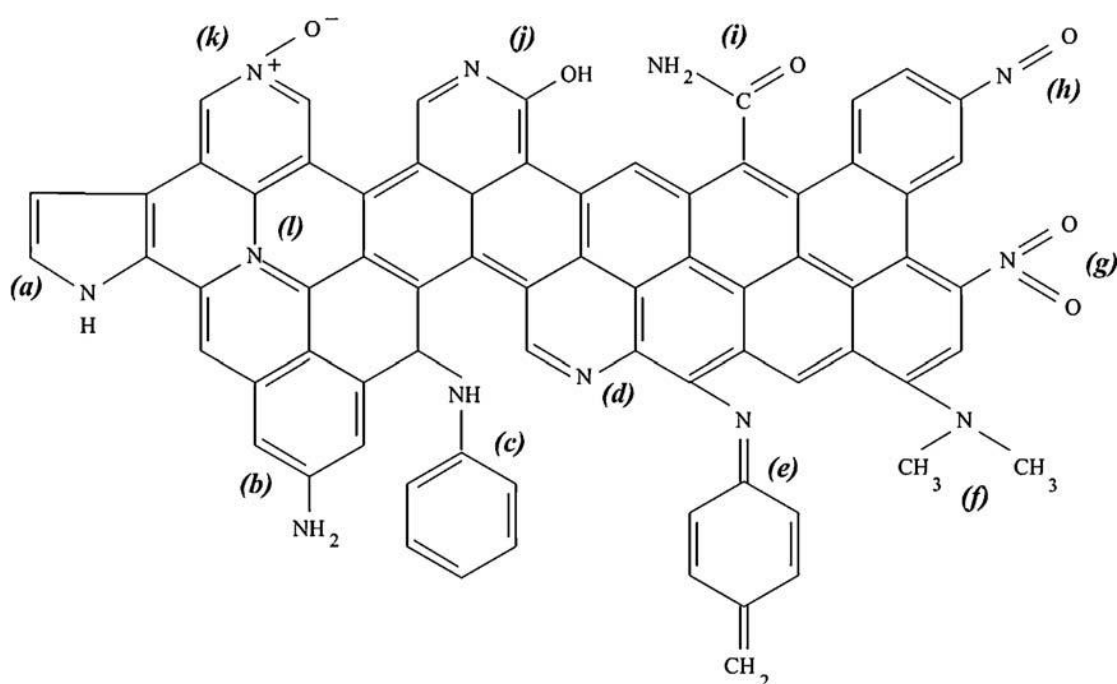


Figure 2 Types of nitrogen surface functional groups: (a) pyrrole, (b) primary amine, (c) secondary amine, (d) pyridine, (e) imine, (f) tertiary amine, (g) nitro, (h) nitroso, (i) amide, (j) pyridone, (k) pyridine-N-oxide, (l) quaternary nitrogen [19]

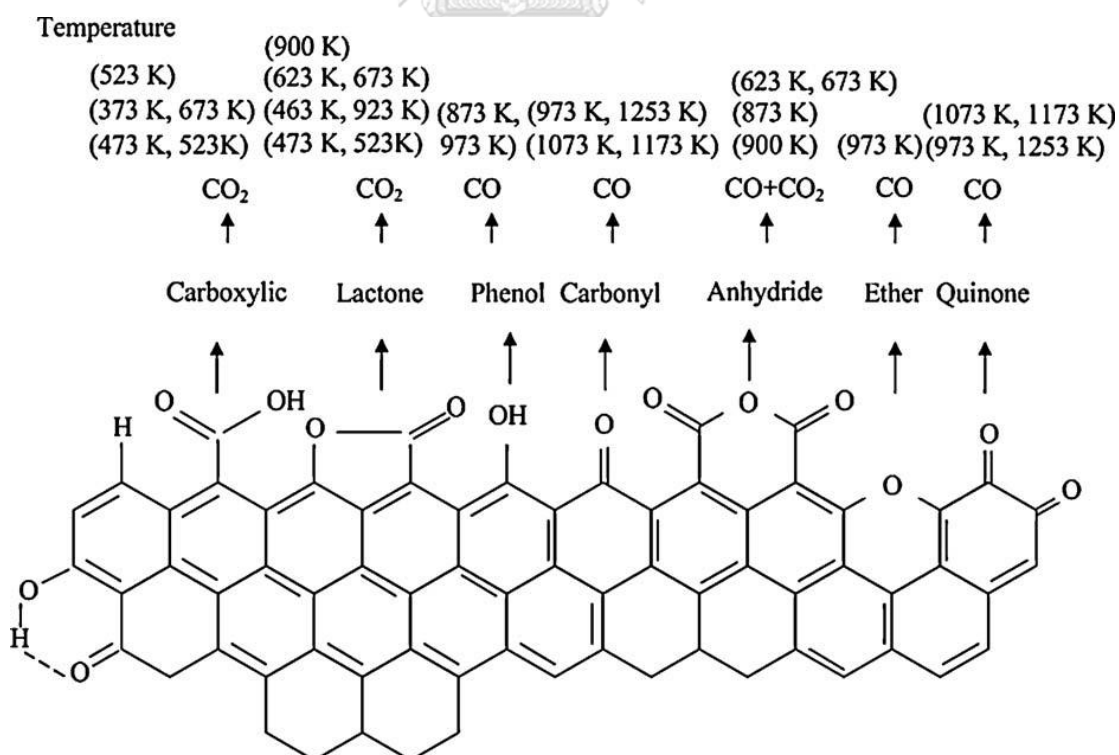


Figure 3 Surface oxygen containing groups on carbon and their decomposition by TPD [20]

2.2 MONTMORILLONITE (MMT CATALYST)

Montmorillonite known as clay. The structure of MMT including two tetrahedral sheets of silica articulated a central octahedral sheet of alumina. The water content of MMT is variable. MMT increases in volume when it absorbs water. The repeating unit formula of structure is hydrated sodium calcium aluminium magnesium silicate hydroxide $(\text{Na,Ca})_{0.33}(\text{Al,Mg})_2(\text{Si}_4\text{O}_{10})(\text{OH})_2 \cdot n\text{H}_2\text{O}$.

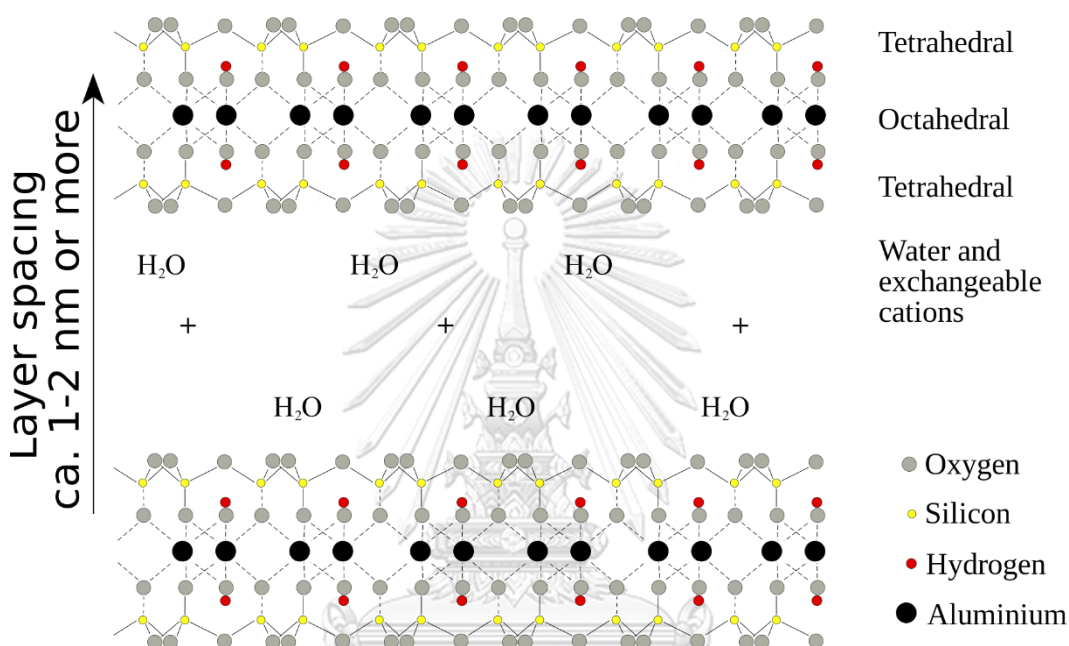


Figure 4 Montmorillonite structure [21]

2.2 AMMONIUM METATUNGSTATE (AMT)

AMT accords with the formula $(\text{NH}_4)_6\text{H}_2\text{W}_{12}\text{O}_{40} \cdot x\text{H}_2\text{O}$. The amount of total water is variable. Usual technical products contain 3 to 4 molecules. Further dehydration may lead to insoluble compounds. The importance of AMT is its high-water solubility. This is why AMT has gained the increasing usage as an intermediate in a variety of applications like chemicals and catalysts[22].

Properties of AMT is a white crystallized powder and its density is 4 g/cm^3 . Decomposition of AMT starts at $100 \text{ }^\circ\text{C}$ and, between $200 \text{ }^\circ\text{C}$ and $300 \text{ }^\circ\text{C}$, it converts into anhydrous form. Then decomposition leads to WO_3 . The solubility in water at $22 \text{ }^\circ\text{C}$ is 1635 g/l or $1500 \text{ g WO}_3/\text{l}$ and at $80 \text{ }^\circ\text{C}$ is 2200 g/l . The pH of the aqueous

solution depends on the concentration of the AMT and vary between 2.5 and 5 at 25 °C, indicating that different species are presented simultaneously[22].

AMT is high solubility in water, Providing the possibility of highly concentrated preparation, alkali-free tungsten solutions. AMT solutions are in use to treat supports for catalyst production. AMT is further used in nuclear shielding, as corrosion inhibitor, and as a precursor for other tungsten chemicals[23].

Table 1 Ammonium metatungstate properties

Properties	Specification
Formula	$(\text{NH}_4)_6\text{H}_2\text{W}_{12}\text{O}_{40} \cdot x\text{H}_2\text{O}$
Compound Formula	$\text{H}_{26}\text{N}_6\text{O}_{40}\text{W}_{12}$
Molecular Weight	2956.3
Appearance	Beige Powder
Melting Point	100 °C
Solubility in H_2O	high solubility

2.3 TUNGSTEN TRIOXIDE

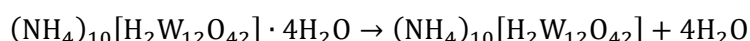
Tungsten trioxide or WO_3 is a chemical compound containing oxygen and the transitioned metal tungsten. Tungsten trioxide is a strong oxidative agent, it reacts to rare-earth elements such as; iron, copper, aluminium, manganese, zinc, molybdenum, chromium, hydrogen, carbon, and silver to make the pure tungsten metal and reacts to gold and platinum to make the tungsten dioxide[24].

WO_3 is almost produced by calcination of APT under oxidizing conditions. General equipment including furnaces operates at 500-700 °C. Excessive supply of air must be provided to inhibit the reduction reaction of the partial cracked ammonia. The evolved ammonia can be recovered by absorption in cold water and can be concentrated by subsequent distillation[22].

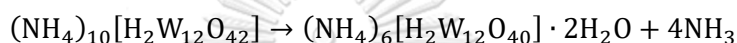
The WO_3 particles are pseudomorphous to APT. This means that the shape and size of the particles are the same as the APT crystals, but they are built WO_3 grains forming oxide sponge with a high degree of specific surface area. Their grain

size and agglomerate structure depend on the calcination conditions (temperature, time, and heating rate). Low-temperature calcined WO_3 (approximately 500-550 °C) is dissolved in water and is highly reactive, but higher-temperature calcined WO_3 is insoluble in water[22].

Under oxidizing conditions, the APT decomposition to WO_3 path is as follows: Between 20 and 100 °C only dehydration occurs, and the product is crystallized, dehydrated APT:



In the temperature range 180-225 °C, ammonia is released and the APT converts to amorphous ammonium meta tungstate (AMT):



Between 230 and 325 °C, ammonia as well as water vapor are evolved. The product is also amorphous:



By increasing the temperature to 400-500 °C, all residual ammonia and water is released, and the reaction product is tungsten trioxide:



Under a slightly reducing atmosphere between 220 and 325 °C amorphous, and above 325 °C, crystallized, ammonium tungsten bronzes form: $(\text{NH}_4)_x \text{WO}_3$. Under stronger reducing conditions, conversion to lower tungsten oxides takes place[22].


Table 2 Tungsten trioxide properties

Properties	Specification
Chemical formula	WO_3
Molecular Weight	231.84
Appearance	Canary yellow powder
Density	7.16 g/cm ³
Melting point	1,473 °C
Boiling point	1,700 °C approximation

2.4 ETHYLENE

Ethylene is a hydrocarbon which has formula C_2H_4 . It is a colorless flammable gas. It is one of alkene group hydrocarbon. Ethylene is widely used in the chemical industry. The most of its product is polyethylene. Ethylene can produce from dehydration of ethanol[25]. some of ethylene properties and some of importance safety data sheet are shown in **table 3**.


Table 3 Ethylene properties

Properties	Specification
Chemical formula	C_2H_4
Molecular Weight	28.054
Appearance	colorless gas
Density	1.178 kg/m ³ at 15 °C, gas[26]
Boiling point	-103.7°C
Flash point	-136 °C
Autoignition temperature	542.8 °C
NFPA 704 (fire diamond)	

2.5 DIETHYL ETHER (DEE)

Diethyl ether is an organic compound in ether class. Its formula $(C_2H_5)_2O$. it is colorless, sweet-smelling, high volatile flammable liquid. It is usually used as a solvent in laboratory. In general, diethyl ether is a byproduct of ethylene hydration to ethanol. however, it can produce from dehydration of ethanol[27]. some of diethyl ether properties and some of importance safety data sheet are shown in **table 4**.


Table 4 Diethyl ether properties

Properties	Specification
Chemical formula	(C ₂ H ₅) ₂ O
Molecular Weight	74.123
Appearance	Colorless liquid
Odor	Ethereal
Density	0.7134 g/cm ³ , liquid
Boiling point	34.6 °C
Flash point	-45 °C
Autoignition temperature	160 °C
NFPA 704 (fire diamond)	
Explosive limits	1.9–48.0%

2.6 ACETALDEHYDE

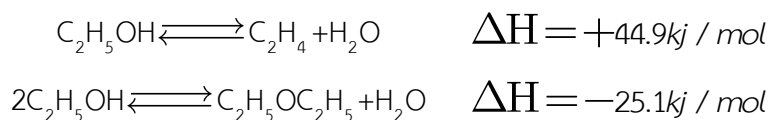
Acetaldehyde is an organic chemical compound. Its formula CH₃CHO. It occurs naturally in coffee, ripe fruit and bread, and is produced by plants[28, 29]. some of diethyl ether properties and some of importance safety data sheet are shown in **table 5**.

Table 5 Acetaldehyde properties

Properties	Specification
Chemical formula	CH ₃ CHO.
Molecular Weight	44.053
Appearance	Colorless liquid
Odor	Ethereal
Density	0.784 g/cm ³ (20 °C)
Boiling point	20.2 °C
Flash point	-39°C
Autoignition temperature	175 °C
NFPA 704 (fire diamond)	
Explosive limits	4.0–60%

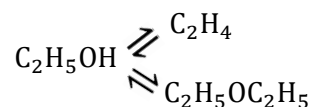
2.7 ETHANOL DEHYDRATION REACTION

Dehydration means to lose or remove water from something. Therefore, ethanol dehydration reaction is a reaction which removes water from ethanol. There are two possibilities of ethanol reaction which are unimolecular ethanol to ethylene and bimolecular ethanol to diethyl ether. Ethylene can occur at high temperatures because it is an endothermic reaction. Meanwhile, diethyl ether occurs at lower temperatures due to the exothermic reaction.

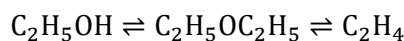


Almost the mechanism research of ethanol dehydration reaction is mainly considered as the generation of ethylene and diethyl ether which can be summarized in 3 routes. These are parallel reaction, a series of reactions[30] and a parallel series reaction.

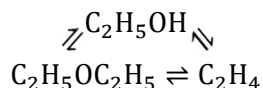
(1) Parallel reaction



(2) A series of reactions

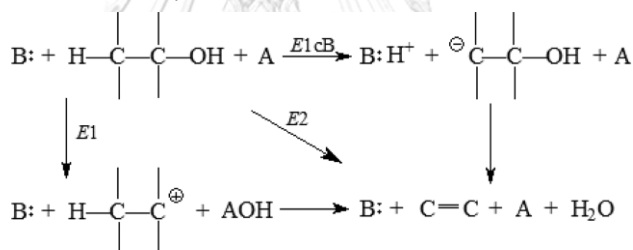


(3) A parallel series reaction



A parallel series reaction refers to three reversible reactions, which are ethanol intramolecular dehydration to ethylene, ethanol intermolecular dehydration to ether, and ether dehydration to ethylene.

Intramolecular dehydration of ethanol to ethylene has three reaction mechanisms (E1, E2 and E1cB) under different reaction conditions[31]. That are E1, E2, and E1cB mechanisms, as is shown as follows, where A and B are the acidic and basic centers of the catalyst, respectively.

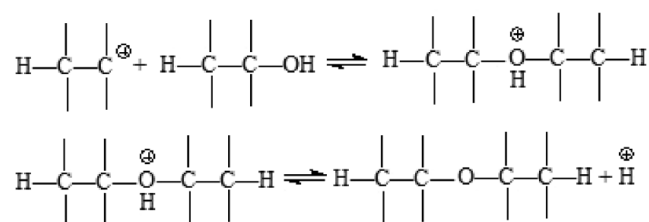


: electrons pair \oplus positive charge \ominus negative charge

These three reactions are elimination reactions[32], and the three are competitive reactions. The E1 reaction is a unimolecular elimination reaction. It has two-steps mechanism. The first step of mechanism is to generate a carbocation intermediate which is the rate-determining step and is a first-order reaction, afterward it rapidly loses β -hydrogen to generate ethylene. The E2 reaction is a bimolecular elimination reaction. It has one-step mechanism, with a single transition state. The reaction rate is the second order, because it is influenced by bimolecular. The E1cB reaction is a unimolecular elimination reaction which occurs under basic conditions. It has two-steps mechanism. In the first step, β -hydrogen of the reactant is captured by the nucleophilic center to generate carbanion (conjugate base), and then the hydroxyl of the conjugate base is unleashed to generate ethylene[33].

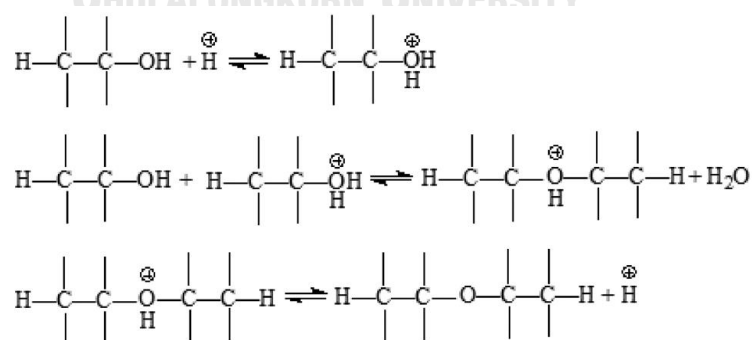
Intermolecular dehydration of ethanol to diethyl ether is a substitution reaction. This reaction has mainly two reaction mechanisms including S_N1 (single-molecule nucleophilic substitution reaction) and S_N2 (bimolecular nucleophilic substitution reaction)[32]. The S_N1 reaction has two steps. The first step is to dissociate ethanol to carbocations by leaving hydroxyl radical, which is the rate-determining step and is the same as the first reaction step of the mechanism E1. In the second step, the nucleophiles immediately associate with carbocations. The S_N2 reaction is like E2 mechanism which has one-step mechanism, with a single transition state. The mechanism of S_N2 is proton attack ethanol forming electrophilic, after that another ethanol was captured with electrophilic forming the intermediate. Finally, the intermediate unleashes water and base group and forming diethyl ether. The S_N1 and S_N2 reaction mechanisms of ethanol intermolecular dehydration to ether are shown as follows[3].

(1) S_N1 reaction mechanisms (the first step is the same as that of E1)



\oplus positive charge

(2) S_N2 reaction mechanisms



\oplus positive charge

However, at the high temperature, the ether bond will break. Then, it will generate a carbocation and may form ethylene, following the E1 reaction mechanism.

2.8 LITERATURE REVIEW

2.8.1 Activated carbon catalyst

In 2019, Ob-eye, J., et al.[34] investigated dehydrogenation of ethanol to acetaldehyde over different metals supported on activated carbon catalyst. They doped various metals, including Ce, Co, Cu, and Ni, on activated carbon catalyst for dehydrogenation of ethanol. The reaction was tested at temperature between 250 °C and 400 °C under atmospheric pressure. They have reported that the type of metal has an important impact on catalytic performance, because it affected the surface acidity. Cu/ACC catalyst represented the highest catalytic activity. Ni/ACC catalyst was appropriate to produce ethylene via ethanol dehydration at 400 °C

2.8.2 Montmorillonite catalyst

In 2016, Krutpijit, C., et al.[35] investigated dehydration of ethanol over montmorillonite catalyst and acid activating montmorillonite catalyst. They were used mineral acid including H₂SO₄ (SA-MMT), HCl (HA-MMT), and HNO₃ (NA-MMT) to acid activating montmorillonite catalyst. They found that HA-MMT exhibited the highest activity in ethanol dehydration. Due to it perform highest yield of ethylene at operating temperature 400°C and high yield of diethyl ether at low operating temperature (200°C to 300°C).

2.8.3 Tungsten oxide

In 2014, Hunyadi, D., et al.[36] studied structure and thermal decomposition of ammonium metatungstate. They have reported that thermal decomposition of AMT had many steps in inert atmosphere including releasing water to dehydrated ATM between 25 °C and 200 °C, formation of an amorphous phase between 200 °C and 380 °C, form hexagonal WO₃ structure between 380 °C and 500 °C, then transformed into more stable m-WO₃ between 500 °C and 600 °C.

2.8.4 Tungsten supported over activated carbon catalyst

In 2000, Alvarez-Merino, M.A., et al.[37] studied preparation of tungsten catalysts supported on granular activated carbon and characterization after Their Heat Treatments in Inert Atmosphere. They have reported that the surface area of supported catalysts was decreased with the amount of the tungsten precursor and was decreased with higher temperature of heat treatment. The reduction of tungsten occurs at temperatures of more than 700 °C. Total surface acidity was increased with the amount of the tungsten precursor but was decreased with higher temperature of heat treatment.

In 2000, Moreno-Castilla, C., et al.[38] investigated decomposition reactions of methanol and ethanol catalyzed by tungsten oxide supported on granular activated carbon. All catalysts were operated at temperature between 100 °C and 200 °C under atmospheric pressure. The reaction was occurred in He flow saturated with alcohol. They have reported that the activity of supported catalysts in the dehydration reactions of methanol and ethanol is linear relationship with their total surface acidity. Moreover, the activated carbon that had a basic character reduced the acid strength of the tungsten oxide.

2.8.5 Tungsten supported over catalyst

In 2019, Tresatayawed, A., et al.[11] studied ethanol dehydration over WO_3/TiO_2 catalysts using Titania came from sol-gel and solvothermal methods. He has reported that WO_3/TiO_2 from solvothermal methods (WO_3/TiO_2 -SV) was suitable for ethanol dehydration and TiO_2 -SV was appropriate for ethanol dehydrogenation.

From all of literature reviews, activity dehydration of ethanol by activated carbon catalyst was low. But it has high degree of surface area. Tungsten could form tungsten trioxide which could enhance the dehydration of ethanol. Nevertheless, tungsten trioxide catalyst had low surface area. Therefore, tungsten oxide supported over AC catalyst and MMT catalyst was interesting for improved activity in catalytic ethanol dehydration.

CHAPTER 3

EXPERIMENT

This chapter explains detail in experiment, which consists of modification catalyst with tungsten loading by implantation process, procedure in testing ethanol dehydration reaction and catalyst characterization such as N₂ physisorption (BET), X-ray diffraction (XRD), Scanning electron microscope (SEM) and Energy dispersive X-ray spectroscopy (EDX), and Ammonia temperature programmed desorption (NH₃-TPD).

3.1 Materials

Chemicals, which was used for preparation of the catalysts were commercial activated carbon from TPI Polene Public Company Ltd. and Sigma-Aldrich, montmorillonite from Sigma-Aldrich, ethanol (99.99%) from Merck Company Ltd., and ammonium metatungstate hydrate (99.99% metals) from Sigma-Aldrich. Furthermore, ultrahigh purity nitrogen gas (99.99%) from Linde (Thailand) Public Company Ltd. was used as carrier for the reaction study.

3.2 CATALYST PREPARATION

3.2.1 Synthesis Tungsten supported on activated carbon catalyst

In this study, the activated carbon from TPI Polene Public Company Ltd. was in the form of fine powder which was referred to the text as AC. In addition, the activated carbon from Sigma-Aldrich was granular activated carbon which was referred to the text as ACG. before W loading, granular AC catalyst necessary was mashed to fine particle.

WO₃ on activated carbon catalysts were prepared by incipient wetness impregnation method. Ammonium metatungstate hydrate was used as a tungsten precursor. Later, the catalyst sample was dried overnight at 110 °C and was calcined at 475°C with the heating rate of 10°C per minute for 4 hours. Finally, the catalysts were loaded with tungsten as referred to in the letter W before text AC or ACG. The tungsten content (wt%) of the catalysts is denoted before the letter W.

3.2.2 Synthesis Tungsten supported on montmorillonite catalyst

WO₃ on montmorillonite catalysts were prepared by incipient wetness impregnation method. Ammonium metatungstate hydrate was used as a tungsten precursor. Later, the catalyst sample was dried overnight at 110 °C and was calcined at 475°C with the heating rate of 10°C per minute for 4 hours. Finally, the catalysts were loaded with tungsten as referred to in the letter W before text MMT. The tungsten content (wt%) of the catalysts is denoted before the letter W.

3.3 CATALYST CHARACTERIZATION

3.3.1 X-ray diffraction (XRD)

The SIEMENS D-5000 X-ray diffractometer using CuK_α radiation ($\lambda = 1.54439 \text{ \AA}$) was being used to determine the crystalline phase structure of supports and catalysts. The XRD patterns of catalysts were analyzed at the rate of 2.4 min⁻¹ in the range 2θ from 20 to 80 degrees with resolution of 0.02 degrees.

3.3.2 Ammonia temperature-programmed desorption (NH₃-TPD)

The Micromeritics Chemisorb 2750 Pulse Chemisorption system instrument was used to diagnose the acidity of catalysts. In the measurement of modified activated carbon catalysts, 0.1 g of catalysts were packed in a U-tube glass with 0.02 g of quartz wool and were pretreated at 475°C under helium flow until Thermal conductivity detector (TCD) signal equal 0. Then, the catalysts were saturated with 15% of NH₃/He and the physisorbed ammonia was desorbed under helium gas flow after being saturated. The catalysts were heated from 30°C to 450°C at the heating rate of 10 °C per minute and were held for 1 hour to desorb the chemisorbed ammonia. For the measurement of modified montmorillonite catalysts, 0.1 g of catalysts were packed in a U-tube quartz with 0.02 g of quartz wool and were pretreated at 200°C under helium flow for 1 hour. Formerly, the catalysts were saturated with 15% of NH₃/He and the physisorbed ammonia was desorbed under helium gas flow after being saturated. The catalyst was heated from 30°C to 800°C at the heating rate of 10 °C per minute to desorb the chemisorbed ammonia. This process necessary installed or reinstalled the cold trap, because TCD signal was disturbed by vapor water from MMT.

3.3.3 Scanning electron microscope (SEM) and Energy dispersive X-ray spectroscopy (EDX)

The SEM model JEOL mode JSM-6400 and EDX with stand Link Isis series 300 program were operated for analysis the morphology, element composition, and distributions of catalysts.

3.3.4 N₂ physisorption (BET)

The Micromeritics Chemisorb 2750 Pulse Chemisorption system instrument was used to assay the specific surface area of catalysts by a single point on the nitrogen adsorption isotherm method. In the measurement, 0.1 g of catalysts were packed in a U-tube glass with 0.01 g of quartz wool and were pretreated at 200°C under nitrogen flow for 1 hour. Formerly, the catalysts were adsorbed with 30% of N₂/He by reducing the temperature with liquid nitrogen until approaching the boiling point of nitrogen (-196°C). Finally, they were desorbed by being heated to the room temperature. The specific surface area is a peak area divided by weight of sample.

Micromeritics ASAP 2020 was used to assay specific surface area, specific pore volume, pore diameter, isotherm graph, and pore size distribution of catalysts by BET&BJH method to analyzing.

3.4 Catalytic Ethanol dehydration reaction

The catalytic dehydration of ethanol was performed in a fixed-bed continuous flow microreactor. First, 0.02 g of quartz wool was packed in the middle of microreactor, then, 0.1 g of catalyst was poured onto quartz wool. After that, 0.005 g of quartz wool was packed above the previous layers to prevent the backward flow of the catalyst. The catalysts were preheated to remove moisture by flowing N₂ with flow rate of 60 ml/min at 200°C for 1 hour under the atmospheric pressure. Afterwards, catalytic ethanol reaction was performed by feeding gas mixtures of vaporized ethanol and N₂ carrier gas. The ethanol flow rate was maintained at 0.397 ml/h and 1.45 ml/h (WHSV=3.13 and 11.44 g_{ethanol}·g_{cat}⁻¹·h⁻¹) and was controlled by Razel model R99-E syringe pump injection. The reaction was processed at various temperature from 200 to 400°C. When each temperature reaching the steady state, substances which were flowing out of the microreactor

were analyzed by Shimadzu gas chromatography 14-B with flame ionization detector (FID) using DB-5 capillary column. Nitrogen was used as carrier gas in GC using the temperature of auxiliary heater, injector, and detector at 150°C and capillary column at 40°C. which had operating condition as reported in Table 4.

Table 6 The chemical used in ethanol dehydration reaction

Chemical	Formula	Supplier
99 wt % Ethanol	C ₂ H ₅ OH	Merch
UHP Nitrogen gas 99.99 %	N ₂	Linde

Table 7 The operating conditions in gas chromatograph

Gas Chromatograph	Shimadzu GC 14-B
Detector	FID
Capillary column	DB-5
Carrier gas	Nitrogen gas
Column temperature	Initial 40 °C Final 40 °C
Injector temperature	150 °C
Detector temperature	150 °C
Time analysis	4 min.

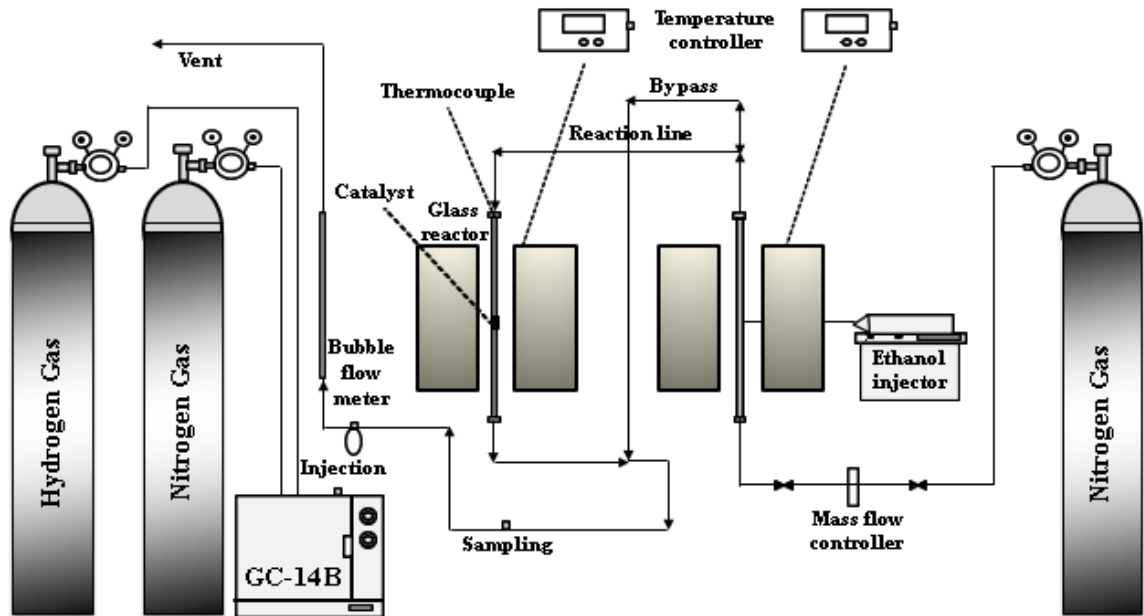


Figure 5 Schematic of the gas phase ethanol dehydration reaction

3.5 Analysis and calculation

The catalytic activities (conversion, selectivity, yield, and reaction rate) were calculated as follow:

The ethanol conversion was defined as follows:

$$X_{\text{EtOH}} = \frac{\dot{n}_{\text{EtOH(in)}} - \dot{n}_{\text{EtOH(out)}}}{\dot{n}_{\text{EtOH(in)}}} \quad (1)$$

The selectivity to *i* product was defined as follows:

$$S_{\text{ethylene}} = \frac{\dot{n}_{\text{ethylene}}}{\dot{n}_{\text{EtOH(in)}} - \dot{n}_{\text{EtOH(out)}}}, \quad (2.1)$$

$$S_{\text{DEE}} = \frac{2 \times \dot{n}_{\text{DEE}}}{\dot{n}_{\text{EtOH(in)}} - \dot{n}_{\text{EtOH(out)}}}, \quad (2.2)$$

$$S_{\text{acetaldehyde}} = \frac{\dot{n}_{\text{acetaldehyde}}}{\dot{n}_{\text{EtOH(in)}} - \dot{n}_{\text{EtOH(out)}}} \quad (2.3)$$

The yield to i product was defined as follows:

$$Y_{\text{ethylene}} = S_{\text{ethylene}} \cdot X_{\text{EtOH}} \quad (3.1)$$

$$Y_{\text{DEE}} = S_{\text{DEE}} \cdot X_{\text{EtOH}} \quad (3.2)$$

$$Y_{\text{acetaldehyde}} = S_{\text{acetaldehyde}} \cdot X_{\text{EtOH}} \quad (3.3)$$

The reaction rate to i product was defined as follows:

$$r_{\text{ethylene}} = \frac{\dot{n}_{\text{EtOH(in)}} \cdot Y_{\text{ethylene}}}{W_{\text{cat}}} \quad (4.1)$$

$$r_{\text{DEE}} = \frac{\dot{n}_{\text{EtOH(in)}} \cdot Y_{\text{DEE}}}{W_{\text{cat}}} \quad (4.2)$$

$$r_{\text{acetaldehyde}} = \frac{\dot{n}_{\text{EtOH(in)}} \cdot Y_{\text{acetaldehyde}}}{W_{\text{cat}}} \quad (4.3)$$

Where $\dot{n}_{\text{EtOH(in)}}$ and $\dot{n}_{\text{EtOH(out)}}$ were defined as molar flow rate ($\mu\text{mol/s}$) of ethanol in feed and product stream, respectively. $\dot{n}_{\text{ethylene}}$, \dot{n}_{DEE} , $\dot{n}_{\text{acetaldehyde}}$ and $\dot{n}_{\text{EtOH(out)}}$ were defined as molar flow rate ($\mu\text{mol/s}$) of ethylene, diethyl ether, and acetaldehyde, respectively. W_{cat} was defined as weight of catalyst (g).

3.5 Research plan

Table 8 Schedule of the research plan

Research plan	Year 2019					Year 2020								
	8	9	10	11	12	1	2	3	4	5	6	7	8	9
Researched and literature review	←---→													
Decide research topic	←---→													
Prepare the AC catalysts		←---→												
Characterized the AC catalysts		←---→					←---→							
Prepare the MMT catalysts							←---→							
Characterized the MMT catalysts							←---→					←---→		
Studying the reaction		←---→					←---→					←---→		
Studying the stability reaction			←---→					←---→				←---→		
Analyzed the result and discussion		←---→					←---→					←---→		
Preparation of the report for presentation		←---→					←---→						←---→	

Note: Dash line (←---→) refers to the duration of experiment planned.
Black line (←---→) refers to the duration of experiment done.

CHAPTER 4

Result and Discussion

This chapter describes the characteristic properties and catalytic activities in ethanol dehydration reaction of all catalysts. It was divided into three parts. The first part and second part explained characteristic properties and catalytic activities in ethanol dehydration reaction of activated carbon support catalyst groups and montmorillonite support catalyst group, Respectively. The final part compared result from the first and second part and discussed suitable catalyst for each application.

4.1 W supported on AC catalysts

4.1.1 Catalyst characterization

4.1.1.1 Scanning electron microscope (SEM) and Energy dispersive X-ray spectroscopy (EDX)

The morphologies of activated carbon and modified activated carbon formed irregular shapes and porous particles are shown in **Figures 6 to 9**. On the surface of catalyst, there are particles from the process of producing activated carbon catalyst. However, ACG support catalysts were rougher surface from AC support catalyst. Since ACG was mashed from gaining to fine particles before catalyst preparation. The rough surface was occurred from the crossed section of gain ACG. The EDX mapping of 2WAC and 5WAC shows that W is absolutely dispersed over surface of catalyst, whereas other W loading catalysts had dense area of W as shown in **Figure 10**. According to **Table 9**, W composition which was obtained by EDX of 13.5WACG was higher than 13.5WAC.

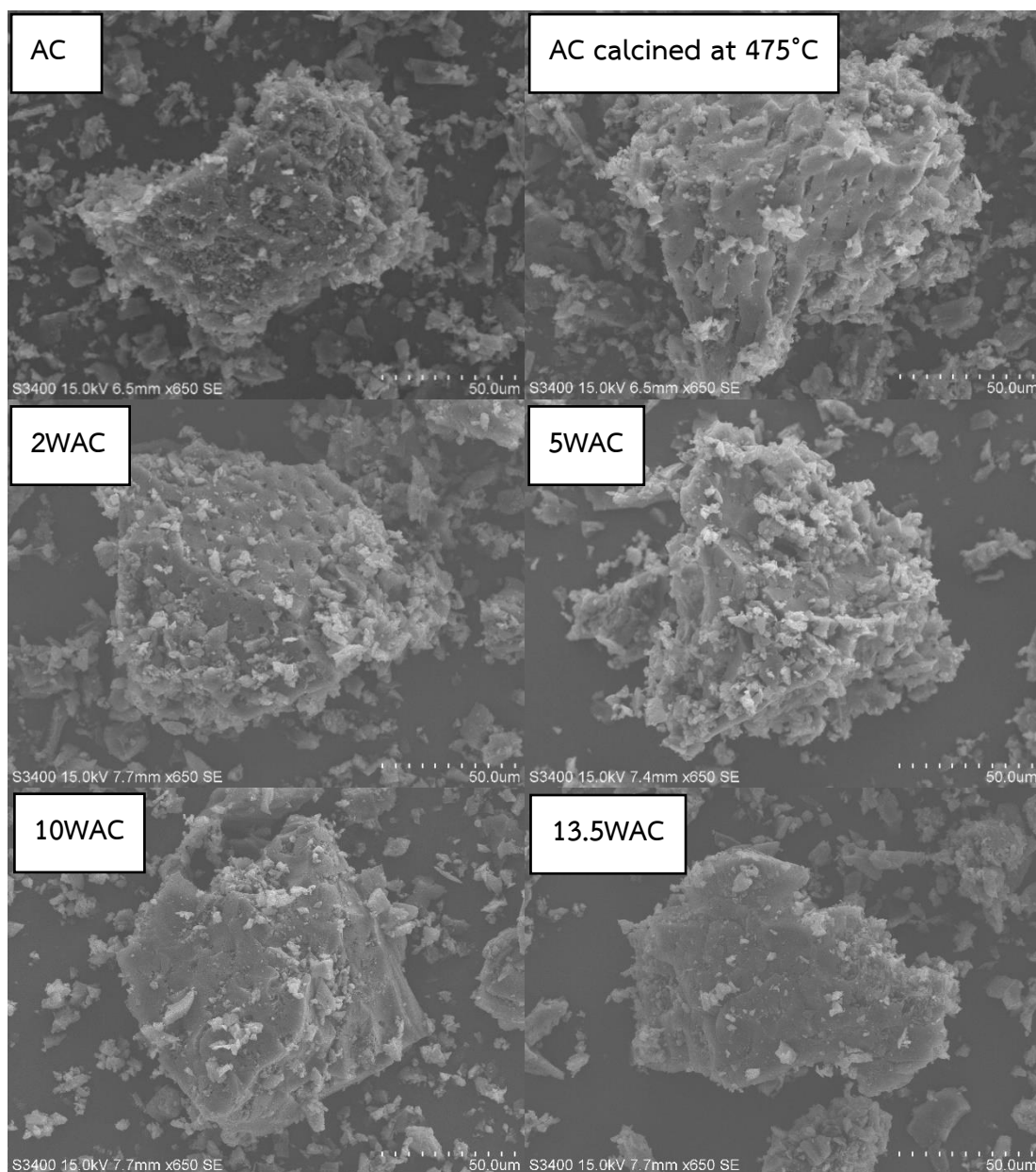


Figure 6 The morphologies of various W supported on AC catalysts (TPI) measured by SEM at mag. X650

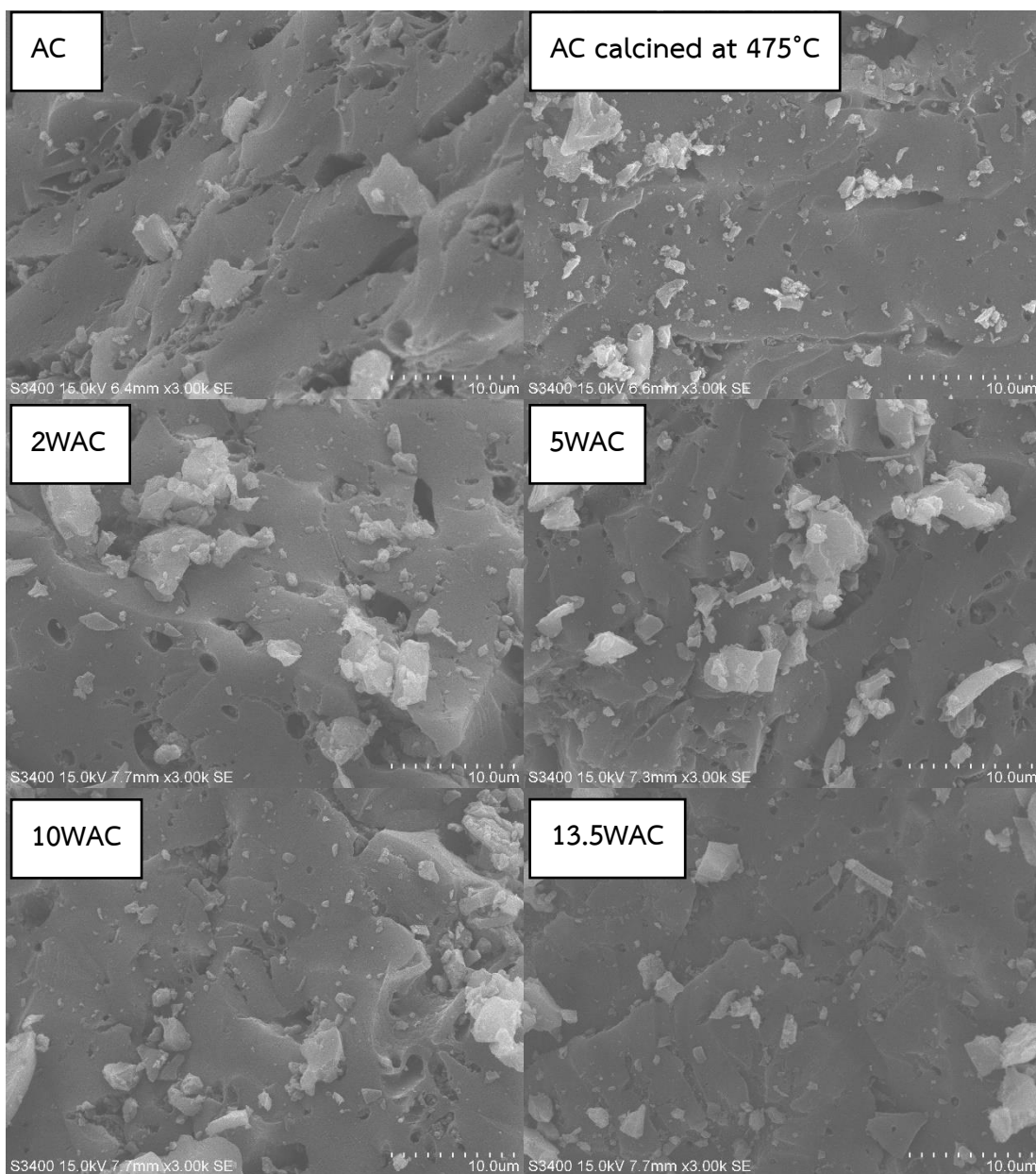


Figure 7 The morphologies of various W supported on AC catalysts (TPI) measured by SEM at mag. X3,000

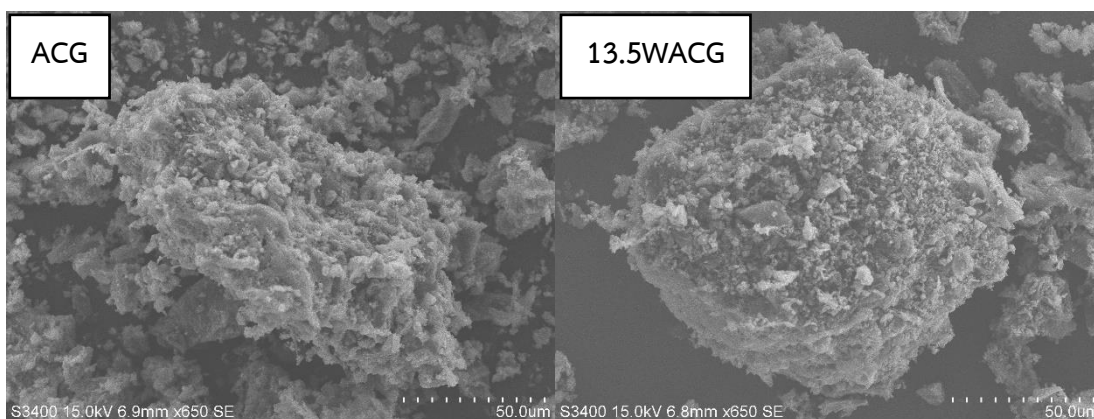


Figure 8 The morphologies of W supported on AC catalysts (Sigma-Aldrich) measured by SEM at mag. X650

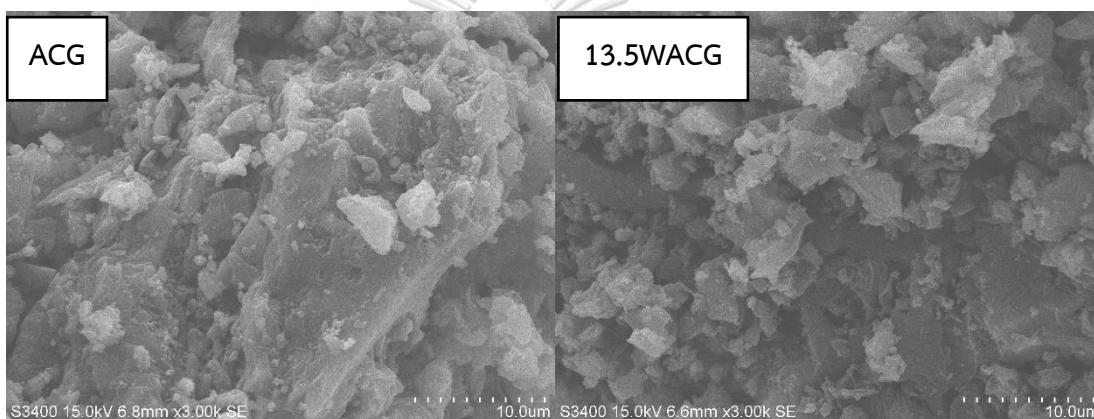


Figure 9 The morphologies of W supported on AC catalysts (Sigma-Aldrich) measured by SEM at mag. X3,000

Table 9 Chemical composition obtained by EDX of W supported on AC catalysts

Catalysts	%weight		
	C	O	W
AC	86.0	14.0	
2WAC	82.9	9.5	7.6
5WAC	81.2	10.5	8.3
10WAC	76.1	9.3	14.6
13.5WAC	73.7	7.6	18.7
ACG	85.5	14.5	
13.5WACG	57.1	9.0	34.0

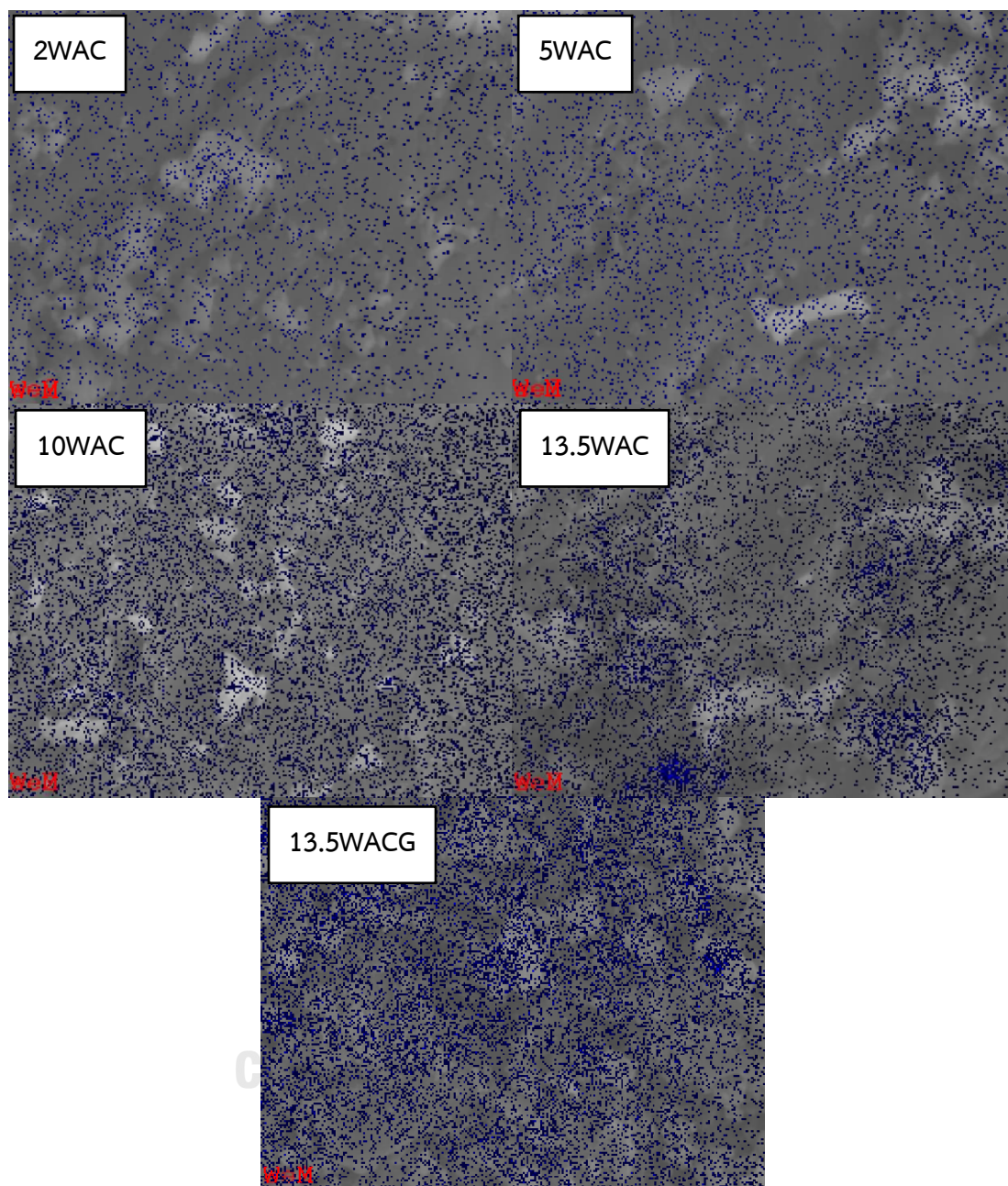


Figure 10 SEM-EDX mapping of various W supported on AC catalysts

4.1.1.2 X-ray Powder Diffraction (XRD)

The XRD patterns of catalysts are shown in **Figure 11**. Considering the XRD pattern of W supported on AC catalysts (TPI), it exhibited the XRD pattern having two broad diffraction peaks located at 2θ degrees of 23° and 43.5° . These broad peaks of the XRD pattern confirm an amorphous state[39]. When AC was impregnated with W, the XRD patterns were also similar with AC, but intensity of broad peaks was decreasing with increased content of W loading. 2WAC exhibited peak located at 2θ degrees 28.7° (Monoclinic- WO_3). However, intensive of this peak decreased in 5WAC. 10WAC and 13.5WAC were exhibited the mixed phase of WO_3 . They exhibited peak located at 2θ degrees of 23.3° (Hexagonal- WO_3), 28.0° (Hexagonal- WO_3), and 36.8° (Hexagonal- WO_3). The intensity of peaks increased with content of W loading. [40-44]. In **Figure 12**, considering the XRD pattern of W supported on AC catalysts (Sigma-Aldrich), it exhibited the XRD pattern having two broad diffraction peaks location same as AC. However, ACG exhibited peak located at 2θ degrees of 26.3° . It can refer to graphite[45]. Moreover, ACG exhibited other peak located at 2θ degrees of 20.8° and 26.6° . They referred to quartz which was impurity from manufacturing. When ACG was impregnated with W, the XRD patterns were also similar with ACG, but intensity of broad peaks was being decreased. The 13.5WACG exhibited peak located at 2θ degrees of 28.7° (Monoclinic- WO_3) [41, 42, 46].

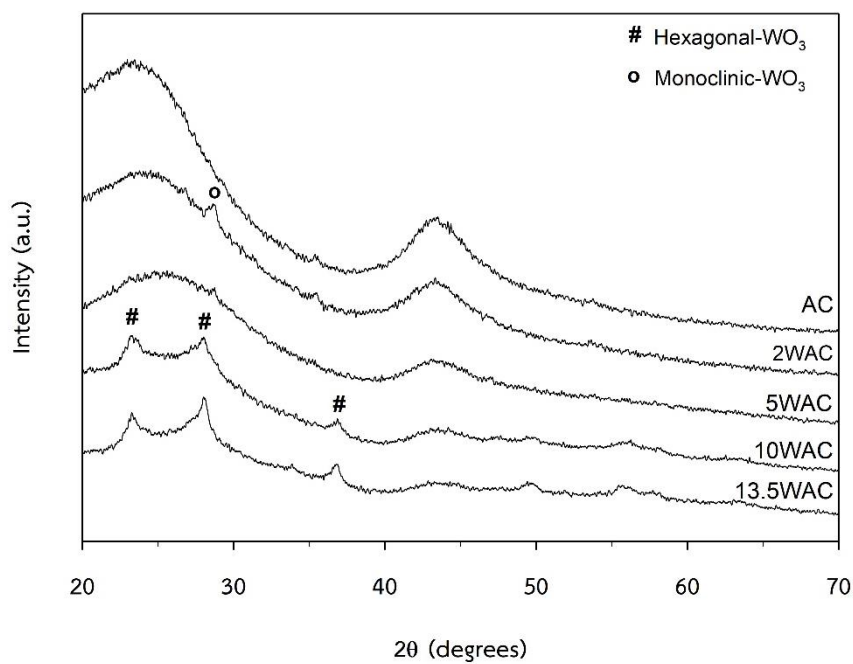


Figure 11 X-ray Powder diffraction patterns of various W supported on AC catalysts (TPI)

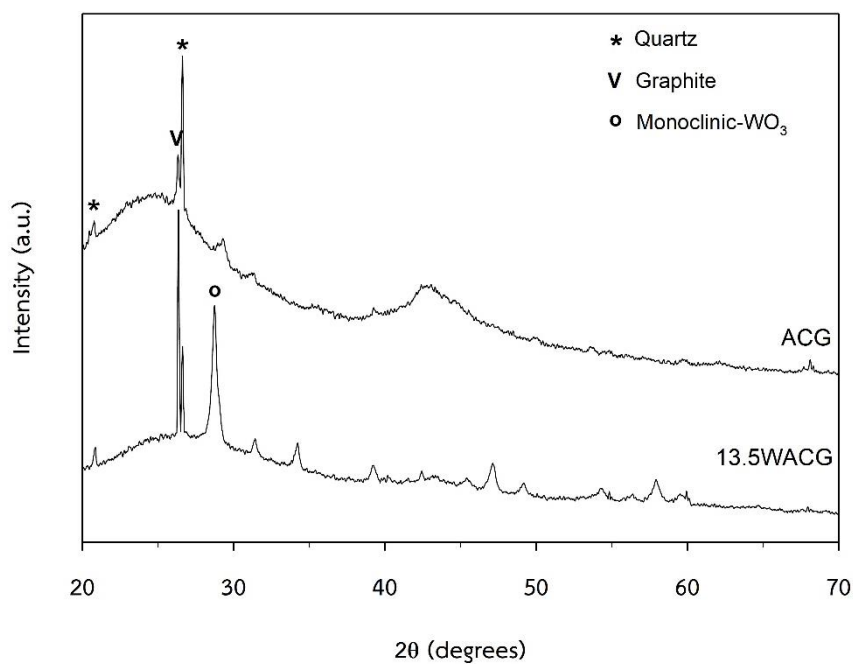


Figure 12 X-ray Powder diffraction patterns of W supported on AC catalysts (Sigma-Aldrich)

4.1.1.3 N₂ physisorption (BET)

Multipoint N₂ physisorption was used to assay specific surface area, specific pore volume, pore diameter, isotherm graph, and pore size distribution of AC, 13.5WAC, ACG, and 13.5WACG. As shown in **Figures 5 to 17**, the activated carbon catalyst and modified activated carbon catalyst from two manufacturer exhibited a combination of type I (major) and IV (minor) isotherms with type H4 hysteresis loop according to IUPAC classification[47], and capillary condensation in the pores at relative pressure (P/P_0) close 0.40. They indicated presence of narrow slit pores including pores in the micropore and mesopore region. Higher pressure hysteresis of ACG and 13.5WACG indicated higher volume of mesopore. Since the instrument were not conducive to measure particle with micropore, the pore size distribution was started to report with 2 nm, furthermore, the average pore diameter was not calculated with micropore. **Figures 18 to 22** shows the pore size distribution of ACG and 13.5WACG which had higher mesopore than AC and 13.5WAC. W loading reduced specific pore volume and specific surface. However, it did not affect the average pore diameter, as shown in **Table 10**.

Single point N₂ physisorption was used to assay the specific surface area of W supported on AC catalysts (TPI). **Table 11** shows specific surface areas which were decreased with content of W. After loading W 13.5 wt% on support, specific surface area of AC was decreased 26% and specific surface area of MMT was decreased 41%.

Table 10 Textural properties of AC, 13.5WAC, ACG, and 13.5WACG

Catalyst	AC	13.5WAC	ACG	13.5WACG
S_{BET} (m^2g^{-1})	922	747	572	489
$S_{\text{micropore}}$ (m^2g^{-1})	730	573	336	291
S_{external} (m^2g^{-1})	192	174	236	198
V_{M} (cm^3g^{-1})	0.340	0.267	0.156	0.134
V_{T} (cm^3g^{-1})	0.466	0.374	0.380	0.324
D_{A} (nm)	2.02	2.00	2.66	2.65

* S_{BET} = specific surface area by BET, $S_{\text{micropore}}$ = t-Plot micropore Area, S_{external} = t-Plot external surface Area V_{M} = t-Plot micropore volume, V_{T} = Single point total pore volume of pores, and D_{A} = average pore diameter by BET

Table 11 Specific surface area of various W supported on AC catalysts (TPI)

Catalyst	$S_1(\text{m}^2 \text{g}^{-1})$
AC	984
2WAC	961
5WAC	886
10WAC	796
13.5WAC	742

* S_1 =specific surface area by single point N_2 physisorption

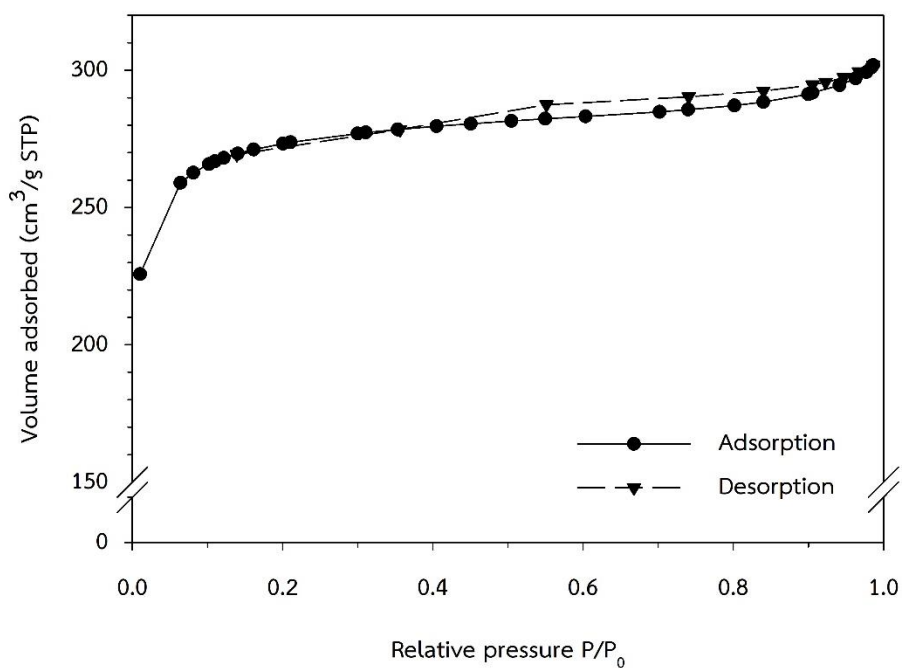


Figure 13 N₂ adsorption-desorption isotherms of AC

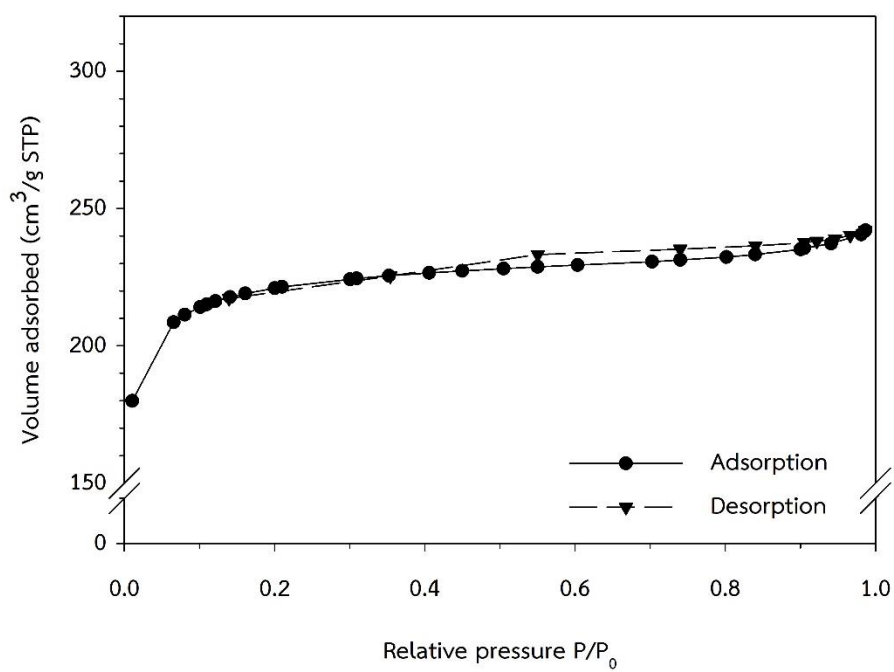


Figure 14 N₂ adsorption-desorption isotherms of 13.5WAC

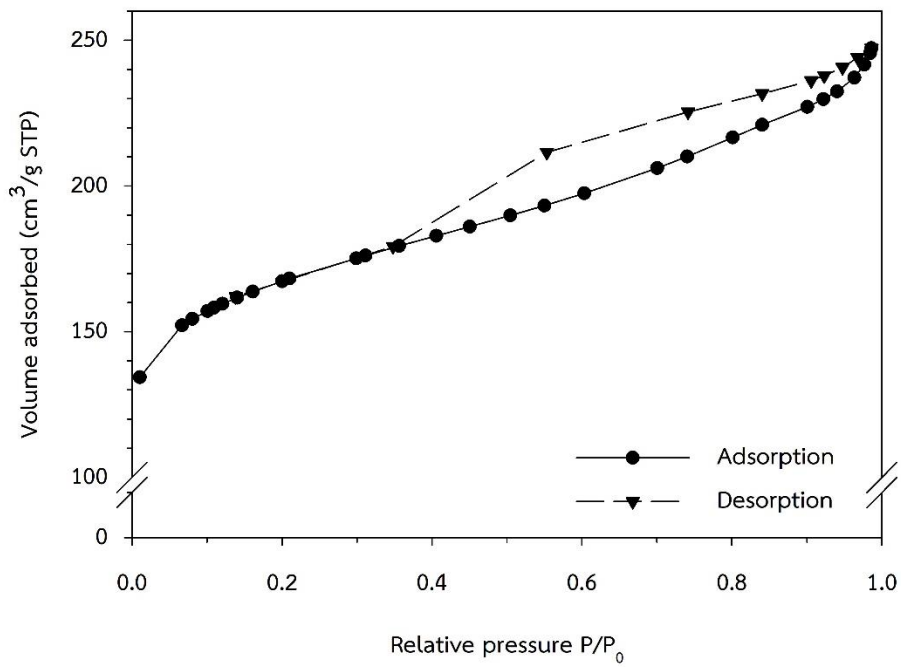


Figure 15 N₂ adsorption-desorption isotherms of ACG

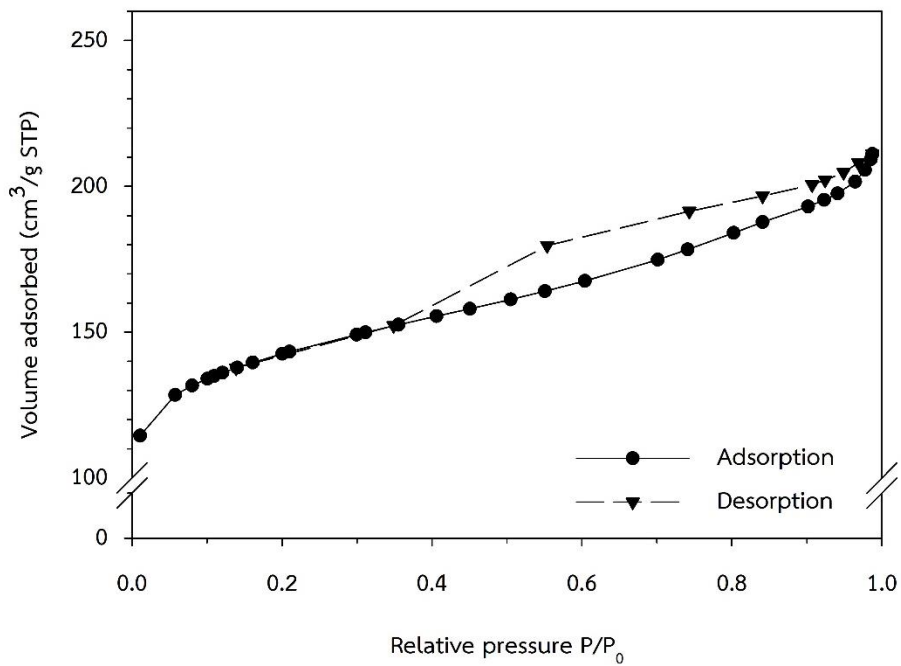


Figure 16 N₂ adsorption-desorption isotherms of 13.5WACG

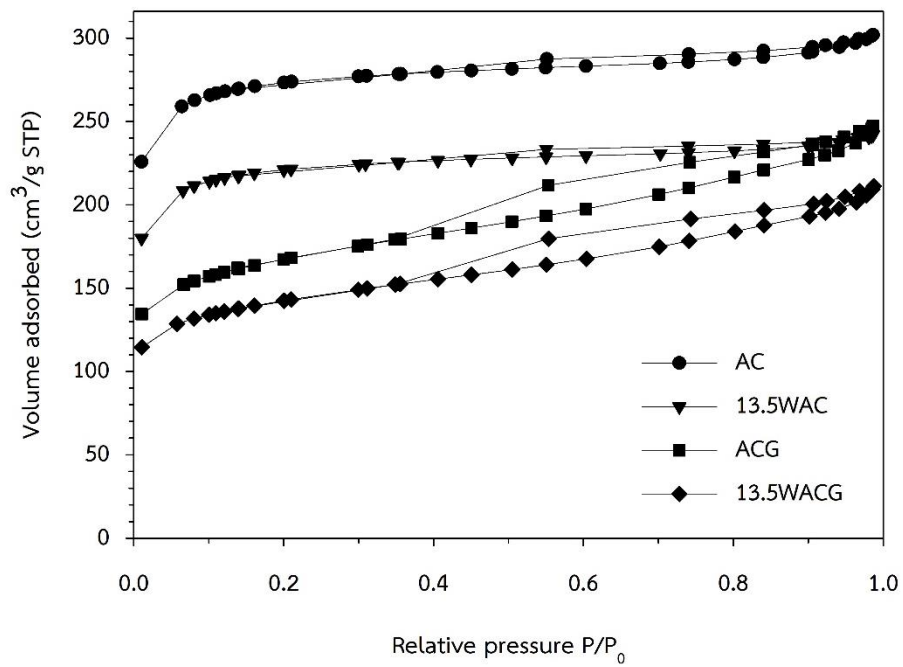


Figure 17 N_2 adsorption-desorption isotherms of AC, 13.5WAC, ACG, and 13.5WACG

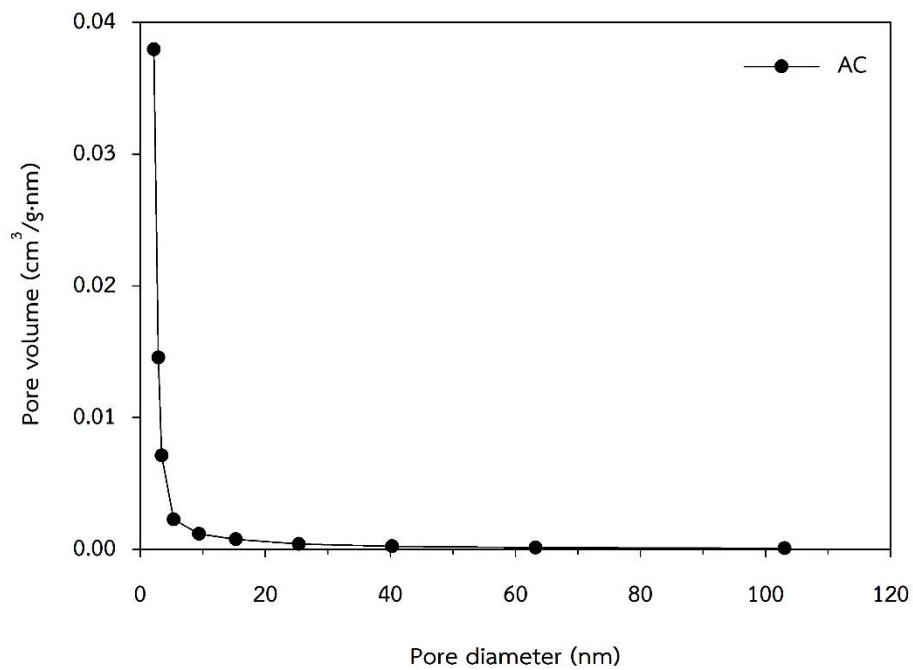


Figure 18 Pore size distribution of AC

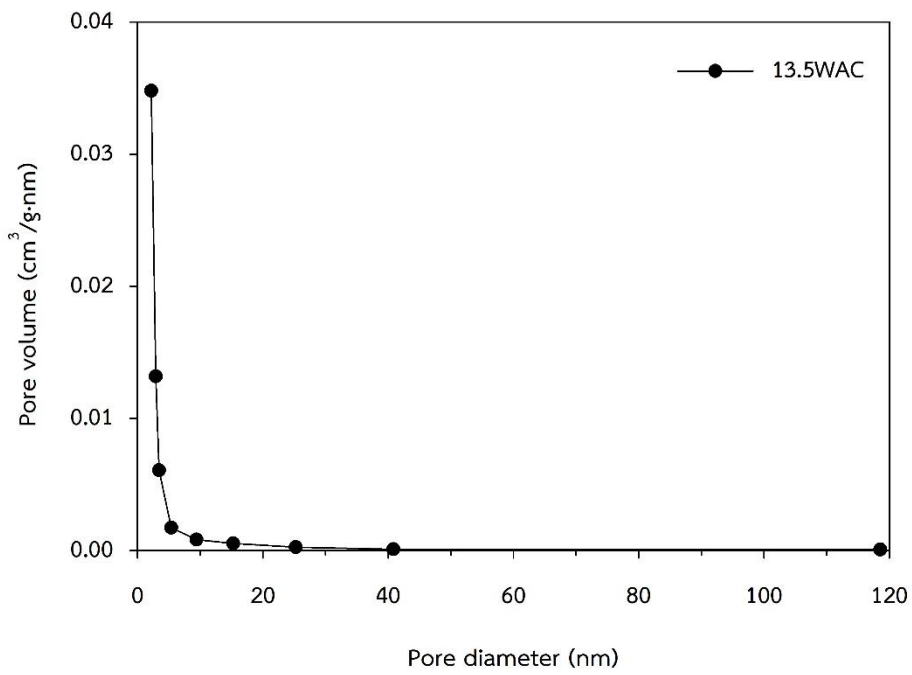


Figure 19 Pore size distribution of 13.5WAC

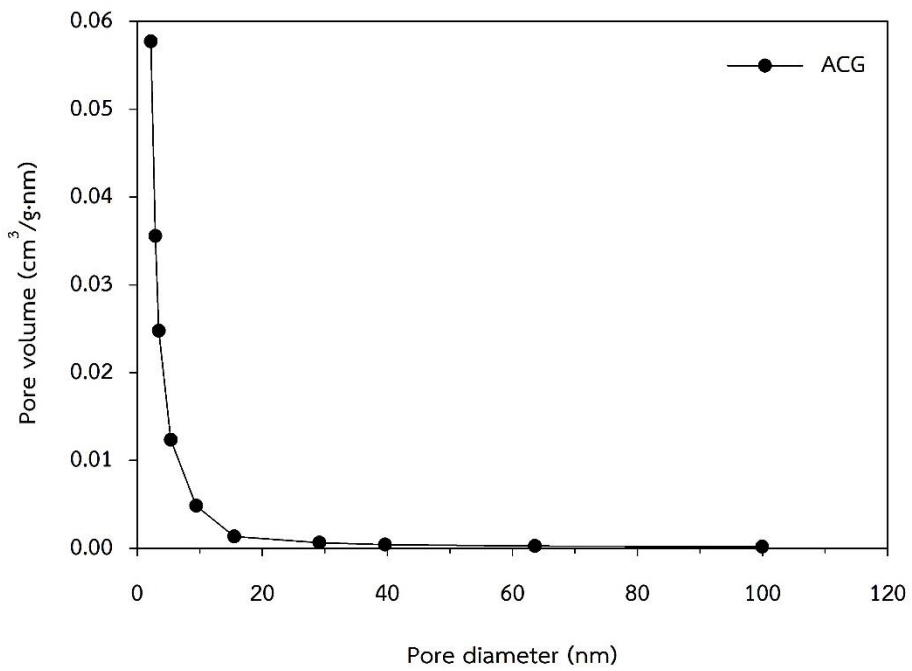


Figure 20 Pore size distribution of ACG

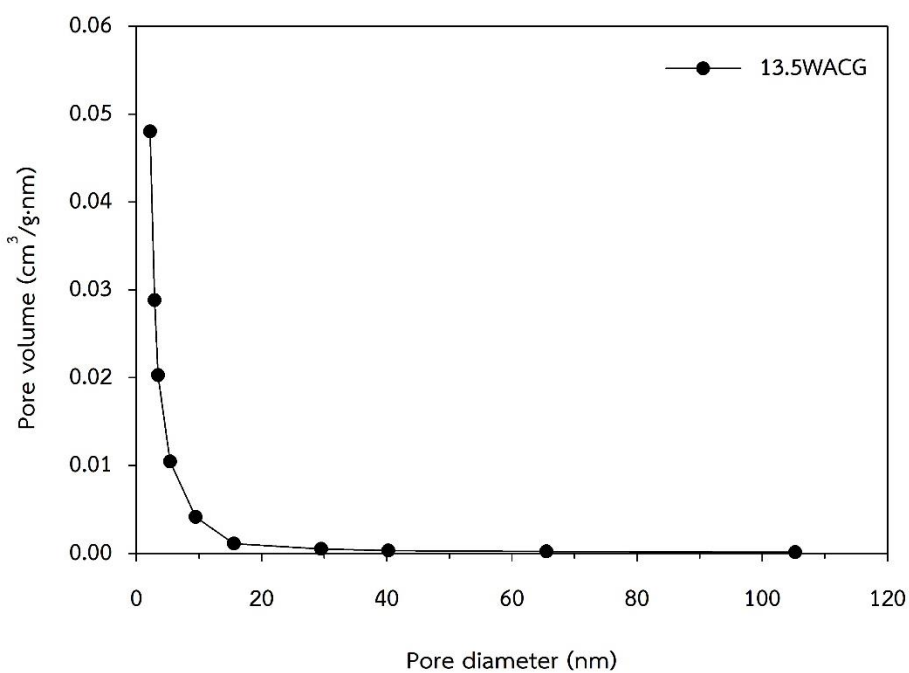


Figure 21 Pore size distribution of 13.5WACG

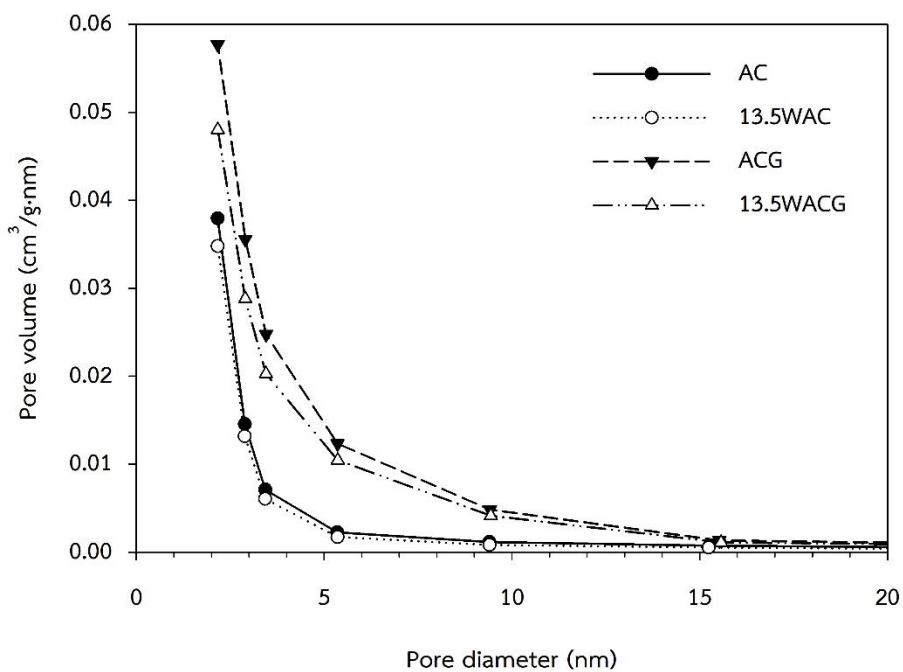


Figure 22 Pore size distribution of AC, 13.5WAC, ACG, and 13.5WACG

4.1.1.4 Ammonia temperature-programmed desorption (NH₃-TPD)

In this study, the strength was classified to 2 tiers including weak strength acid (<200°C), and strong strength acid (>200°C). In **Figures 23 to 26**, considering W loading on activated carbon was most likely to increase weak strength acid and to reduce strong strength acid. After all, NH₃-TPD profile of all catalyst was crucial to analyze. The post process used Fityk program to predict suitable fitting curve. Gaussian distribution was applied to fitting the NH₃-TPD profile. More detail was shown in **appendix A. Table 12** shown properties of all catalysts. Considering low W loading which was decreased the total acidity such as 2WAC. However, additional W loading was increased the total acidity. The increasing total acidity of W loading was 25% from AC to 13.5WAC. Nonetheless, it was increased 149% from ACG to 13.5WACG. This might be involved with high crystalline of WO₃.

Table 12 Properties of various W supported on AC catalysts

catalyst	S ₁ (m ² /g _{cat})	NH ₃ desorption (μmol NH ₃ /g _{cat})		Total acidity (μmol NH ₃ /g _{cat})	Acid density (μmol NH ₃ /m ²)
		Weak	Strong		
AC	984	98	173	271	0.28
2WAC	961	69	138	207	0.22
5WAC	886	97	125	222	0.25
10WAC	796	140	132	272	0.34
13.5WAC	742	202	136	338	0.46
ACG	572*	70	155	224	0.39
13.5WACG	489*	260	329	588	1.20

*Specific surface of ACG and 13.5WACG were from BET

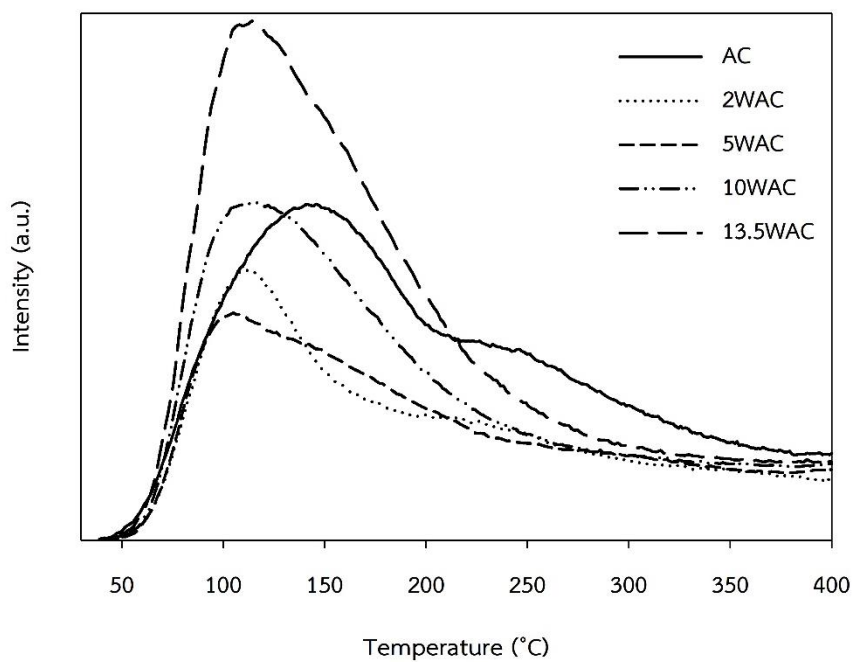


Figure 23 NH₃-TPD profile of various W supported on AC catalysts (TPI)

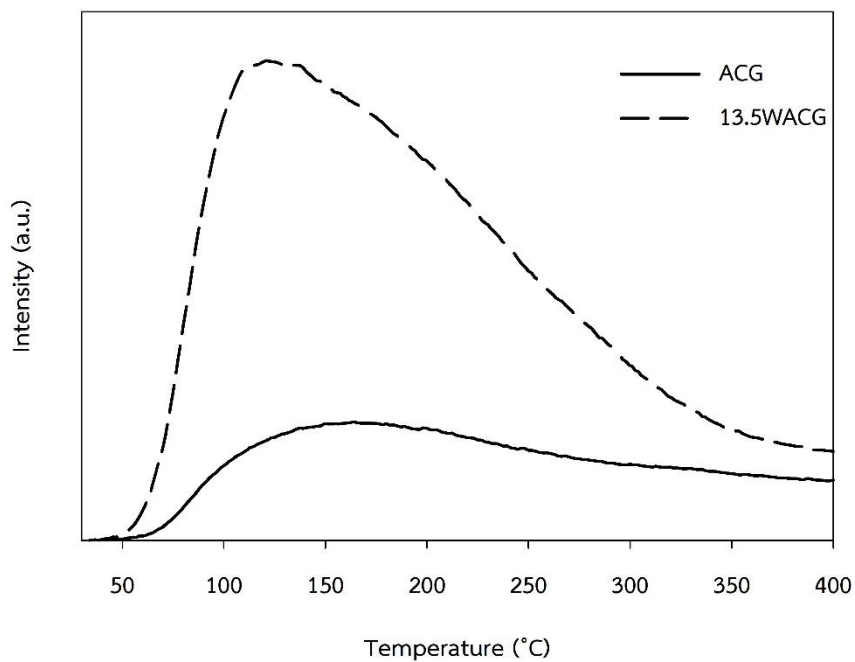


Figure 24 NH₃-TPD profile of ACG and 13.5WACG

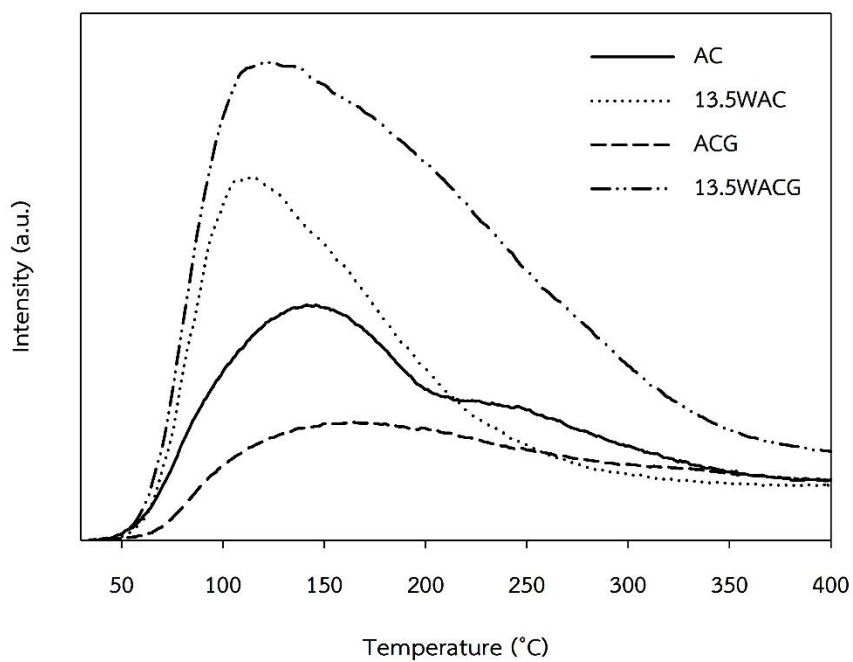


Figure 25 NH₃-TPD profile of W loading on different manufacturer of AC catalyst

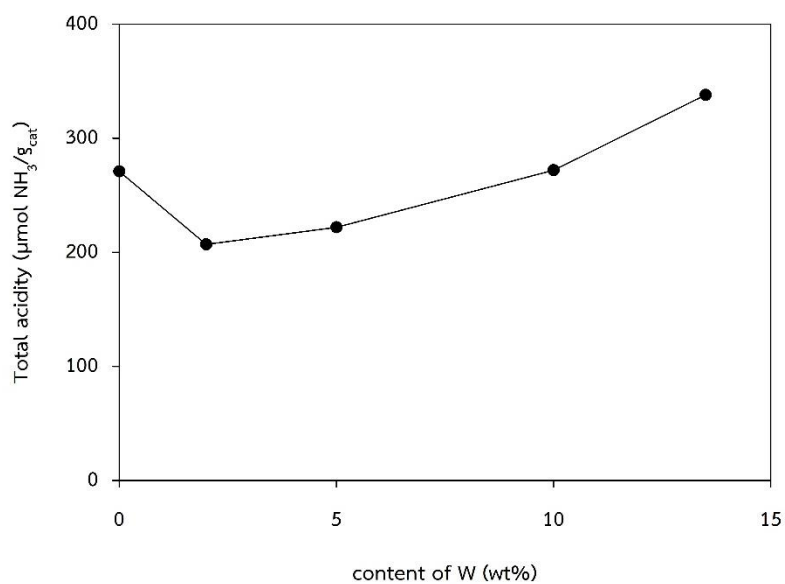


Figure 26 Total acidity of various W supported on AC catalysts (TPI)

4.1.2 Catalytic ethanol dehydration reaction

All catalysts were tested toward ethanol dehydration reaction in gas phase at temperature ranging from 200°C to 400°C and atmospheric pressure. Where W supported on AC catalysts were tested with ethanol flow rate at 0.397 mL/h and 1.45 mL/h (WHSV=3.13 and 11.44 $\text{g}_{\text{ethanol}} \cdot \text{g}_{\text{cat}}^{-1} \cdot \text{h}^{-1}$). The catalytic activity and product distribution for all catalysts were shown in **Figures 27 to 30 and Tables 13 to 16**. Moreover, ethyl acetate was neglected due to rarely occurred.

Considering catalytic ethanol dehydration reaction of W supported on AC catalysts (TPI) with ethanol flow rate at 0.397 mL/h (WHSV=3.13 $\text{g}_{\text{ethanol}} \cdot \text{g}_{\text{cat}}^{-1} \cdot \text{h}^{-1}$). The main product of this condition was acetaldehyde. The yield of acetaldehyde increased with operating temperature, whereas low of W loading can improved its yield such as 2WAC, however, additional W loading decreased yield of acetaldehyde such as 5WAC, 10WAC, and 13.5WAC. The yield of ethylene increased with operating temperature and content of W. However, ethylene did not occur at operating temperature 200°C and 250°C.

Considering catalytic ethanol dehydration reaction of W supported on AC catalysts (Sigma-Aldrich) with ethanol flow rate at 0.397 mL/h (WHSV=3.13 $\text{g}_{\text{ethanol}} \cdot \text{g}_{\text{cat}}^{-1} \cdot \text{h}^{-1}$). Acetaldehyde was the main product of ACG in which ethanol conversion was 50% more than ethanol conversion of AC. Although, W loading can improve ethanol conversion from 30% to 90%. The yield of acetaldehyde was not affected at operating temperature 200°C and 250°C. however, yield of acetaldehyde was decreased at operating temperature 300°C to 400°C. Moreover, yield of diethyl ether and ethylene were increased with W loading. Their turned to main product instead acetaldehyde at low operating temperature and high operating temperature, respectively.

Considering catalytic ethanol dehydration reaction of activated carbon groups catalyst with ethanol flow rate at 1.45 mL/h (WHSV=11.44 $\text{g}_{\text{ethanol}} \cdot \text{g}_{\text{cat}}^{-1} \cdot \text{h}^{-1}$). the catalytic properties were like lower ethanol flow condition. Whereas the highest yield of acetaldehyde was 5WAC instead of 2WAC. Moreover, almost reaction rate of acetaldehyde was lower than ethanol flow condition. Therefore, reaction rate of ethylene was higher, contribute higher ethylene selectivity. The yield to diethyl ether

of 13.5WACG was significant increased and remaining high yield at operating temperature 300°C and 350°C.

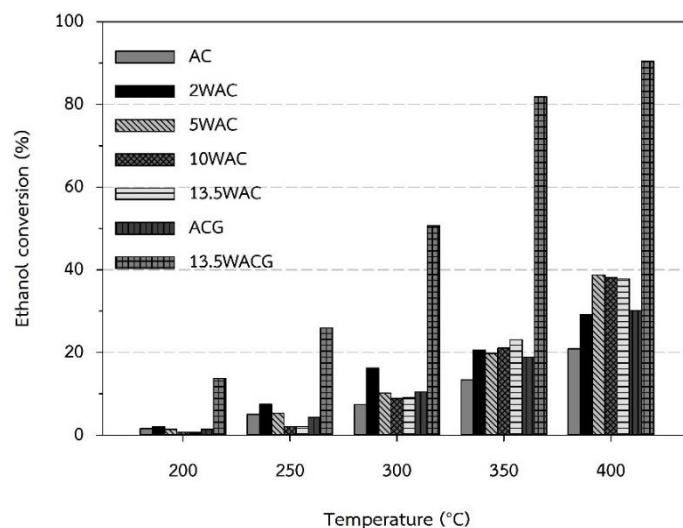


Figure 27 Ethanol conversion of various W supported on AC catalysts for ethanol dehydration at various operating temperature (WHSV=3.13 $\text{g}_{\text{ethanol}} \cdot \text{g}_{\text{cat}}^{-1} \cdot \text{h}^{-1}$)

Table 13 Product distribution of W supported on AC catalysts (Sigma-Aldrich) (WHSV=3.13 $\text{g}_{\text{ethanol}} \cdot \text{g}_{\text{cat}}^{-1} \cdot \text{h}^{-1}$)

Catalyst	Temp. (°C)	Conversion (%)	Selectivity (%)			Yield (%)		
			ET	ACT	DEE	ET	ACT	DEE
ACG	200	1.4		100			1.42	
	250	4.2		100			4.21	
	300	10.5		100			10.50	
	350	18.9	2.5	94.3		0.47	17.80	
	400	30.1	7.4	91.5		2.22	27.54	
13.5WACG	200	13.7	0.8	9.6	89.6	0.11	1.32	6.15
	250	25.9	8.4	16.4	73.2	2.17	4.25	9.47
	300	50.7	38.5	16.7	44.0	19.49	8.44	11.14
	350	81.8	76.7	12.1	10.7	62.81	9.91	4.36
	400	90.5	85.1	11.2	3.4	77.00	10.12	1.55

*ET = Ethylene, ACT = Acetaldehyde, and DEE = diethyl ether

Table 14 Product distribution of W supported on AC catalysts (TPI)(WHSV=3.13 $\text{g}_{\text{ethanol}} \cdot \text{g}_{\text{cat}}^{-1} \cdot \text{h}^{-1}$)

Catalyst	Temp. (°C)	Conversion (%)	Selectivity (%)		Yield (%)	
			ET	ACT	ET	ACT
AC	200	1.6		100		1.58
	250	5.0		100		5.02
	300	7.4		100		7.45
	350	13.4	2.8	97.2	0.38	13.02
	400	20.9	4.4	95.6	0.91	19.94
2WAC	200	2.0		100		2.05
	250	7.5		100		7.50
	300	16.2	1.4	98.6	0.23	16.00
	350	20.5	7.4	91.7	1.51	18.83
	400	29.1	14.6	85.4	4.25	24.87
5WAC	200	1.4		100		1.38
	250	5.0		100		5.00
	300	10.1	3.1	93.8	0.31	9.51
	350	19.7	20.6	77.4	4.08	15.29
	400	38.7	40.6	58.7	15.73	22.75
10WAC	200	0.7		100		0.71
	250	2.1		100		2.10
	300	8.8	8.3	86.8	0.73	7.67
	350	21.0	33.4	63.8	7.02	13.43
	400	38.1	52.5	46.6	19.99	17.76
13.5WAC	200	0.6		100		0.61
	250	2.0		100		2.05
	300	9.1	16.3	80.8	1.49	7.36
	350	23.1	42.6	56.1	9.84	12.94
	400	37.8	59.0	40.1	22.29	15.13

*ET = Ethylene, and ACT = Acetaldehyde

Table 15 Product distribution of W supported on AC catalysts (Sigma-Aldrich)(WHSV=11.44 $\text{g}_{\text{ethanol}} \cdot \text{g}_{\text{cat}}^{-1} \cdot \text{h}^{-1}$)

Catalyst	Temp. (°C)	Conversion (%)	Selectivity (%)			Yield (%)		
			ET	ACT	DEE	ET	ACT	DEE
ACG	200	0.2		100			0.22	
	250	0.5		100			0.51	
	300	0.8	2.4	97.6		0.02	0.82	
	350	1.8	12.0	88.0		0.21	1.56	
	400	4.1	14.4	85.6		0.60	3.54	
13.5WACG	200	0.5	1.5	27.6	70.8	0.01	0.15	0.19
	250	4.6	6.5	5.4	88.2	0.30	0.25	2.03
	300	14.8	22.1	2.7	75.2	3.27	0.39	5.56
	350	25.3	55.7	5.4	38.8	14.06	1.36	4.90
	400	38.3	79.7	11.4	8.6	30.51	4.37	1.66

*ET = Ethylene, ACT = Acetaldehyde, and DEE = diethyl ether

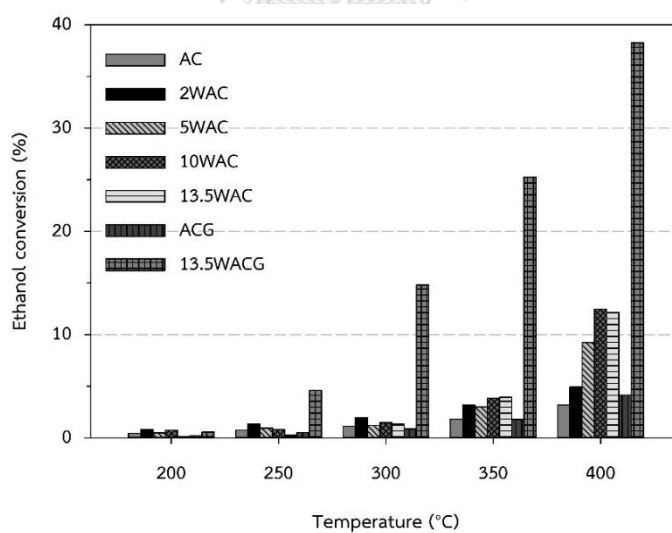
**Figure 28** Ethanol conversion of various W supported on AC catalysts for ethanol dehydration at various operating temperature (WHSV=11.44 $\text{g}_{\text{ethanol}} \cdot \text{g}_{\text{cat}}^{-1} \cdot \text{h}^{-1}$)

Table 16 Product distribution of W supported on AC catalysts (TPI)(WHSV=11.44 g_{ethanol}·g_{cat}⁻¹·h⁻¹)

Catalyst	Temp. (°C)	Conversion (%)	Selectivity (%)			Yield (%)		
			ET	ACT	DEE	ET	ACT	DEE
AC	200	0.5		100			0.45	
	250	0.7		96.0			0.70	
	300	1.1	0.8	92.8		0.01	1.04	
	350	1.8	3.7	89.7		0.07	1.62	
	400	3.2	7.3	88.4		0.23	2.82	
2WAC	200	0.8		97.0			0.76	
	250	1.3		93.2			1.25	
	300	1.9	5.1	90.2		0.10	1.75	
	350	3.2	21.4	76.0		0.68	2.40	
	400	4.9	29.4	68.7		1.44	3.37	
5WAC	200	0.5		96.4			0.47	
	250	0.9		94.6			0.90	
	300	1.2	8.5	87.6		0.10	1.05	
	350	3.0	46.3	52.2		1.38	1.56	
	400	9.2	61.3	38.2		5.65	3.52	
10WAC	200	0.8		97.3			0.74	
	250	0.8		97.5			0.80	
	300	1.5	23.3	73.9		0.34	1.08	
	350	3.8	62.6	36.3		2.39	1.39	
	400	12.5	71.5	28.0		8.92	3.50	
13.5WAC	200	0.1		100			0.13	
	250	0.3	9.3	90.7		0.02	0.23	
	300	1.4	36.0	31.9	31.0	0.49	0.43	0.21
	350	3.9	68.7	24.1	6.6	2.69	0.94	0.13
	400	12.1	79.4	18.7	1.5	9.63	2.27	0.09

*ET = Ethylene, ACT = Acetaldehyde, and DEE = diethyl ether

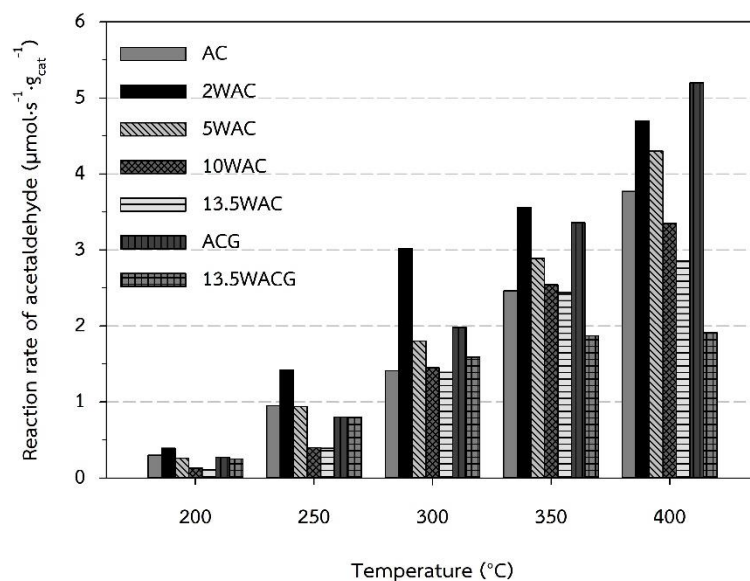


Figure 29 Acetaldehyde reaction rate of various W supported on AC catalysts for ethanol dehydration at various operating temperature (WHSV= $3.13 \text{ g}_{\text{ethanol}}\cdot\text{g}_{\text{cat}}^{-1}\cdot\text{h}^{-1}$)

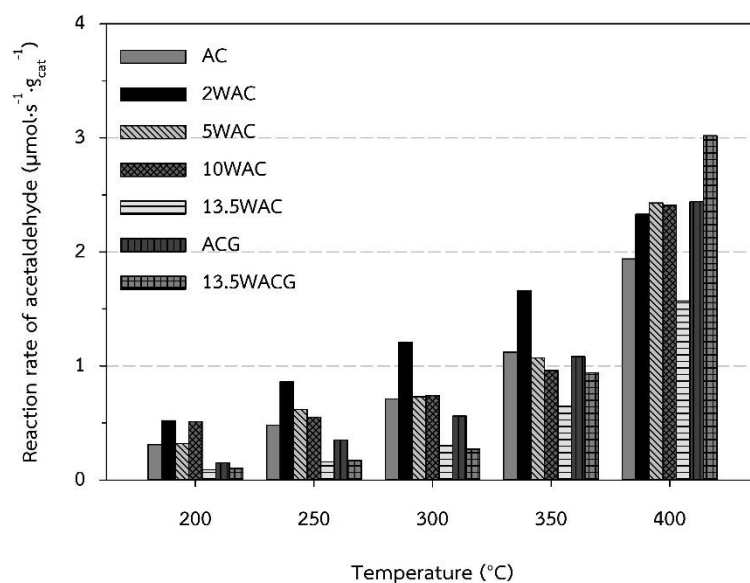


Figure 30 Acetaldehyde reaction rate of various W supported on AC catalysts for ethanol dehydration at various operating temperature (WHSV= $11.44 \text{ g}_{\text{ethanol}}\cdot\text{g}_{\text{cat}}^{-1}\cdot\text{h}^{-1}$)

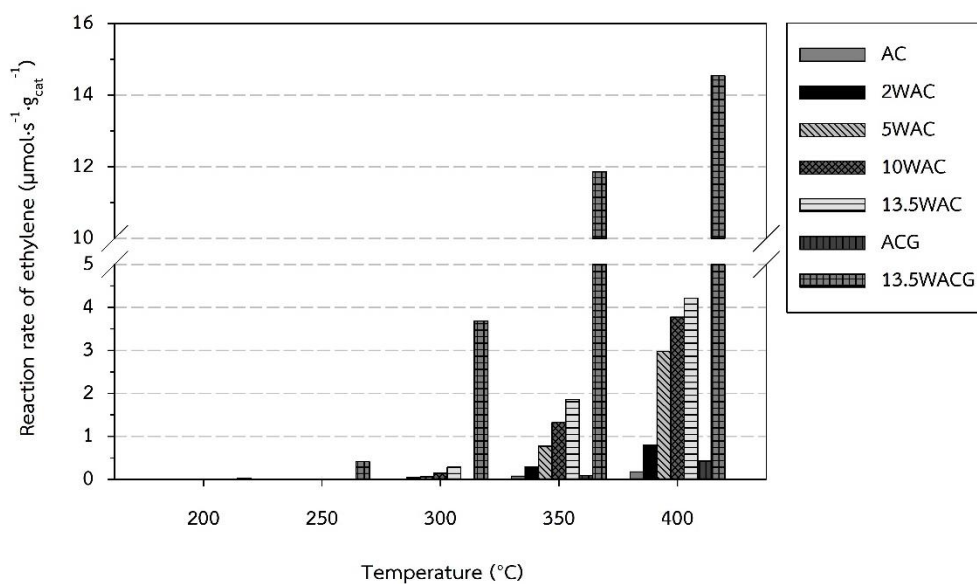


Figure 31 Ethylene reaction rate of various W supported on AC catalysts for ethanol dehydration at various operating temperature ($\text{WHSV}=3.13 \text{ g}_{\text{ethanol}}\cdot\text{g}_{\text{cat}}^{-1}\cdot\text{h}^{-1}$)

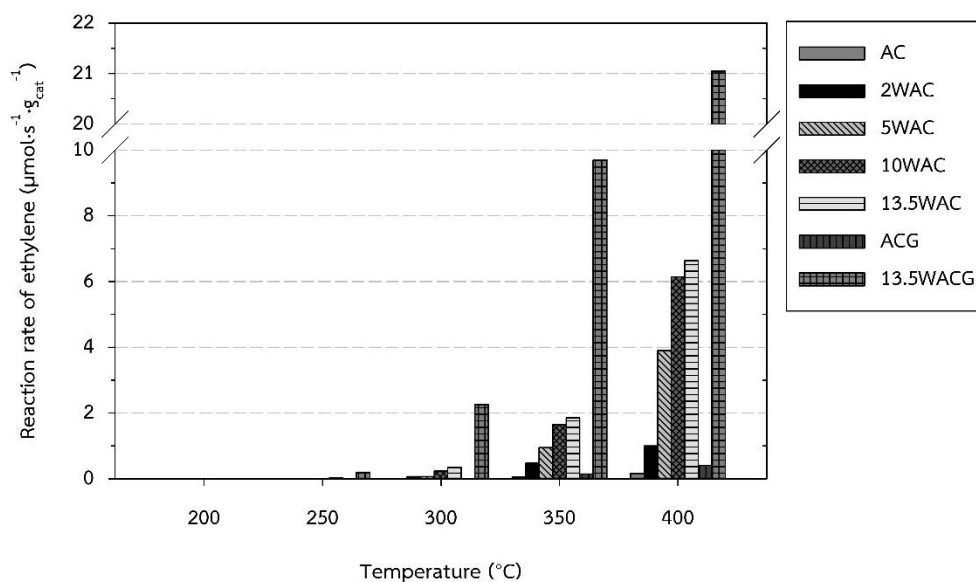


Figure 32 Ethylene reaction rate of various W supported on AC catalysts for ethanol dehydration at various operating temperature ($\text{WHSV}=11.44 \text{ g}_{\text{ethanol}}\cdot\text{g}_{\text{cat}}^{-1}\cdot\text{h}^{-1}$)

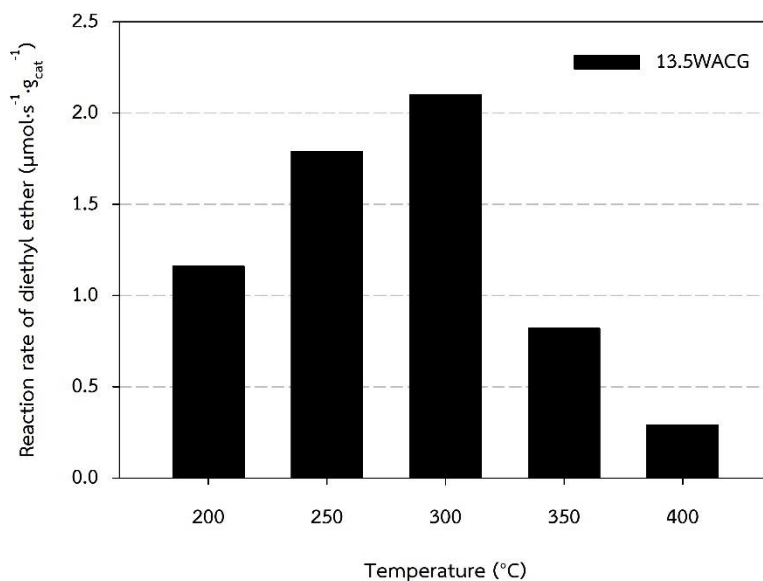


Figure 33 Diethyl ether reaction rate of various W supported on AC catalysts for ethanol dehydration at various operating temperature (WHSV=3.13 $\text{g}_{\text{ethanol}}\cdot\text{g}_{\text{cat}}^{-1}\cdot\text{h}^{-1}$)

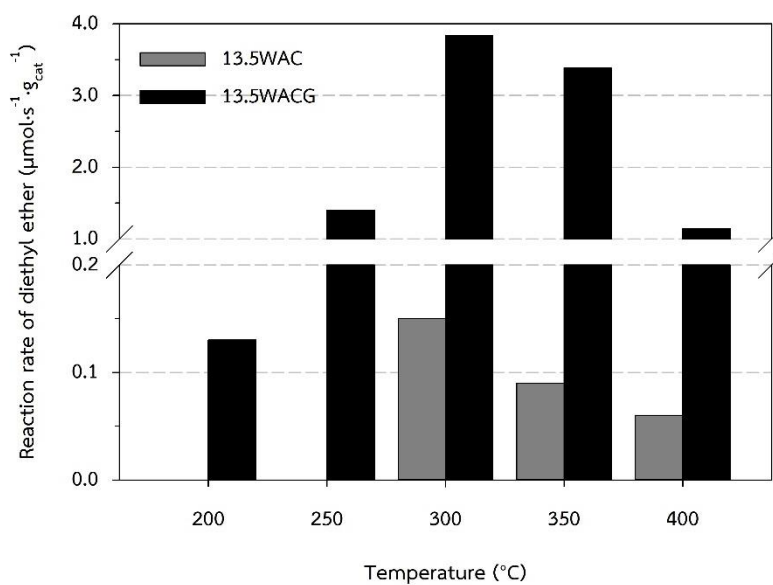


Figure 34 Diethyl ether reaction rate of various W supported on AC catalysts for ethanol dehydration at various operating temperature (WHSV=11.44 $\text{g}_{\text{ethanol}}\cdot\text{g}_{\text{cat}}^{-1}\cdot\text{h}^{-1}$)

4.1.3 Stability test

Considering stability test of catalytic ethanol dehydration reaction. In this study, the AC support catalyst and MMT support catalyst were considered. In ethanol flow rate at 0.375 ml/h condition, 13.5WAC exhibit the highest yield of ethylene at operating temperature 400°C. **Figure 35** shown the ethanol conversion of 13.5WAC decreased from initial conversion to stable around 30%. Whereas AC was stable around 15%. 13.5WAC was also tested under ethanol flow rate at 0.375 ml/h and operating temperature 400°C condition. **Figure 36** shown the ethanol conversion of 13.5WAC decreased from initial conversion to stable around 4%.

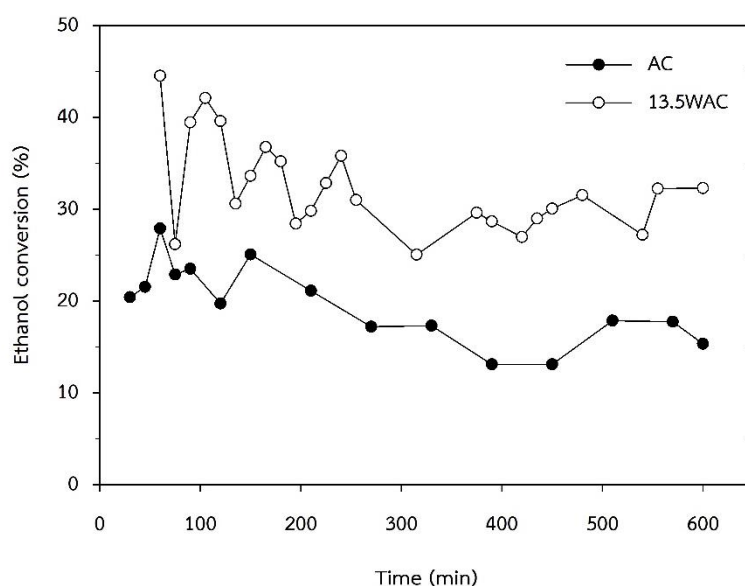


Figure 35 Ethanol conversion of AC and 13.5WAC in stability test of catalytic ethanol dehydration reaction (the reaction condition: $T = 400^{\circ}\text{C}$ and $\text{WHSV} = 3.13 \text{ h}^{-1}$)

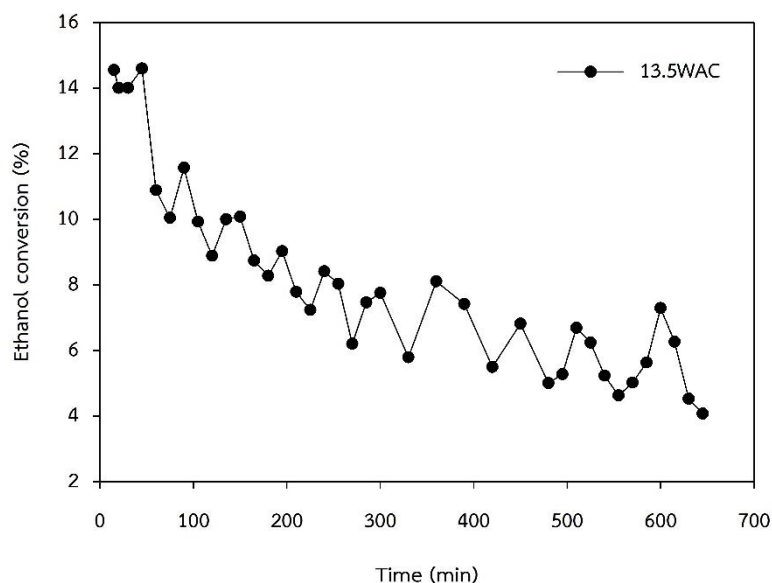


Figure 36 Ethanol conversion of 13.5WAC in stability test of catalytic ethanol dehydration reaction (the reaction condition: $T = 400^{\circ}\text{C}$ and $\text{WHSV} = 11.44 \text{ h}^{-1}$)

4.1.4 Summary

Low tungsten loading over catalyst exhibited isolated monotungstate or oligomeric tungstate [48, 49]. W loading on AC exhibited crystalline phase of WO_3 from XRD pattern. Whereas 5WAC exhibited the lowest crystalline phase of WO_3 . In **Figure 11**, The intensity of NH_3 desorption around 250°C which represent by residual acid function group after pretreated or calcined at 475°C dramatic decreased after W loading. Cause of decreasing of total acidity after low tungsten loading was replacement of some WO_3 over AC catalyst acid site. Considering catalytic ethanol dehydration reaction, low tungsten loading over AC catalyst and low ethanol flow rate enhanced ethanol dehydrogenation to acetaldehyde. The additional W loading enhanced ethanol dehydration to ethylene and diethyl ether. However, source of AC catalyst which W loading was affect to catalytic properties. 13.5ACG was exhibited much higher total acidity than 13.5WAC and it also exhibited higher activity in catalytic ethanol dehydration reaction. the stability tests show the AC catalyst and W loading over catalyst were stability catalysts.

4.2 W supported on MMT catalysts

4.2.1 Catalyst characterization

4.2.1.1 Scanning electron microscope (SEM) and Energy dispersive X-ray spectroscopy (EDX)

The morphologies of W supported on MMT catalysts formed irregular shapes and porous particles as shown in **Figures 37 and 38**. The outer surface of all MMT were rough than ACG and 13.5WACG. The EDX cannot report since characteristic X-ray of Si and W was interception.

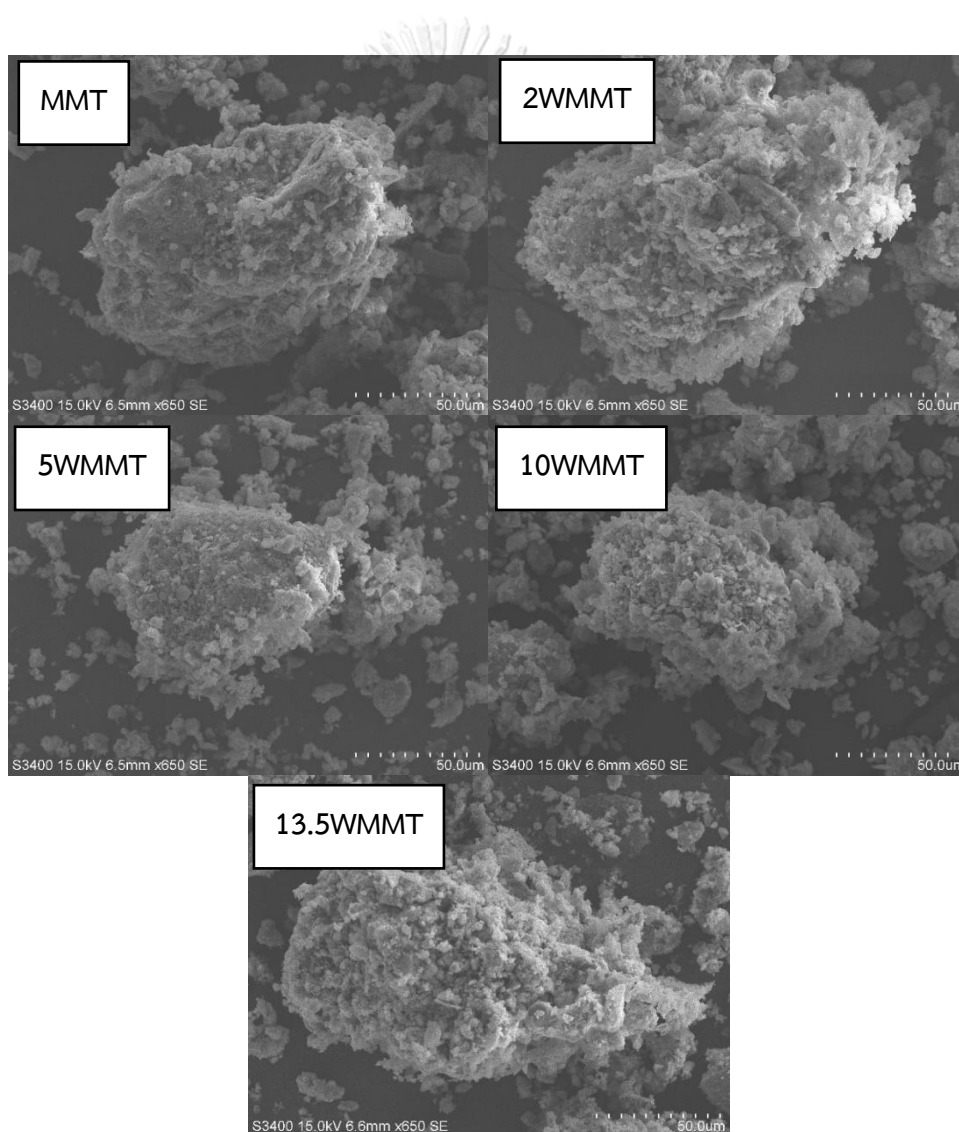


Figure 37 The morphologies of various W supported on MMT catalysts measured by SEM at mag. X650

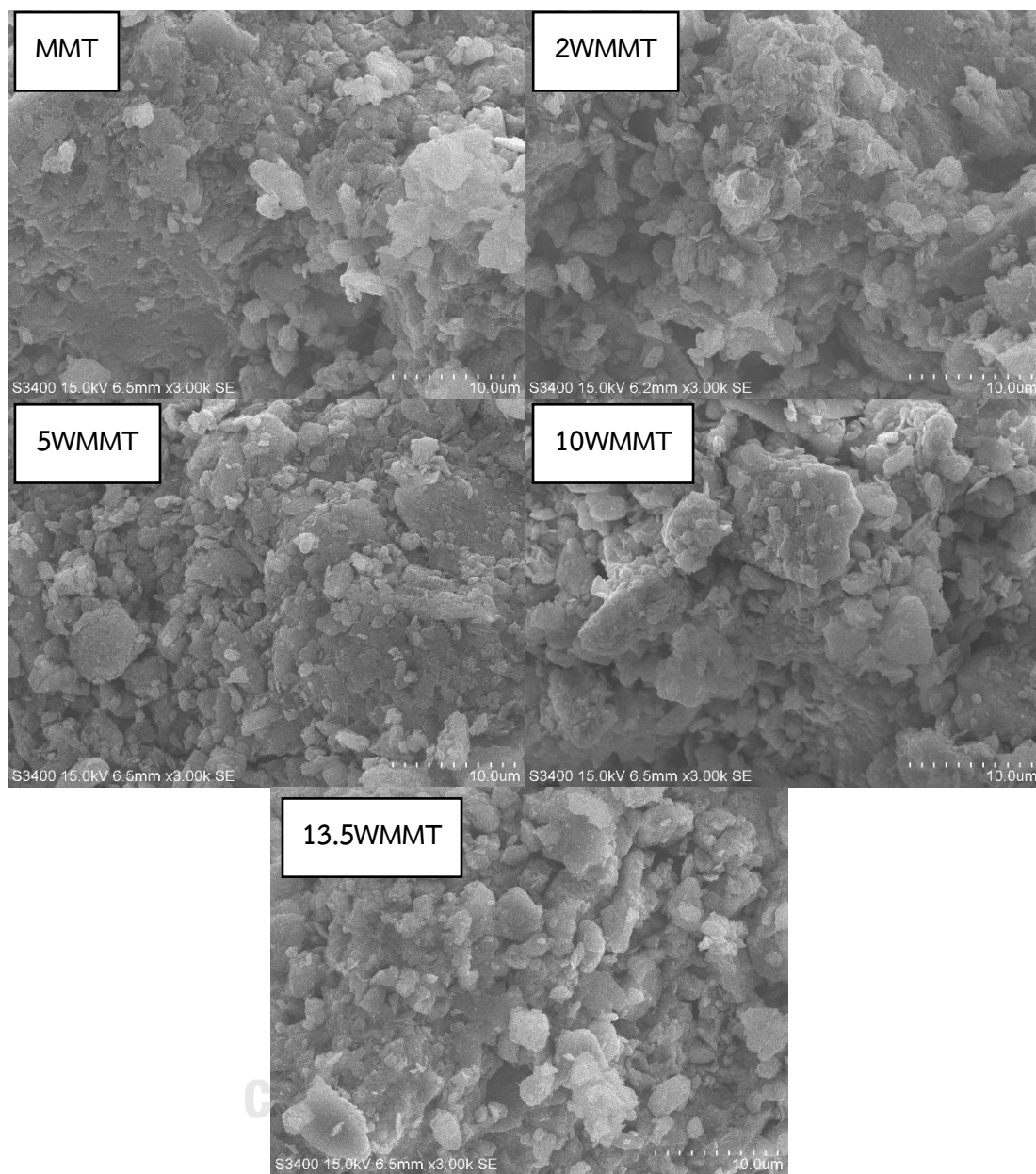


Figure 38 The morphologies of various W supported on MMT catalysts measured by SEM at mag. X3,000

4.2.1.2 X-ray Powder Diffraction (XRD)

In **Figure 39**, Considering the XRD pattern of W supported on MMT catalysts, their XRD pattern were like XRD pattern of MMT. It can refer to high dispersion of WO_3 . However, 10WMMT exhibited low intensive peak located at 2θ degrees of 27.3° which can refer to Hexagonal- WO_3 . Moreover, 13.5WMMT exhibited low intensive peak located at 2θ degrees of 24.2° which can refer to Hexagonal- WO_3 [41, 42, 46].

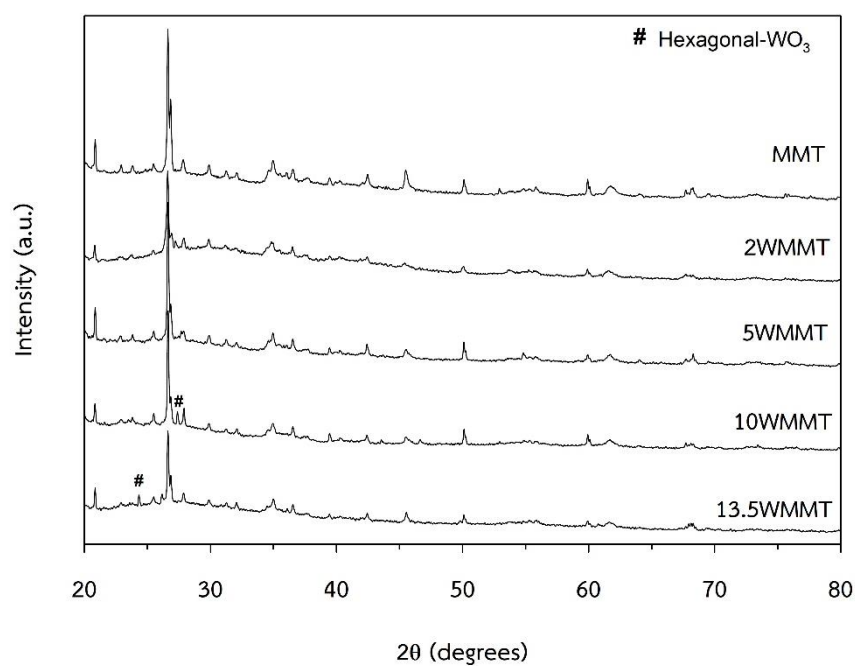


Figure 39 X-ray Powder Diffraction patterns of various W supported on MMT catalysts

4.2.1.3 N₂ physisorption (BET)

Multipoint N₂ physisorption was used to assay specific surface area, specific pore volume, pore diameter, isotherm graph, and pore size distribution of MMT and 13.5WMMT. As shown in **Figures 40 to 45**, the MMT catalyst and modified MMT catalyst exhibited a type IV isotherm with type H3 hysteresis loop according to IUPAC classification[47], and capillary condensation in the pores at relative pressure (P/P₀) close 0.40. They indicated presence of non-rigid aggregates of plate-like particles (slit-shaped pores). Higher pressure hysteresis of MMT indicated higher volume of mesopore. Since the instrument were not conducive to measure particle with micropore, the pore size distribution was started to report with 2 nm, furthermore, the average pore diameter was not calculated with micropore. **Figures 40 to 42 and Table 17** show the pore size distribution of MMT and 13.5WMMT. W loading reduced specific pore volume. However, the negative volume adsorbed was occurred by 13.5WMMT. It indicated negative t-plot micropore or non-micropore particles and it also indicated error on BET result. Nevertheless, single point surface area of multipoint N₂ physisorption closed to surface area of single point N₂ physisorption.

Single point N₂ physisorption was used to assay the specific surface area of W supported on MMT catalysts. **Table 18** shows specific surface areas which were decreased with content of W. After loading W 13.5wt% on support, specific surface area of MMT was decreased 41%.

Table 17 Textural properties of MMT and 13.5WMMT

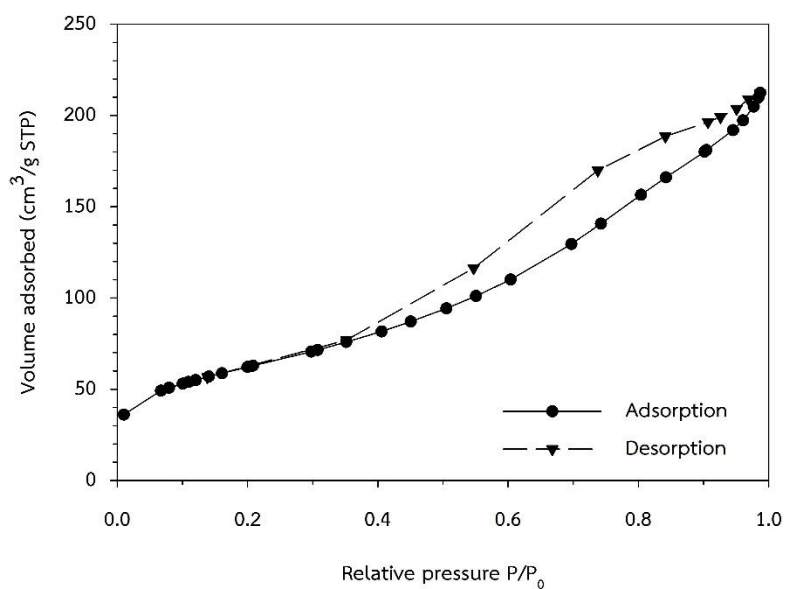
Catalyst	S _{BET} (m ² g ⁻¹)	S _{micropore} (m ² g ⁻¹)	S _{external} (m ² g ⁻¹)	V _M (cm ³ g ⁻¹)	V _T (cm ³ g ⁻¹)	D _p (nm)
MMT	224	17.7	206.3	0.006	0.325	5.38
13.5WMMT	n.a.	0	n.a.	0	0.275	5.46

* S_{BET}= specific surface area by BET, S_{micropore}= t-Plot micropore Area, S_{external}= t-Plot external surface Area V_M= t-Plot micropore volume, V_T= Single point total pore volume of pores, D_p= average pore diameter by BJH (calculated from mesopore) and n.a.= not applicable

Table 18 Specific surface area of various W supported on MMT catalysts

Catalyst	S_1 ($\text{m}^2 \text{g}^{-1}$)
MMT	210
2WMMT	179
5WMMT	154
10WMMT	146
13.5WMMT	124

* S_1 =specific surface area by single point N_2 physisorption

**Figure 40** N_2 adsorption-desorption isotherms of MMT

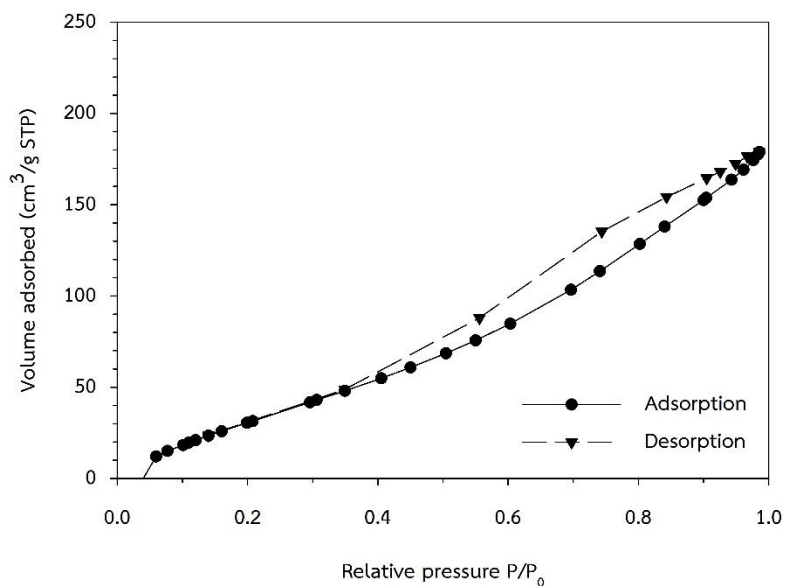


Figure 41 N₂ adsorption-desorption isotherms of 13.5WMMT

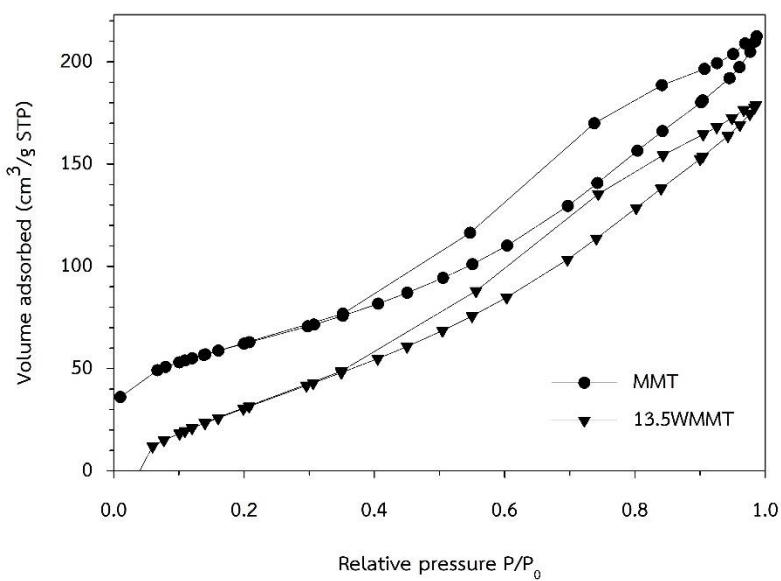


Figure 42 N₂ adsorption-desorption isotherms of MMT and 13.5WMMT

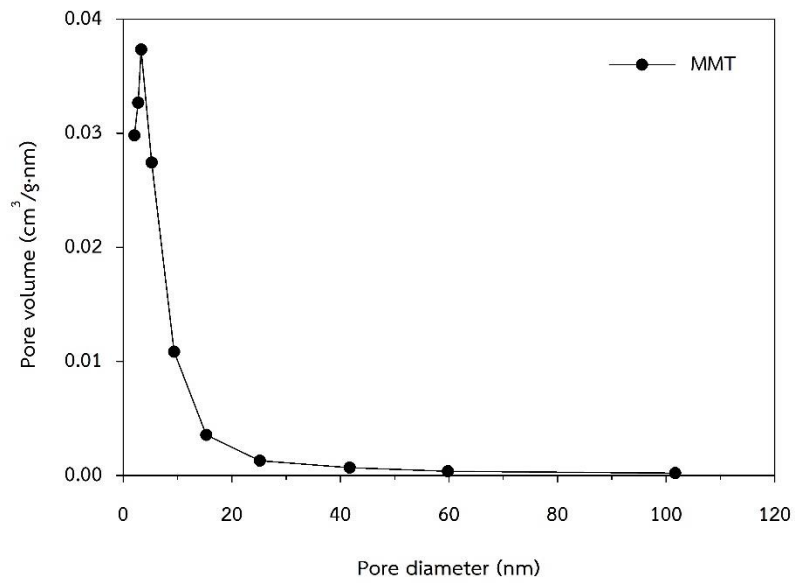


Figure 43 Pore size distribution of MMT

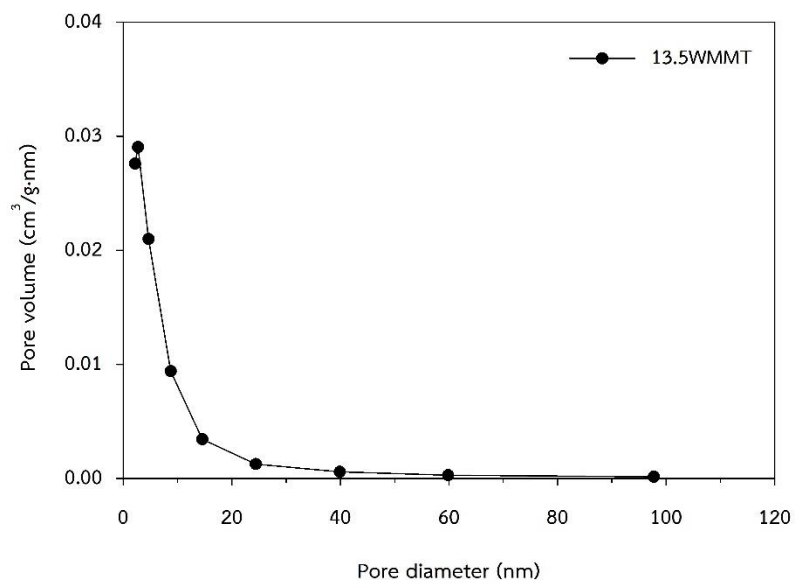


Figure 44 Pore size distribution of 13.5WMMT

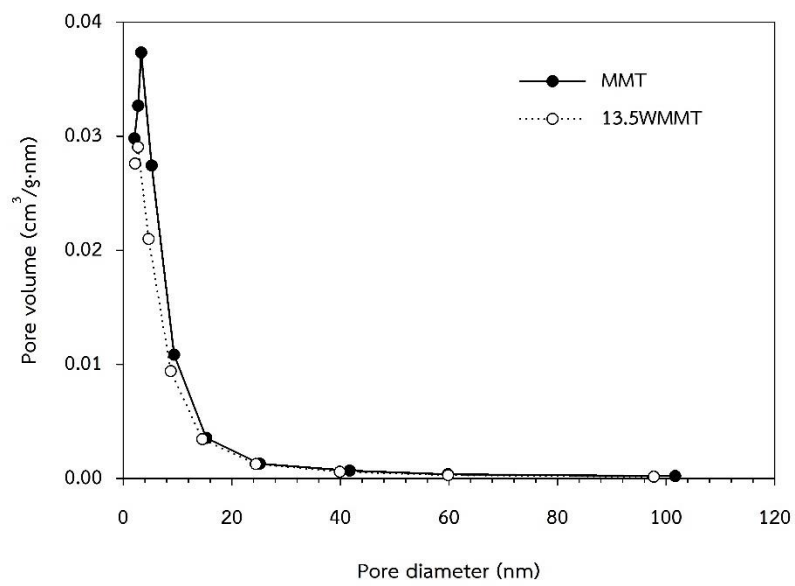


Figure 45 Pore size distribution of MMT and 13.5WMMT



4.2.1.4 Ammonia temperature-programmed desorption (NH₃-TPD)

In this study, the strength was classified to 2 tiers including weak strength acid (<200°C), and strong strength acid (>200°C). In **Figures 46 and 47**, considering W loading on MMT reduced weak strength acid and increased strong strength acid. After all, NH₃-TPD profile of all catalyst was crucial to analyze. The post process used Fityk program to predict suitable fitting curve. Gaussian distribution was applied to fitting the NH₃-TPD profile. More detail was shown in **appendix A. Table 19** shown properties of all catalysts. Considering low W loading which was decreased the total acidity such as 2WAC and 2WMMT. However, more W loading was increased the total acidity. The increasing total acidity of W loading was 7% from MMT to 13.5WMMT

Table 19 Properties of various W supported on MMT catalysts

catalyst	S ₁ (m ² /g _{cat})	NH ₃ desorption (μmol NH ₃ /g _{cat})		Total acidity (μmol NH ₃ /g _{cat})	Acid density (μmol NH ₃ /m ²)
		Weak	Strong		
MMT	210	334	324	658	3.13
2WMMT	179	310	268	578	3.23
5WMMT	154	350	257	607	3.94
10WMMT	146	330	346	677	4.65
13.5WMMT	124	260	442	703	5.66

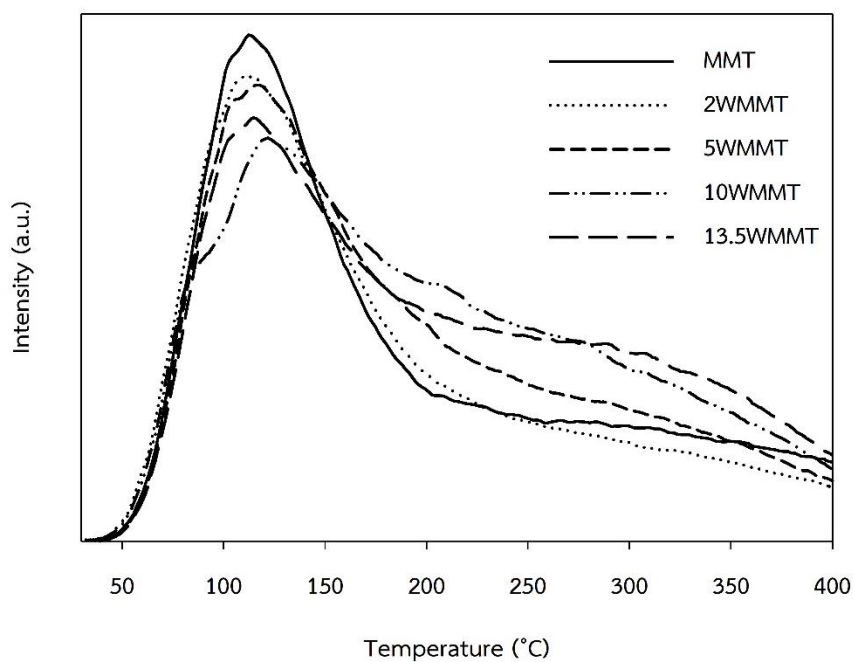


Figure 46 NH₃-TPD profile of various W supported on MMT catalysts

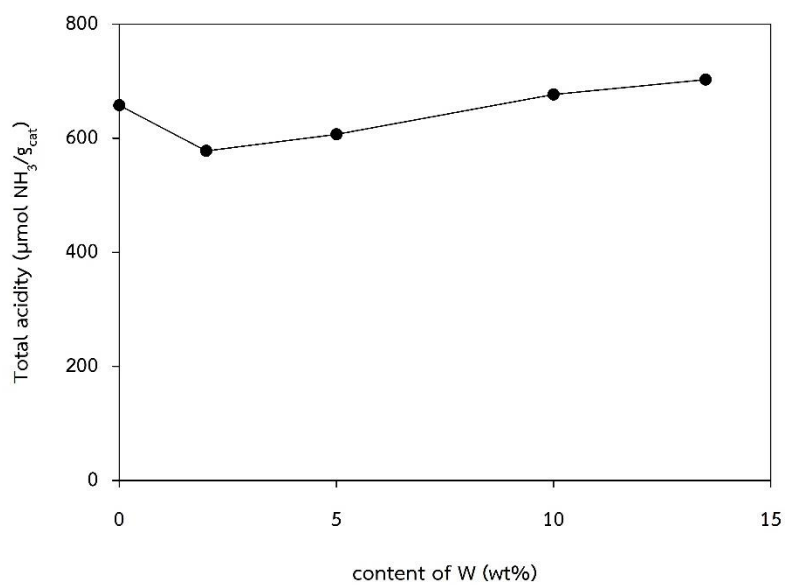


Figure 47 Total acidity of various W supported on MMT catalysts

4.2.2 Catalytic ethanol dehydration reaction

All catalysts were tested toward ethanol dehydration reaction in gas phase at temperature ranging from 200°C to 400°C and atmospheric pressure. Where W supported on MMT catalysts were tested with ethanol flow rate at 1.45 ml/h (WHSV=11.44 $\text{g}_{\text{ethanol}} \cdot \text{g}_{\text{cat}}^{-1} \cdot \text{h}^{-1}$). The catalytic activity and product distribution for all catalysts were shown in **Figures 48 to 51 and Table 20**.

Considering catalytic ethanol dehydration reaction of montmorillonite groups catalyst with ethanol flow rate at 1.45 ml/h. The almost acetaldehyde reaction rate of MMT groups were lower than activated carbon groups. Moreover, acetaldehyde reaction rate cloud does not compare with reaction rate of ethylene and diethyl ether at higher operating temperature than 200°C. the reaction rate of ethylene increased with operating temperature and content of W. The yield of ethylene was reach to 92.88% by 13.5WMMT at operating temperature 400°C. However, the reaction rate of diethyl ether increased with operating temperature, but it also decreased with additional operating temperature. The yield of diethyl ether was reach to 21.3% by 13.5WMMT at operating temperature 250°C. The reaction rate and yield of ethylene and diethyl ether of 2WMMT were lower than MMT. This can refer to its lower total acidity.

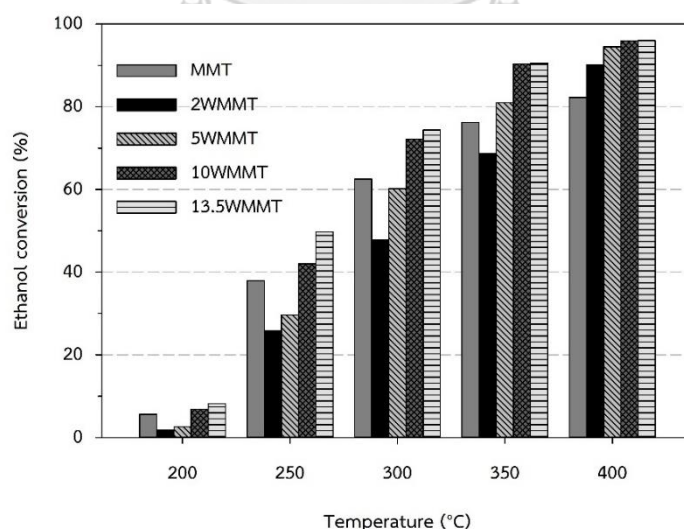


Figure 48 Ethanol conversion of various W supported on MMT catalysts for ethanol dehydration at various operating temperature (WHSV=11.44 $\text{g}_{\text{ethanol}} \cdot \text{g}_{\text{cat}}^{-1} \cdot \text{h}^{-1}$)

Table 20 Product distribution of W supported on MMT catalysts

Catalyst	Temp. (°C)	Conversion (%)	Selectivity (%)			Yield (%)		
			ET	ACT	DEE	ET	ACT	DEE
MMT	200	5.6	6.5	1.8	91.7	0.37	0.10	2.57
	250	37.9	14.2	0.6	85.2	5.39	0.21	16.16
	300	62.5	42.8	0.8	56.3	26.78	0.53	17.60
	350	76.2	74.6	1.1	24.3	56.81	0.85	9.27
	400	82.3	79.7	1.5	18.8	65.55	1.21	7.75
2WMMT	200	1.8	3.8	19.8	76.4	0.07	0.35	0.67
	250	25.8	4.5	2.2	93.1	1.17	0.57	12.02
	300	47.9	23.2	2.1	74.6	11.09	1.01	17.86
	350	68.6	57.7	2.4	40.0	39.59	1.62	13.72
	400	90.2	88.7	1.3	10.0	79.96	1.21	4.51
5WMMT	200	2.6	3.6	10.6	85.7	0.10	0.28	1.13
	250	29.6	6.3	2.8	90.9	1.86	0.84	13.47
	300	60.2	29.1	3.1	67.7	17.52	1.89	20.36
	350	81.0	71.1	1.2	27.7	57.59	0.93	11.22
	400	94.5	94.3	1.0	4.7	89.14	0.92	2.22
10WMMT	200	6.8	5.3	0.7	94.0	0.36	0.05	3.21
	250	42.0	13.2	0.3	86.5	5.54	0.13	18.15
	300	72.2	41.5	0.3	58.2	29.98	0.21	21.01
	350	90.4	87.2	0.5	12.2	78.85	0.49	5.53
	400	96.0	96.7	0.8	2.6	92.75	0.75	1.23
13.5WMMT	200	8.2	4.1	1.2	94.6	0.34	0.10	3.87
	250	49.8	14.0	0.4	85.6	6.98	0.19	21.30
	300	74.4	44.2	0.8	55.0	32.89	0.60	20.44
	350	90.5	88.3	0.5	11.2	79.91	0.46	5.06
	400	96.0	96.7	0.9	2.4	92.88	0.86	1.14

*ET = Ethylene, ACT = Acetaldehyde, and DEE = diethyl ether

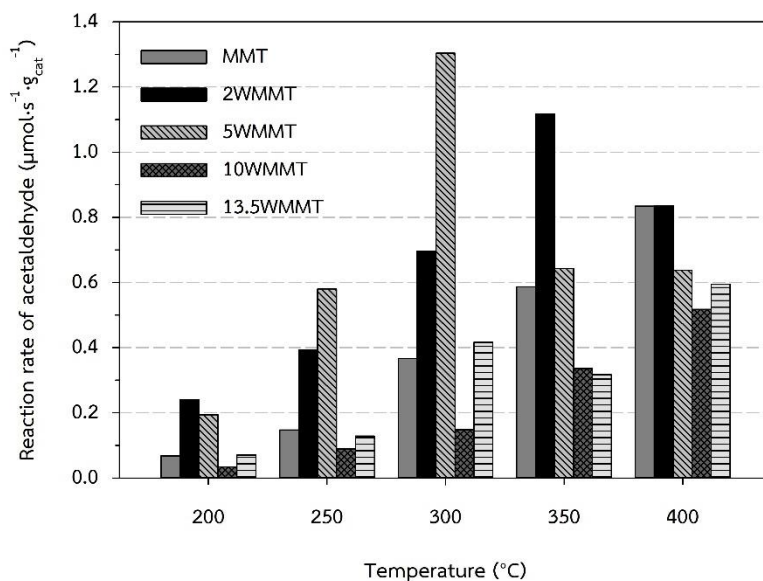


Figure 49 Acetaldehyde reaction rate of various W supported on MMT catalysts for ethanol dehydration at various operating temperature (WHSV=11.44 $\text{g}_{\text{ethanol}} \cdot \text{g}_{\text{cat}}^{-1} \cdot \text{h}^{-1}$)

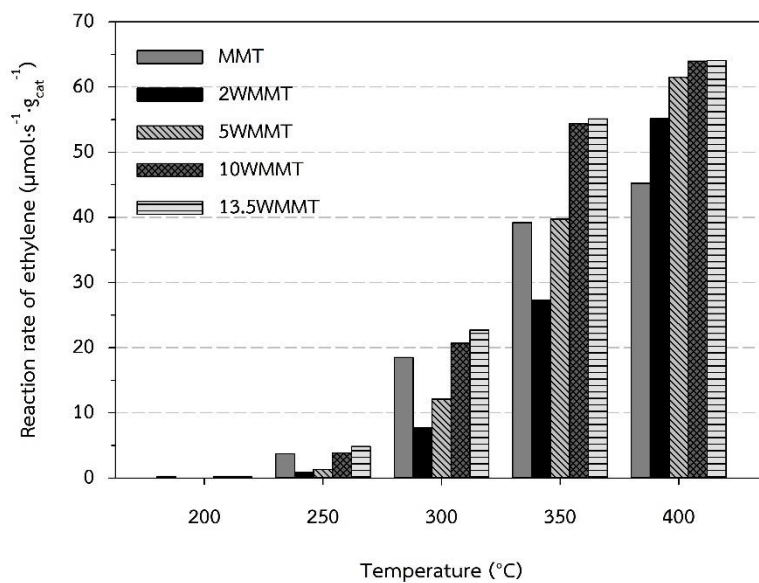


Figure 50 Ethylene reaction rate of various W supported on MMT catalysts for ethanol dehydration at various operating temperature (WHSV=11.44 $\text{g}_{\text{ethanol}} \cdot \text{g}_{\text{cat}}^{-1} \cdot \text{h}^{-1}$)

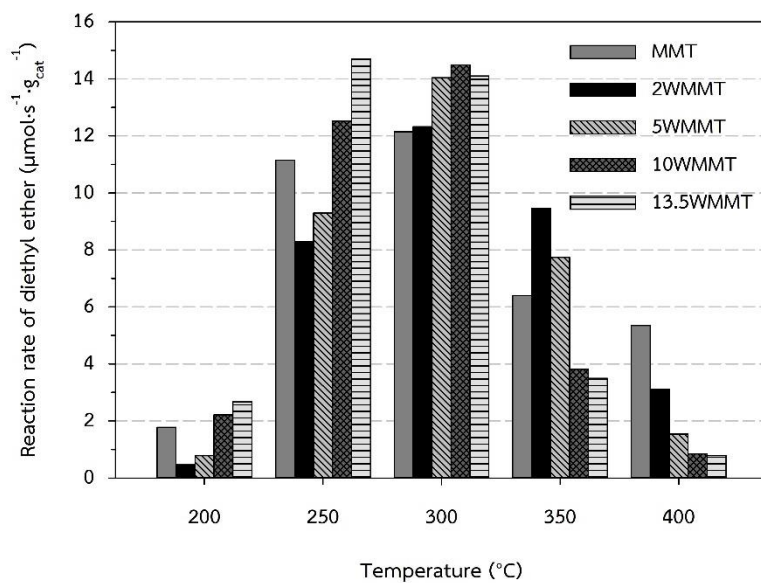
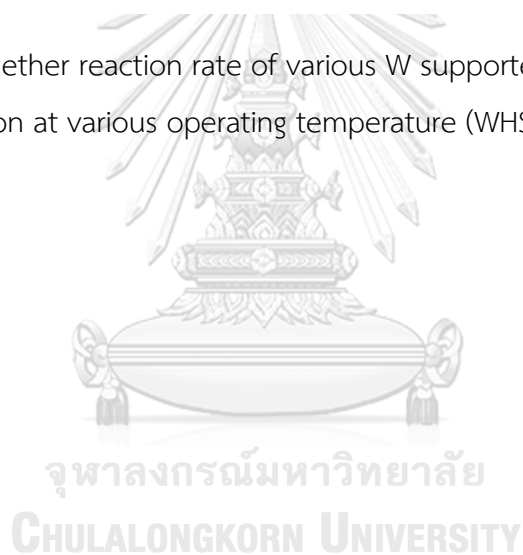


Figure 51 Diethyl ether reaction rate of various W supported on MMT catalysts for ethanol dehydration at various operating temperature (WHSV=11.44 $\text{g}_{\text{ethanol}} \cdot \text{g}_{\text{cat}}^{-1} \cdot \text{h}^{-1}$)



4.1.3 Stability test

Considering 13.5WMMT which exhibited the highest yield of ethylene at operating temperature 400°C and exhibited the highest yield of diethyl ether at operating temperature 250°C. **Figure 52** shows the ethanol conversion of 13.5WMMT was continuous decrease from initial conversion. After 10h of tested, ethanol conversion of 13.5WMMT did not reach the stable conversion. However, under operating temperature 250°C can assumed the stable ethanol conversion at 40%

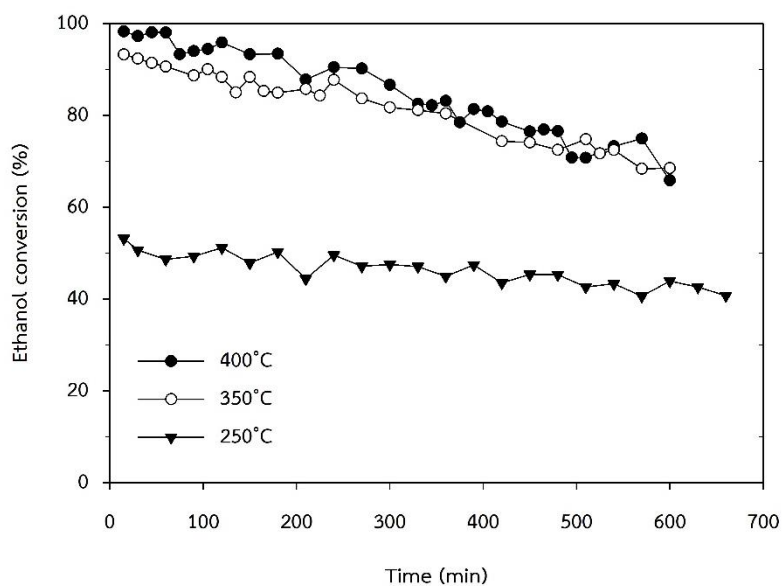


Figure 52 Ethanol conversion of 13.5WMMT in stability test of catalytic ethanol dehydration reaction with various operating temperature (the reaction condition: $WHSV = 11.44 \text{ g}_{\text{ethanol}} \cdot \text{g}_{\text{cat}}^{-1} \cdot \text{h}^{-1}$)

4.2.4 Summary

Low tungsten loading over catalyst exhibited isolated monotungstate or oligomeric tungstate[48, 49], whereas 10wt% and 13.5wt% of W loading on MMT catalyst exhibited crystalline phase of tungsten from XRD pattern in **Figure 39**. Cause of decreasing of total acidity after low tungsten loading was replacement of some WO_3 over MMT catalyst acid site. Considering catalytic ethanol dehydration reaction, low tungsten loading over MMT catalyst and low operating temperature enhanced ethanol dehydrogenation to acetaldehyde. The additional W loading enhanced ethanol dehydration to ethylene and diethyl ether. The stability tests for 10 h show that the 13.5WMMT catalyst was stable at operating temperature of 250°C.

4.3 Comparison and discussion of W supported on AC catalysts and W supported on MMT catalysts

The catalytic activity of both catalysts apparently depended on their morphology and acidity. The MMT catalyst with mesoporous structure exhibits higher mass diffusion than the AC catalyst having the microporous structure. Thus, the poor mass diffusion affected to limitation of reaction rate, but this will result in increased contact time between reactant and active site. For AC catalyst with low ethanol flow rate, this condition also increased contact time. Thus, high contact time was usually increased possibility of acetaldehyde and ethyl acetate formation. However, low contact time was increased possibility of ethylene formation. Considering W supported on AC catalyst, W was filled or block in micropore which less efficiency than other position. Due to AC catalyst and MMT catalyst had high surface area compare to other catalysts, the form of WO_3 was isolated as monotungstate and oligomeric tungstate. The effect of interaction of W cation and support was occurred which reduced or increased WO_3 particle acidity properties[50]. Nevertheless, addition content of W increased number of WO_3 , which resulted in increased total acidity. Finally, acidity of WO_3 with high crystalline was not affect by interaction of support. The total acidity and NH_3 -TPD pattern were major exhibited by crystalline WO_3 domain such as 13.5WACG.

The MMT catalyst exhibited higher activity in catalytic ethanol dehydration reaction than AC catalyst. Low W loading could enhance ethanol dehydrogenation, but high W loading could enhance ethanol dehydration. However, AC catalyst performed high acetaldehyde selectivity. Moreover, low ethanol flow rate apparently enhanced reaction rate of acetaldehyde. Nevertheless, MMT catalyst performed high diethyl ether selectivity at low temperature and high ethylene selectivity at high temperature. Additionally, it performed low acetaldehyde yield selectivity. Although, 13.5WACG performed high activity in dehydration, but it was still low compared with MMT catalyst. After all, ACG was suitable to produce acetaldehyde under low ethanol flow rate at 400°C due to its high reaction rate. Furthermore, 2WAC was also suitable like ACG and predictive catalytic properties of 2WACG might be more suitable than ACG due to higher reaction rate. From stability result, 13.5WMMT was suitable to produce diethyl ether at operating temperature of 250°C due to high yield and high stability. However, 13.5WMMT can be operated at temperature of 350°C and 400°C, which was suitable to produce ethylene.

CHAPTER 5

CONCLUSION AND RECOMMENDATIONS

In this study, characteristics and catalytic performance of various catalysts including W supported on AC catalysts and W supported on MMT catalysts for ethanol dehydration were investigated. This chapter summarized the results for all studies in section 5.1 and recommendations about this research in section 5.2.

5.1 Conclusions

The various W loading (2 to 13.5wt%) on AC catalysts and MMT catalyst did not affect to their morphology, as shown in SEM. From EDX result, the O/W on outer surface of 13.5WACG was closely to O/W of WO_3 . This could refer to WO_3 was completely replacement over AC catalyst acid site. Moreover, the W/C of 13.5WACG was higher than 13.5WAC. This could refer to higher W content on external surface area. The XRD pattern of all catalysts showed low crystalline of WO_3 . This could refer to well dispersed form either an amorphous phase or microcrystals. However, 13.5WACG exhibited high crystalline phase of monoclinic- WO_3 . The low crystalline of WO_3 could refer by isolated monotungstate and some oligomeric tungstate which exhibited major in Lewis acid character but high crystalline of WO_3 could refer by oligomeric tungstate and bulk WO_3 which exhibited major in Brønsted acid character. In previous work [1], the surface acidity of tungsten oxide particles was depending on the nature of the support. In general, characteristics of surface acidity of metal oxide depend on species of support[2]. The decreasing of total acidity at low W loading could be explained by many theories. The interesting theories were replacement of WO_3 over support domain[3] and local coordinative unsaturation of the doping agent metal cations due to specific interactions between the cations and the support[2].

The ethanol conversion of W supported on AC catalysts was contributed of acetaldehyde reaction rate and ethylene reaction rate. Reaction rate of ethylene was increased with operating temperature and content of W. In whatever way, ethylene did not occur at low operating temperature (200°C and almost at 250°C). However, at low operating temperature, low W loading increased reaction rate of

acetaldehyde. Although, the increased ethanol flow rate decreased reaction rate of acetaldehyde and increased reaction rate of ethylene. Moreover, diethyl ether was occurred after 13.5wt% of W loading (13.5WAC at high ethanol flow rate and 13.5WACG both ethanol flow rate). Reaction rate of diethyl ether was increased with temperature until 300°C. The highest reaction rate of acetaldehyde in AC catalysts was occurred by ACG which reached $5.20 \mu\text{mol}\cdot\text{s}^{-1}\cdot\text{g}_{\text{cat}}^{-1}$ (for AC groups was 2WAC = $4.70 \mu\text{mol}\cdot\text{s}^{-1}\cdot\text{g}_{\text{cat}}^{-1}$) under conditions: $\text{WHSV} = 3.13 \text{ g}_{\text{ethanol}}\cdot\text{g}_{\text{cat}}^{-1}\cdot\text{h}^{-1}$ and operating temperature of 400°C. The highest reaction rate of ethylene in AC catalysts was occurred by 13.5WACG which reached $21.05 \mu\text{mol}\cdot\text{s}^{-1}\cdot\text{g}_{\text{cat}}^{-1}$ (for AC groups was 13.5WAC = $6.64 \mu\text{mol}\cdot\text{s}^{-1}\cdot\text{g}_{\text{cat}}^{-1}$) under conditions: $\text{WHSV} = 11.44 \text{ g}_{\text{ethanol}}\cdot\text{g}_{\text{cat}}^{-1}\cdot\text{h}^{-1}$ and operating temperature of 400°C. Diethyl ether was rarely occurred by AC groups, but 13.5WACG performed the highest diethyl ether rate at $3.84 \mu\text{mol}\cdot\text{s}^{-1}\cdot\text{g}_{\text{cat}}^{-1}$ under conditions: $\text{WHSV} = 11.44 \text{ g}_{\text{ethanol}}\cdot\text{g}_{\text{cat}}^{-1}\cdot\text{h}^{-1}$ and operating temperature of 300°C.

The ethanol conversion of montmorillonite support catalyst groups was contributed of ethylene reaction rate and diethyl ether reaction rate. Reaction rate of ethylene was increased with operating temperature and content of W. Although, low W loading decreased the reaction rate of ethylene under operating temperature between 200°C and 350°C. The reaction rate of diethyl ether was increased by temperature between 250°C and 300°C. Then, it was decreasing due to losing competitive reaction with ethylene pathway. Moreover, at low operating temperature and low W loading decreased reaction rate of diethyl ether. Reaction rate of acetaldehyde was increased with content of W and temperature. Nevertheless, acetaldehyde reaction rate was reduced at high operating temperature, due to the lost of competitive reaction with dehydration. 10WMMT and 13.5WMMT performed the highest ethylene reaction rate which reached $63.98 \mu\text{mol}\cdot\text{s}^{-1}\cdot\text{g}_{\text{cat}}^{-1}$ and $64.07 \mu\text{mol}\cdot\text{s}^{-1}\cdot\text{g}_{\text{cat}}^{-1}$ under conditions: $\text{WHSV} = 11.44 \text{ g}_{\text{ethanol}}\cdot\text{g}_{\text{cat}}^{-1}\cdot\text{h}^{-1}$ and operating temperature 400°C, respectively. The highest diethyl ether reaction rate in montmorillonite groups was occurred by 13.5WMMT which reached $14.70 \mu\text{mol}\cdot\text{s}^{-1}\cdot\text{g}_{\text{cat}}^{-1}$ under conditions: $\text{WHSV} = 11.44 \text{ g}_{\text{ethanol}}\cdot\text{g}_{\text{cat}}^{-1}\cdot\text{h}^{-1}$ and operating temperature 250°C.

The stability test of catalytic ethanol dehydration reaction has found that W loading was highly active at high temperature. However, coke formation was occurred at high operating temperature. It caused the decreasing of catalytic properties. However, after 10 hours of test, ethanol conversion of 13.5WMMT still did not reach stable conversion, but its conversion could promise to reach stable conversion based on stability test of 13.5WAC.

5.2 Recommendations

- The pyridine-adsorbed IR spectra should be used to investigate types of acidity including Lewis acid site and Brønsted acid site.
- More tungsten loading should be investigated due to low crystalline phase of WO_3 on support catalyst.
- The stability of MMT should be investigated to determine stable conversion.
- The long stability test should be applied to determine actual stable conversion.
- The more ethanol flow rate should be investigated due to reaching reaction rate limitation.
- The lower heating rate in NH_3 -TPD should be applied due to accuracy determine weak-medium-strong strength acid site.
- The CO_2 -TPD should be used to investigate total basicity.
- The H_2 reduction of catalyst should be applied to transformation Lewis acid of WO_3 to Bronsted acid.

REFERENCES



จุฬาลงกรณ์มหาวิทยาลัย
CHULALONGKORN UNIVERSITY

1. Gheewala, S., et al., *Biofuel Production from Sugarcane in Thailand*. 2019. p. 157-174.
2. Organization, I.S. *ISO Ethanol Yearbook 2019*. 2019.
3. Zhang, M. and Y. Yu, *Dehydration of Ethanol to Ethylene*. *Industrial & Engineering Chemistry Research*, 2013. **52**: p. 9505–9514.
4. Widayat, W., A. Roesyadi, and M. Rachimoellah, *Diethyl Ether Production Process with Various Catalyst Type*. *International Journal of Science and Engineering*, 2012. **4**.
5. United, S., et al., *Health assessment document for acetaldehyde*. 1987, Research Triangle Park, N.C.: Environmental Criteria and Assessment Office, Office of Health and Environmental Assessment, Office of Research and Development, U.S. Environmental Protection Agency.
6. Phung, T.K., et al., *Dehydration of ethanol over zeolites, silica alumina and alumina: Lewis acidity, Brønsted acidity and confinement effects*. *Applied Catalysis A: General*, 2015. **493**: p. 77-89.
7. Somrudee Chatchawanrat, B.J., *DEHYDROGENATION OF ETHANOL TO ACETALDEHYDE OVER ACTIVATED CARBON CATALYSTS*. 2013.
8. Ai, M., *The activity of WO₃-based mixed-oxide catalysts I. Acidic properties of WO₃-based catalysts and correlation with catalytic activity*. *Journal of Catalysis*, 1977. **49**(3): p. 305-312.
9. Cecilia, J.A., et al., *WO₃ supported on Zr doped mesoporous SBA-15 silica for glycerol dehydration to acrolein*. *Applied Catalysis A: General*, 2016. **516**: p. 30-40.
10. Lebarbier, V., G. Clet, and M. Houalla, *Relations between Structure, Acidity, and Activity of WO_x/TiO₂: Influence of the Initial State of the Support, Titanium Oxyhydroxide, or Titanium Oxide*. *The Journal of Physical Chemistry B*, 2006. **110**(45): p. 22608-22617.
11. Tresatayawed, A., P. Glinrun, and B. Jongsomjit, *Ethanol Dehydration over WO₃ /TiO₂ Catalysts Using Titania Derived from Sol-Gel and Solvothermal Methods*. *International Journal of Chemical Engineering*, 2019. **2019**: p. 1-11.

12. Marsh, H. and F. Rodríguez-Reinoso, *CHAPTER 9 - Production and Reference Material*, in *Activated Carbon*, H. Marsh and F. Rodríguez-Reinoso, Editors. 2006, Elsevier Science Ltd: Oxford. p. 454-508.
13. Chada, N., et al. *Activated carbon monoliths for methane storage*.
14. Soo, Y., et al. *Adsorbed Methane Film Properties in Nanoporous Carbon Monoliths*.
15. Dillon, E.C., et al., *Large surface area activated charcoal and the inhibition of aspirin absorption*. *Annals of Emergency Medicine*, 1989. **18**(5): p. 547-552.
16. Marsh, H. and F. Rodríguez-Reinoso, *CHAPTER 4 - Characterization of Activated Carbon*, in *Activated Carbon*, H. Marsh and F. Rodríguez-Reinoso, Editors. 2006, Elsevier Science Ltd: Oxford. p. 143-242.
17. Marsh, H. and F. Rodríguez-Reinoso, *CHAPTER 2 - Activated Carbon (Origins)*, in *Activated Carbon*, H. Marsh and F. Rodríguez-Reinoso, Editors. 2006, Elsevier Science Ltd: Oxford. p. 13-86.
18. Montes-Morán, M.A., et al., *On the nature of basic sites on carbon surfaces: an overview*. *Carbon*, 2004. **42**(7): p. 1219-1225.
19. Pietrzak, R., *XPS study and physico-chemical properties of nitrogen-enriched microporous activated carbon from high volatile bituminous coal*. *Fuel*, 2009. **88**(10): p. 1871-1877.
20. Figueiredo, J.L., et al., *Modification of the surface chemistry of activated carbons*. *Carbon*, 1999. **37**(9): p. 1379-1389.
21. Trepte, A., *Montmorillonite structure, with English labels*, Montmorillonite-en.svg, Editor. 2007.
22. Lassner, E. and W.-D. Schubert, *Industrial Production*, in *Tungsten: Properties, Chemistry, Technology of the Element, Alloys, and Chemical Compounds*, E. Lassner and W.-D. Schubert, Editors. 1999, Springer US: Boston, MA. p. 179-253.
23. Lassner, E. and W.-D. Schubert, *Tungsten Compounds and Their Application*, in *Tungsten: Properties, Chemistry, Technology of the Element, Alloys, and Chemical Compounds*, E. Lassner and W.-D. Schubert, Editors. 1999, Springer US: Boston, MA. p. 133-177.

24. Patnaik, P. and Knovel, *Handbook of Inorganic Chemicals*. McGraw-Hill handbooks. 2003: McGraw-Hill.
25. Wikipedia. *Ethylene*. 2020 [28/8/2020]; Available from: <https://en.wikipedia.org/wiki/Ethylene>.
26. (IFA), t.l.f.A.d.D.G.U. *Ethylene*. [28/8/2020]; Available from: [http://gestis-en.itrust.de/nxt/gateway.dll/gestis_en/012710.xml?f=templates\\$fn=default.htm\\$3.0](http://gestis-en.itrust.de/nxt/gateway.dll/gestis_en/012710.xml?f=templates$fn=default.htm$3.0).
27. Wikipedia. *Diethyl ether*. 2020 [28/8/2020]; Available from: https://en.wikipedia.org/wiki/Diethyl_ether.
28. Uebelacker, M. and D.W. Lachenmeier, *Quantitative determination of acetaldehyde in foods using automated digestion with simulated gastric fluid followed by headspace gas chromatography*. *Journal of automated methods & management in chemistry*, 2011. **2011**: p. 907317-907317.
29. Wikipedia. *Acetaldehyde*. 2020 [28/8/2020]; Available from: <https://en.wikipedia.org/wiki/Acetaldehyde>.
30. Brey, W.S. and K.A. Krieger, *The Surface Area and Catalytic Activity of Aluminum Oxide*. *Journal of the American Chemical Society*, 1949. **71**(11): p. 3637-3641.
31. Tanabe, K., et al., *New Solid Acids and Bases: Their Catalytic Properties*. *Studies in Surface Science and Catalysis*, ed. K. Tanabe, et al. Vol. 51. 1989: Elsevier.
32. Smith, M.B. and J. March, *March's Advanced Organic Chemistry: Reactions, Mechanisms, and Structure, Sixth Edition*. Vol. 6. 2006.
33. Noller, H. and K. Thomke, *Transition states of catalytic dehydration and dehydrogenation of alcohols*. *Journal of Molecular Catalysis*, 1979. **6**(5): p. 375-392.
34. Ob-eye, J., P. Prasertdam, and B. Jongsomjit, *Dehydrogenation of Ethanol to Acetaldehyde over Different Metals Supported on Carbon Catalysts*. *Catalysts*, 2019. **9**: p. 66.
35. Krutpijit, C. and B. Jongsomjit, *Catalytic Ethanol Dehydration over Different Acid-activated Montmorillonite Clays*. 2016. **65**(4): p. 347-355.

36. Hunyadi, D., I. Sajó, and I.M. Szilágyi, *Structure and thermal decomposition of ammonium metatungstate*. Journal of Thermal Analysis and Calorimetry, 2014. **116**(1): p. 329-337.
37. Alvarez-Merino, M.A., et al., *Tungsten catalysts supported on activated carbon: I. Preparation and characterization after their heat treatments in inert atmosphere*. Journal of Catalysis, 2000. **192**(2): p. 363-373.
38. Moreno-Castilla, C., M.A. Alvarez-Merino, and F. Carrasco-Marín, *Decomposition Reactions of Methanol and Ethanol Catalyzed by Tungsten Oxide Supported on Activated Carbon*. Reaction Kinetics and Catalysis Letters, 2000. **71**(1): p. 137-142.
39. Shang, H., et al., *Preparing high surface area porous carbon from biomass by carbonization in a molten salt medium*. RSC Advances, 2015. **5**(92): p. 75728-75734.
40. Nukui, Y., et al., *Vertically aligned hexagonal WO₃ nanotree electrode for photoelectrochemical water oxidation*. Chemical Physics Letters, 2015. **635**: p. 306-311.
41. Hasan, B., L. Hamza, and D. Uamran, *Enhanced sensing properties of WO₃ and its binary systems for thin films gas sensors*. Journal of Physics: Conference Series, 2019. **1234**.
42. Szilágyi, I.M., et al., *Preparation of hexagonal WO₃ from hexagonal ammonium tungsten bronze for sensing NH₃*. Materials Research Bulletin, 2009. **44**(3): p. 505-508.
43. Kalhori, H., et al., *Flower-like nanostructures of WO₃: Fabrication and characterization of their in-liquid gasochromic effect*. Sensors and Actuators B: Chemical, 2016. **225**: p. 535-543.
44. Breedon, M., et al., *Synthesis of nanostructured tungsten oxide thin films: A simple, controllable, inexpensive, aqueous sol-gel method*. Cryst Growth des, 2009. **10**.
45. Siburian, R., et al., *New Route to Synthesize of Graphene Nano Sheets*. Oriental Journal of Chemistry, 2018. **34**: p. 182-187.

46. Yuan, H.-J., et al., *Hydrothermal synthesis and chromic properties of hexagonal WO₃ nanowires*. Chinese Physics B - CHIN PHYS B, 2011. **20**.
47. Matthias, T., et al., *Physisorption of gases, with special reference to the evaluation of surface area and pore size distribution (IUPAC Technical Report)*. Pure and Applied Chemistry, 2015. **87**(9-10): p. 1051-1069.
48. Baertsch, C.D., S.L. Soled, and E. Iglesia, *Isotopic and Chemical Titration of Acid Sites in Tungsten Oxide Domains Supported on Zirconia*. The Journal of Physical Chemistry B, 2001. **105**(7): p. 1320-1330.
49. Lai, J.-K. and I.E. Wachs, *A Perspective on the Selective Catalytic Reduction (SCR) of NO with NH₃ by Supported V₂O₅-WO₃/TiO₂ Catalysts*. ACS Catalysis, 2018. **8**(7): p. 6537-6551.
50. Datka, J., *Acidic properties of supported niobium oxide catalysts: An infrared spectroscopy investigation*. Journal of Catalysis, 1992. **135**(1): p. 186-199.
51. Bernholc, J., et al., *Broensted acid sites in transition metal oxide catalysts: modeling of structure, acid strengths, and support effects*. The Journal of Physical Chemistry, 1987. **91**(6): p. 1526-1530.



APPENDIX

จุฬาลงกรณ์มหาวิทยาลัย
CHULALONGKORN UNIVERSITY

APPANDIX A

Calculation for acid site of catalysts

Calculation of acidity

The acidity was measured by NH₃-TPD, it can be calculated from NH₃-TPD profile as follow.

$$\text{Acidity of catalysts} = \text{mol of NH}_3 \text{ desorption per } g_{cat} \quad (\text{A.1})$$

Where g_{cat} was weight of dry catalyst

To calculate mole of NH₃ desorption from the calibration curve of NH₃ as follow:

$$\text{mol of NH}_3 \text{ desorption per } g_{cat} = 2.628 \times 10^{-5} \times A \quad (\text{A.2})$$

Where, A was area under peak per weight of dry catalyst of the NH₃ -TPD profile.

Then combine equation (A.1) and (A.2). So, the equation (A.1) can be take place as equation (A.3)

$$\text{Acidity of catalysts} = 2.628 \times 10^{-5} \times A \quad (\text{A.3})$$

Curve fitting by Fityk

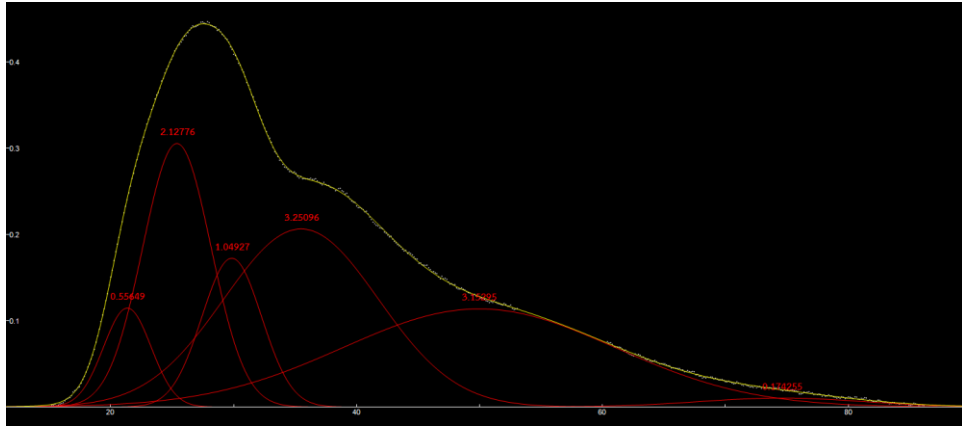


Figure A.1 TCD-time curve fitting of AC by Gaussian curve in Fityk program

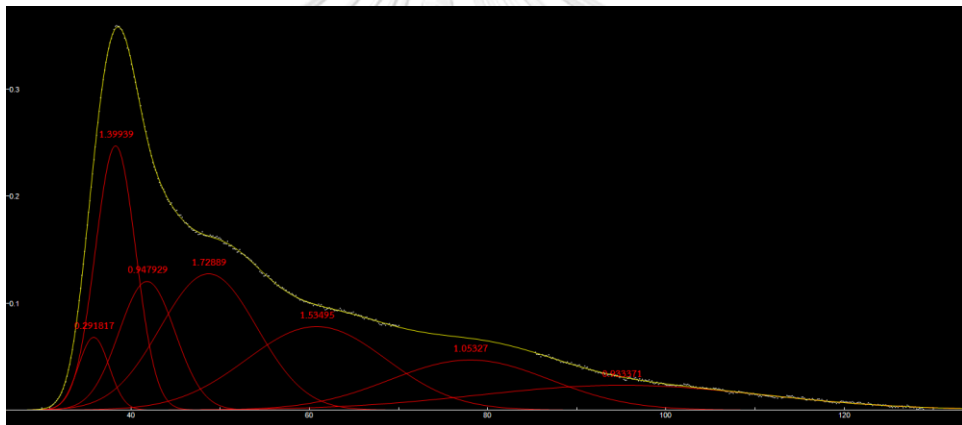


Figure A.2 TCD-time curve fitting of 2WAC by Gaussian curve in Fityk program

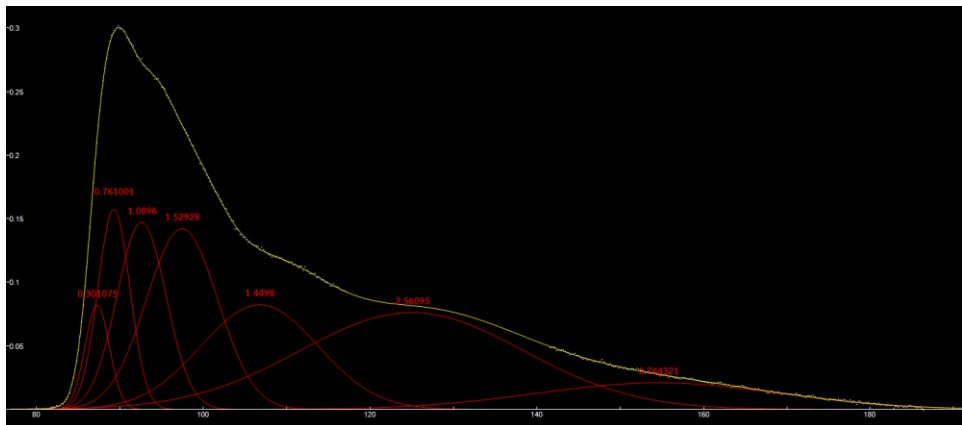


Figure A.3 TCD-time curve fitting of 5WAC by Gaussian curve in Fityk program

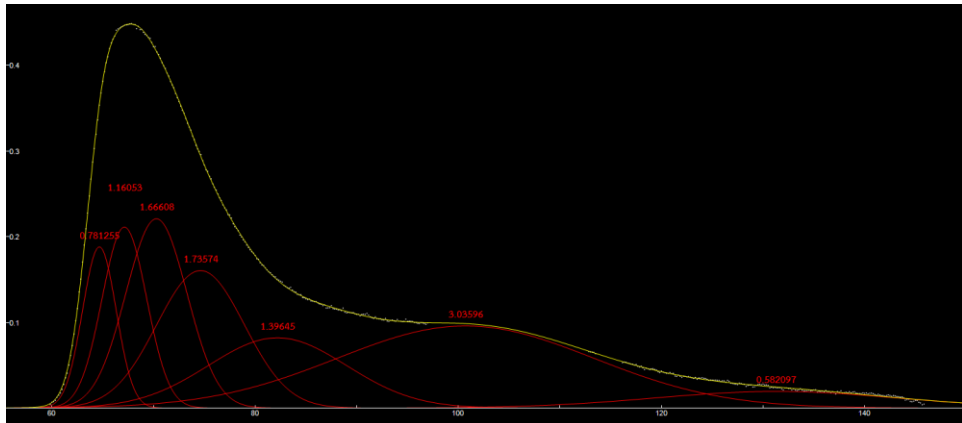


Figure A.4 TCD-time curve fitting of 10WAC by Gaussian curve in Fityk program

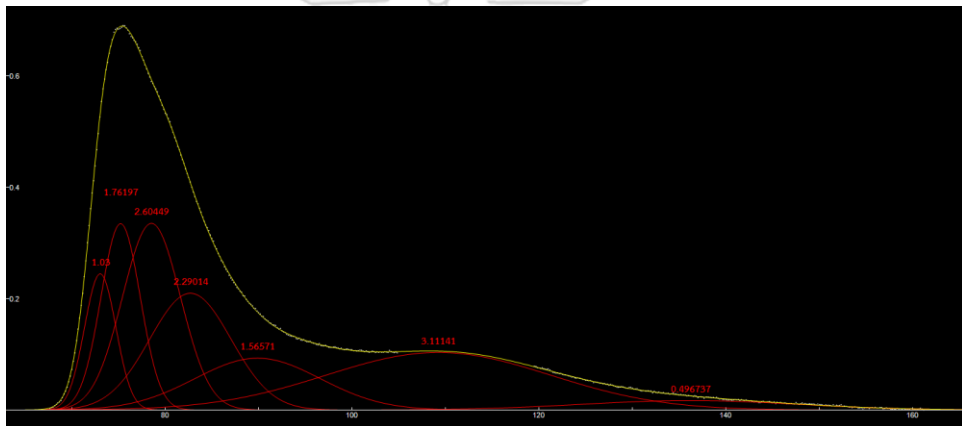


Figure A.5 TCD-time curve fitting of 13.5WAC by Gaussian curve in Fityk program

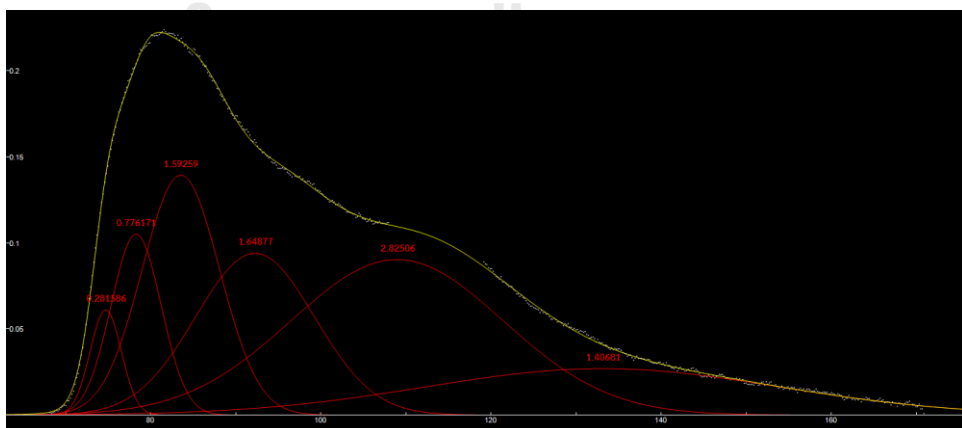


Figure A.6 TCD-time curve fitting of ACG by Gaussian curve in Fityk program

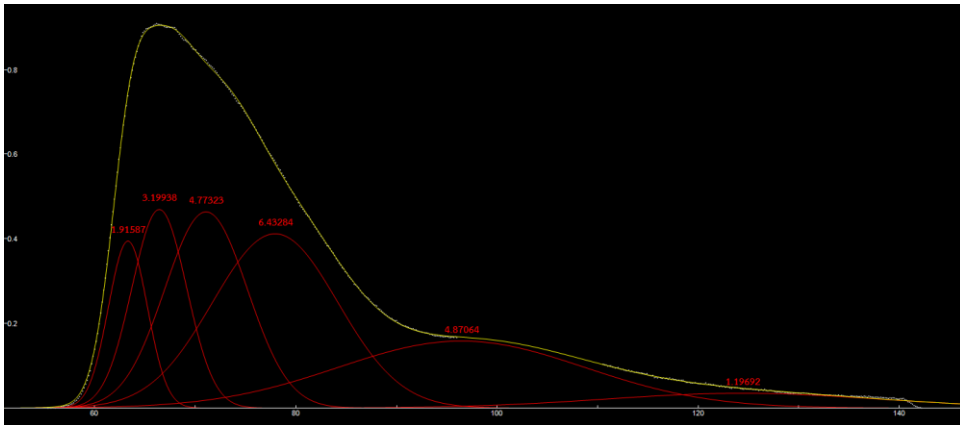


Figure A.7 TCD-time curve fitting of 13.5WACG by Gaussian curve in Fityk program

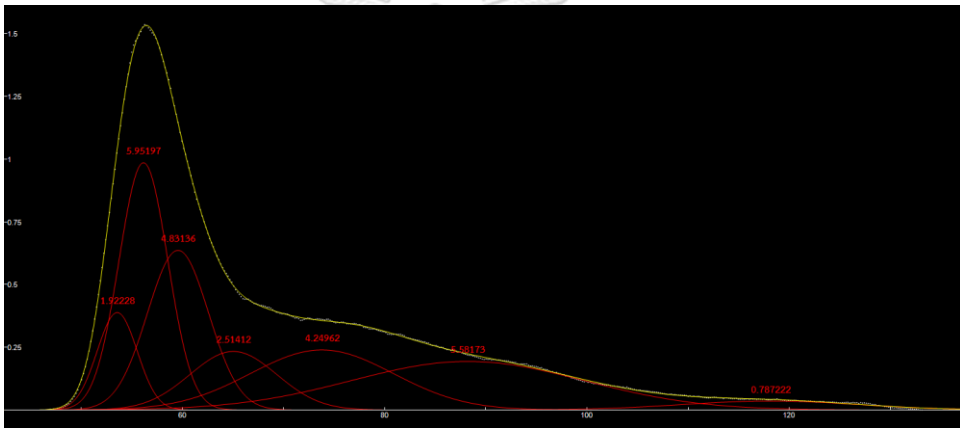


Figure A.8 TCD-time curve fitting of MMT by Gaussian curve in Fityk program

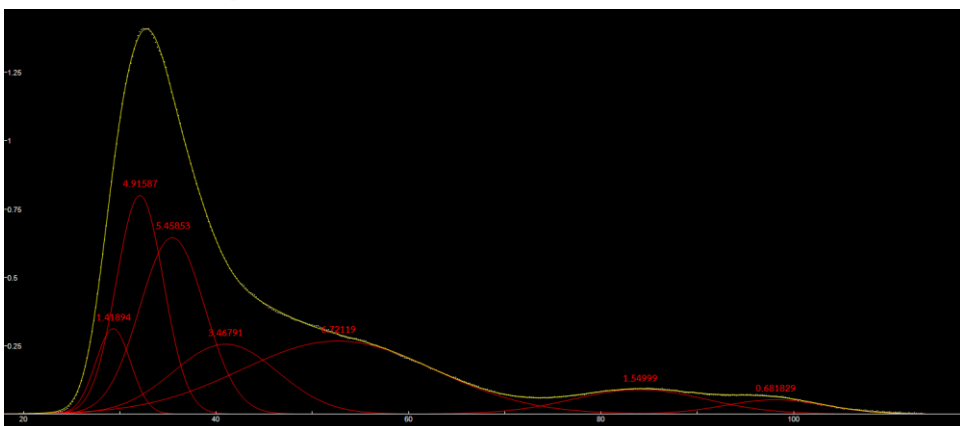


Figure A.9 TCD-time curve fitting of 2WMMT by Gaussian curve in Fityk program

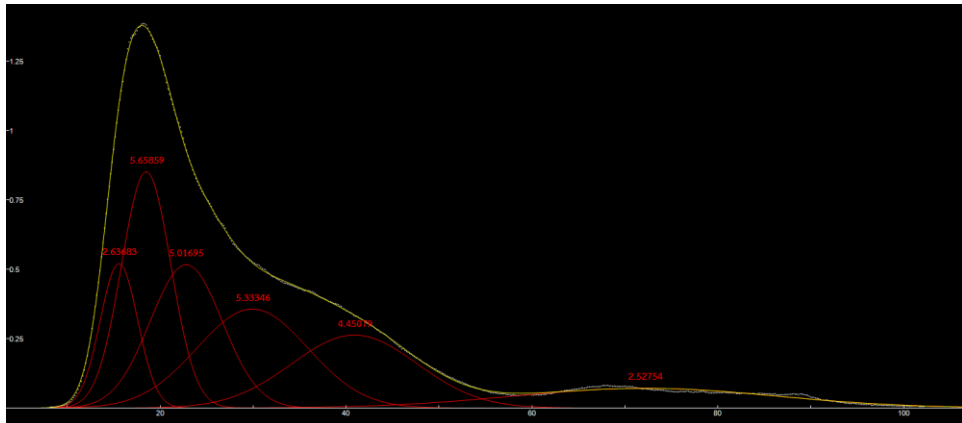


Figure A.10 TCD-time curve fitting of 5WMMT by Gaussian curve in Fityk program

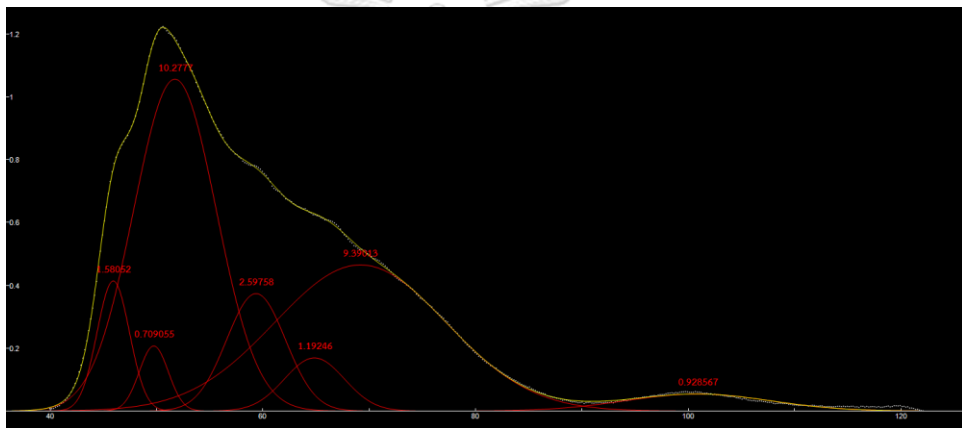


Figure A.11 TCD-time curve fitting of 10WMMT by Gaussian curve in Fityk program

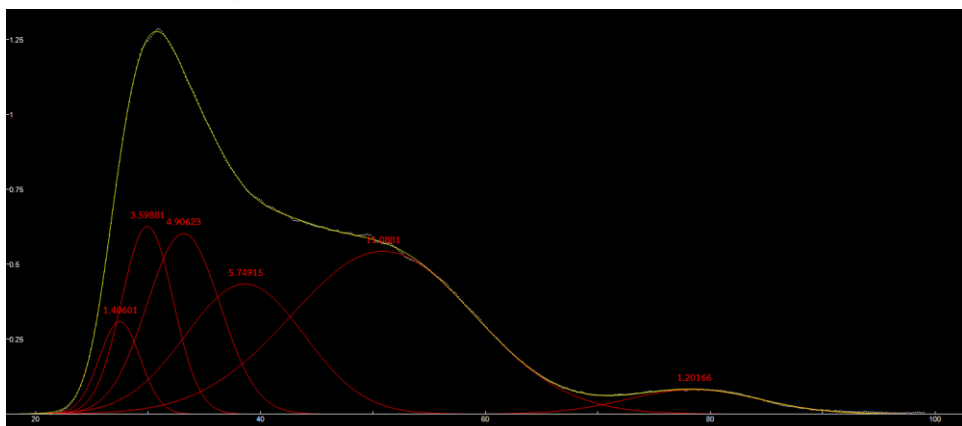


Figure A.12 TCD-time curve fitting of 13.5WMMT by Gaussian curve in Fityk program

APPENDIX B

Calibration curve of Reactant and Product

The calibration curve was calculated by injection substance into GC-FID and detected by chromatogram in area of substance versus amount of injection substance. The calibration curve of reactant and product were shown in Figure B.1 to B4.

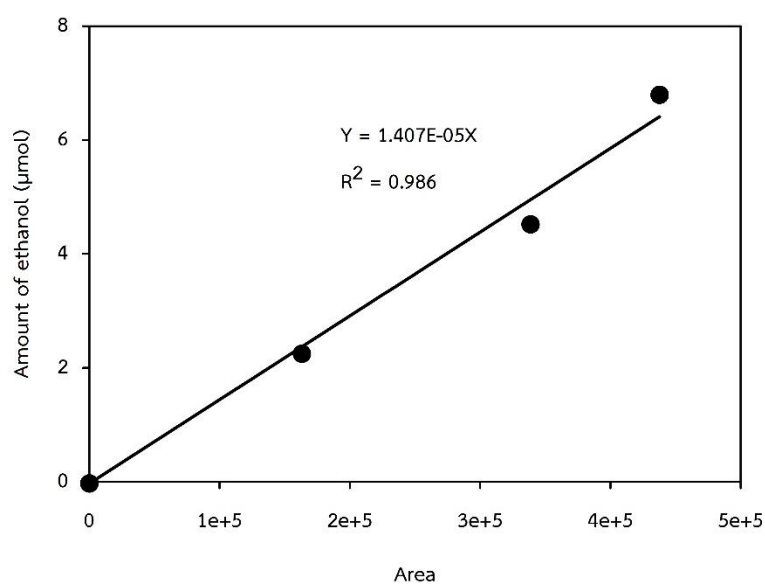


Figure B.1 The calibration curve of ethanol

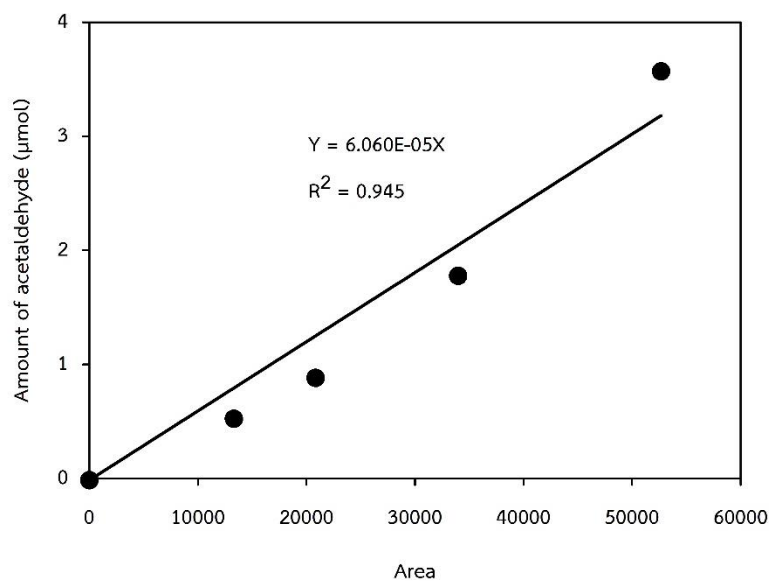


Figure B.2 The calibration curve of acetaldehyde

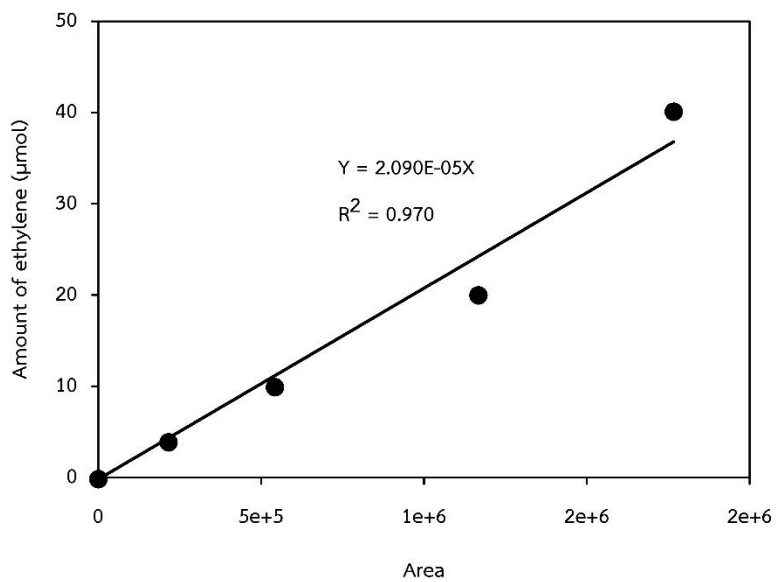


Figure B.3 The calibration curve of ethylene

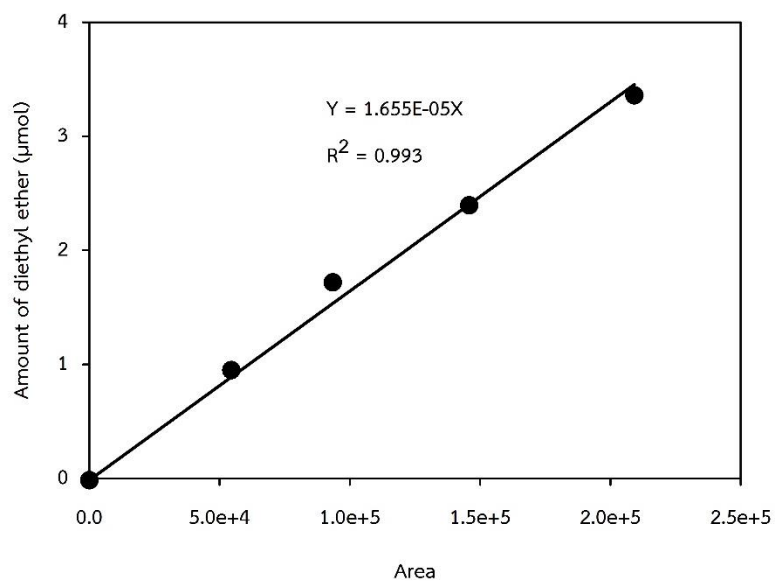


Figure B.4 The calibration curve of diethyl ether

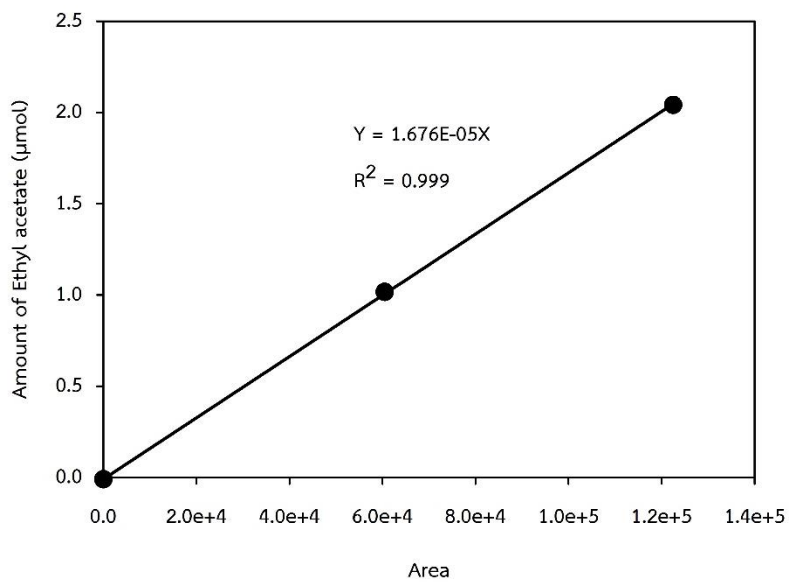


Figure B.5 The calibration curve of ethyl acetate

APPENDIX C

Catalytic activity, selectivity, and yield of product over all catalysts

Addition Figure of yield and selectivity of product over all catalysts

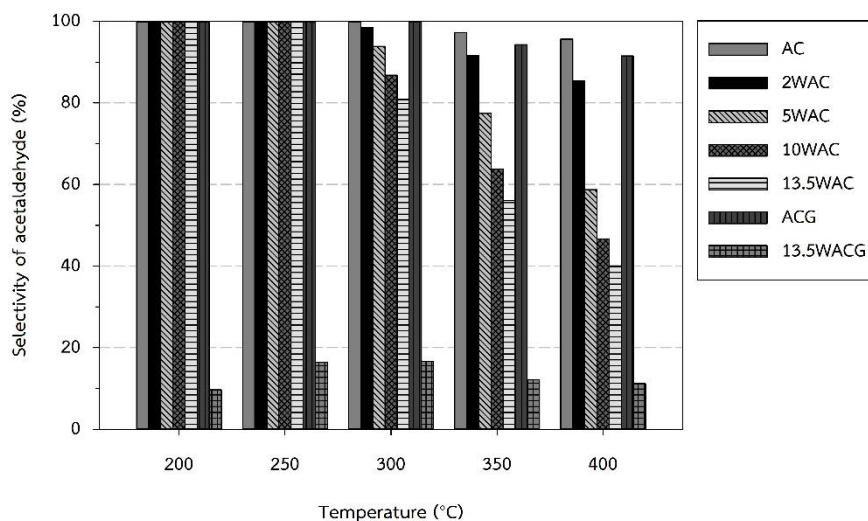


Figure C.1 Acetaldehyde selectivity of various W supported on AC catalysts for ethanol dehydration at various operating temperature ($WHSV=3.13 \text{ g}_{\text{ethanol}} \cdot \text{g}_{\text{cat}}^{-1} \cdot \text{h}^{-1}$)

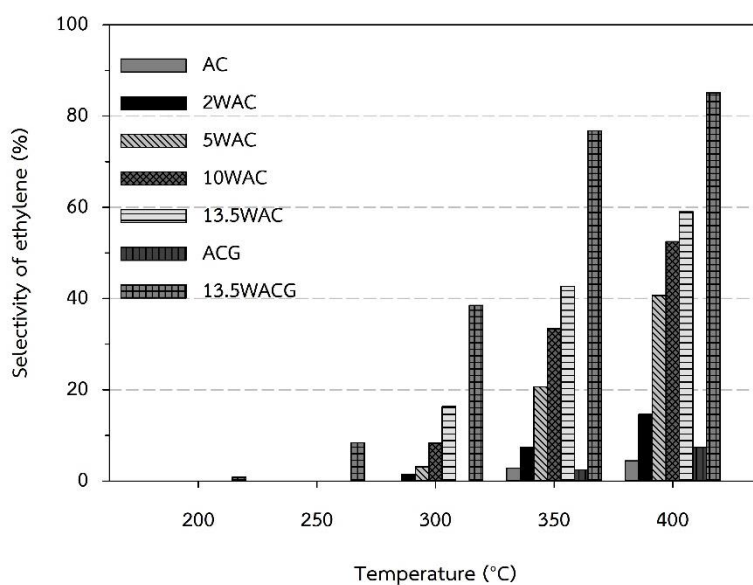


Figure C.2 Ethylene selectivity of various W supported on AC catalysts for ethanol dehydration at various operating temperature ($WHSV=3.13 \text{ g}_{\text{ethanol}} \cdot \text{g}_{\text{cat}}^{-1} \cdot \text{h}^{-1}$)

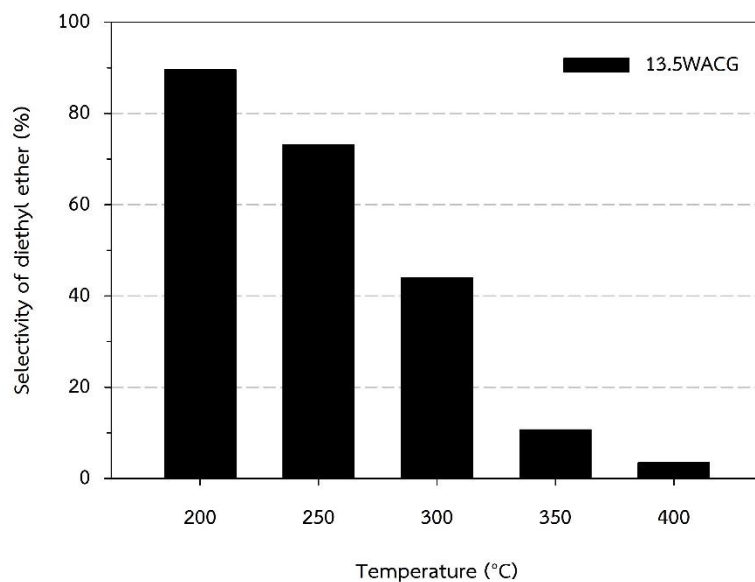


Figure C.3 Diethyl ether selectivity of various W supported on AC catalysts for ethanol dehydration at various operating temperature (WHSV=3.13 $\text{g}_{\text{ethanol}} \cdot \text{g}_{\text{cat}}^{-1} \cdot \text{h}^{-1}$)

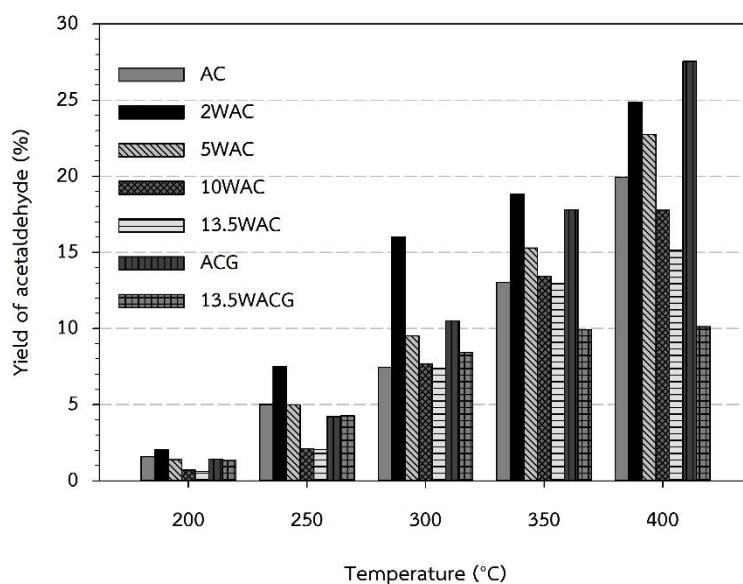


Figure C.4 Acetaldehyde yield of various W supported on AC catalysts for ethanol dehydration at various operating temperature (WHSV=3.13 $\text{g}_{\text{ethanol}} \cdot \text{g}_{\text{cat}}^{-1} \cdot \text{h}^{-1}$)

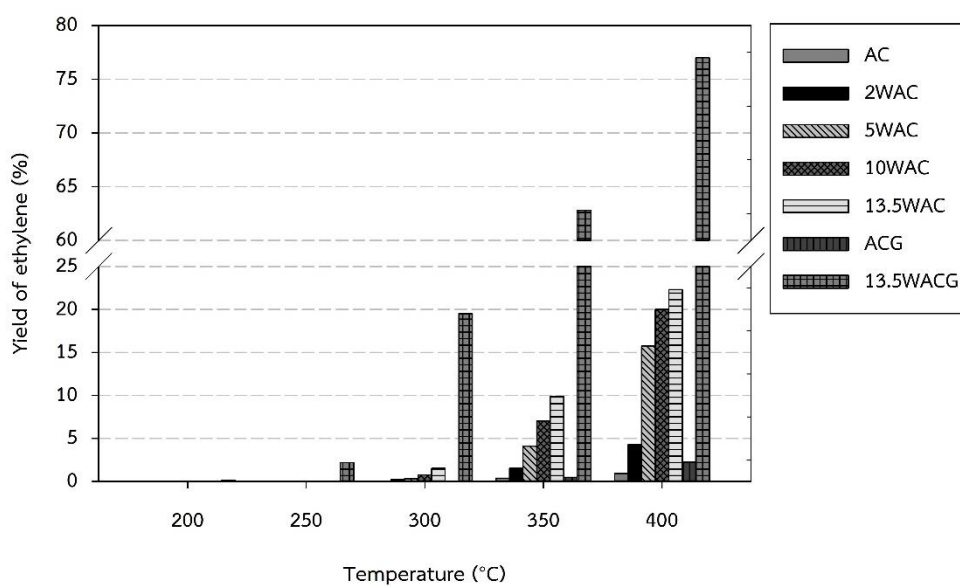


Figure C.5 Ethylene yield of various W supported on AC catalysts for ethanol dehydration at various operating temperature (WHSV=3.13 $\text{g}_{\text{ethanol}} \cdot \text{g}_{\text{cat}}^{-1} \cdot \text{h}^{-1}$)

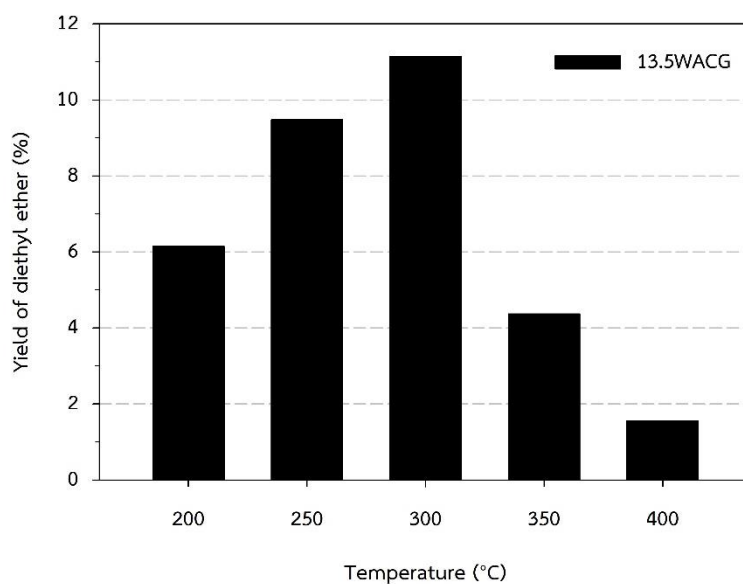


Figure C.6 Diethyl ether yield of various W supported on AC catalysts for ethanol dehydration at various operating temperature (WHSV=3.13 $\text{g}_{\text{ethanol}} \cdot \text{g}_{\text{cat}}^{-1} \cdot \text{h}^{-1}$)

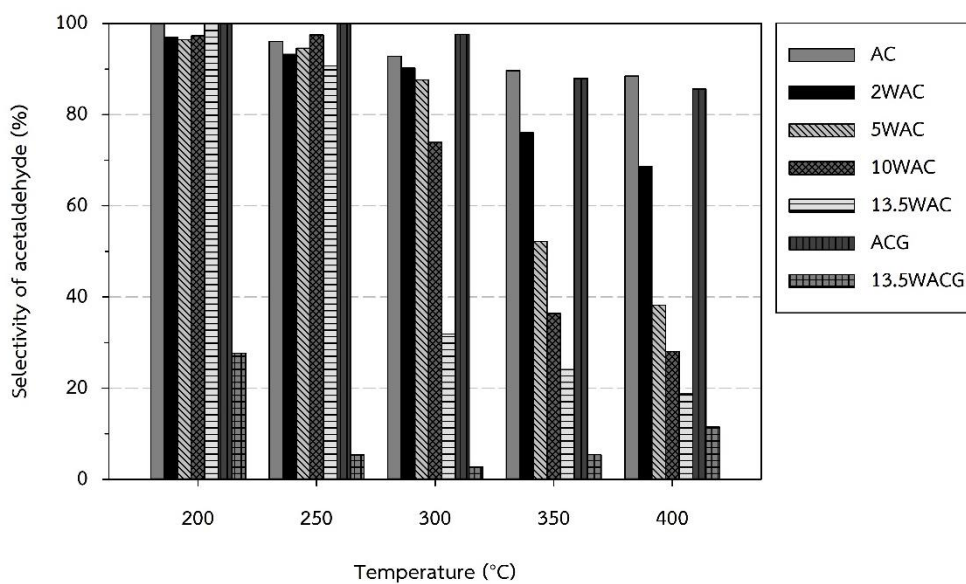


Figure C.7 Acetaldehyde selectivity of various W supported on AC catalysts for ethanol dehydration at various operating temperature (WHSV=11.44 $\text{g}_{\text{ethanol}} \cdot \text{g}_{\text{cat}}^{-1} \cdot \text{h}^{-1}$)

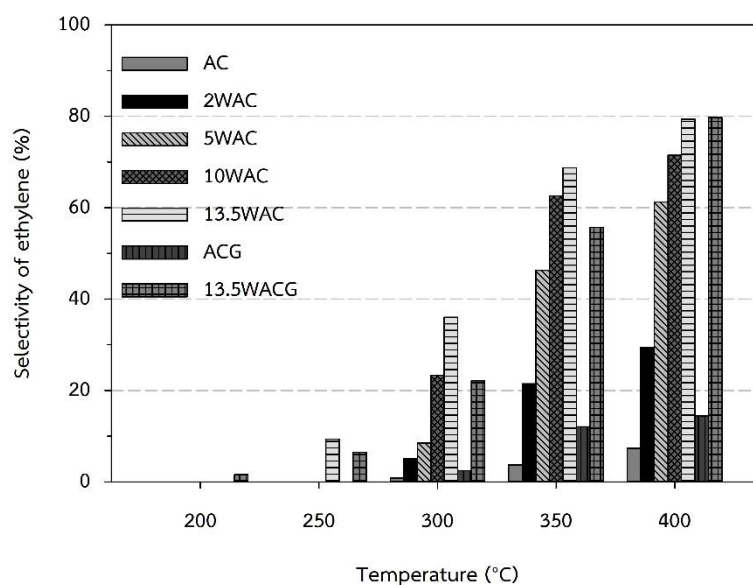


Figure C.8 Ethylene selectivity of various W supported on AC catalysts for ethanol dehydration at various operating temperature (WHSV=11.44 $\text{g}_{\text{ethanol}} \cdot \text{g}_{\text{cat}}^{-1} \cdot \text{h}^{-1}$)

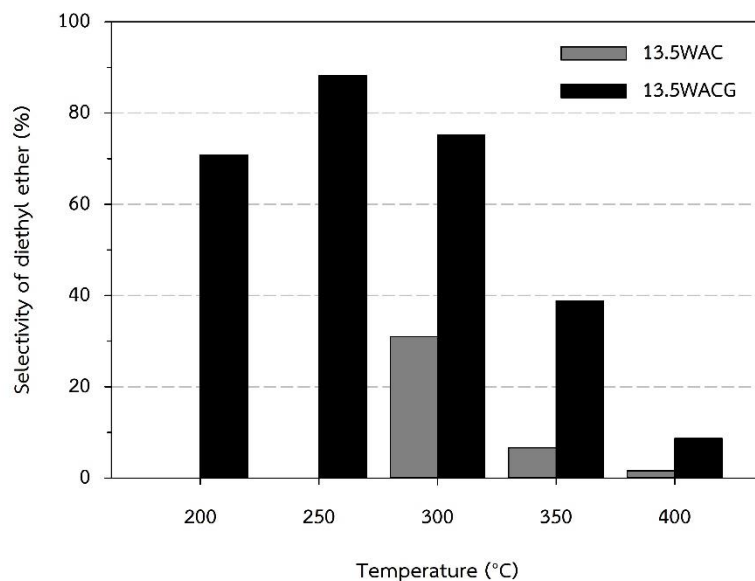


Figure C.9 Diethyl ether selectivity of various W supported on AC catalysts for ethanol dehydration at various operating temperature (WHSV=11.44 $\text{g}_{\text{ethanol}} \cdot \text{g}_{\text{cat}}^{-1} \cdot \text{h}^{-1}$)

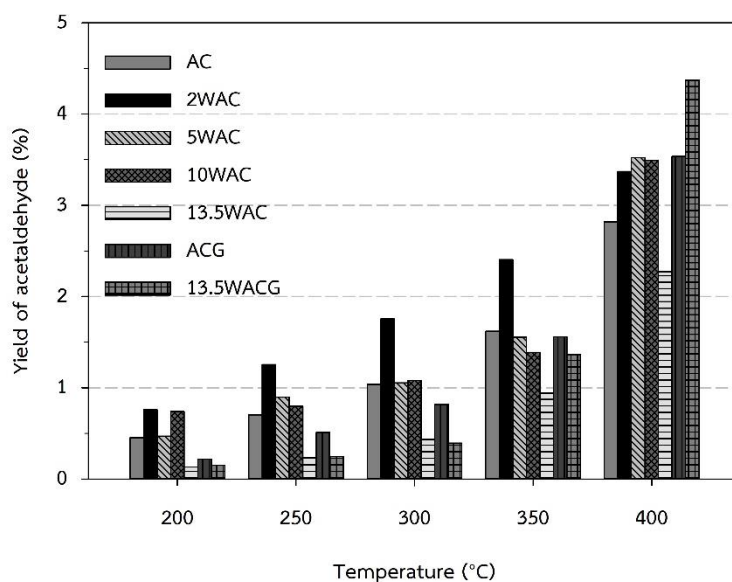


Figure C.10 Acetaldehyde yield of various W supported on AC catalysts for ethanol dehydration at various operating temperature (WHSV=11.44 $\text{g}_{\text{ethanol}} \cdot \text{g}_{\text{cat}}^{-1} \cdot \text{h}^{-1}$)

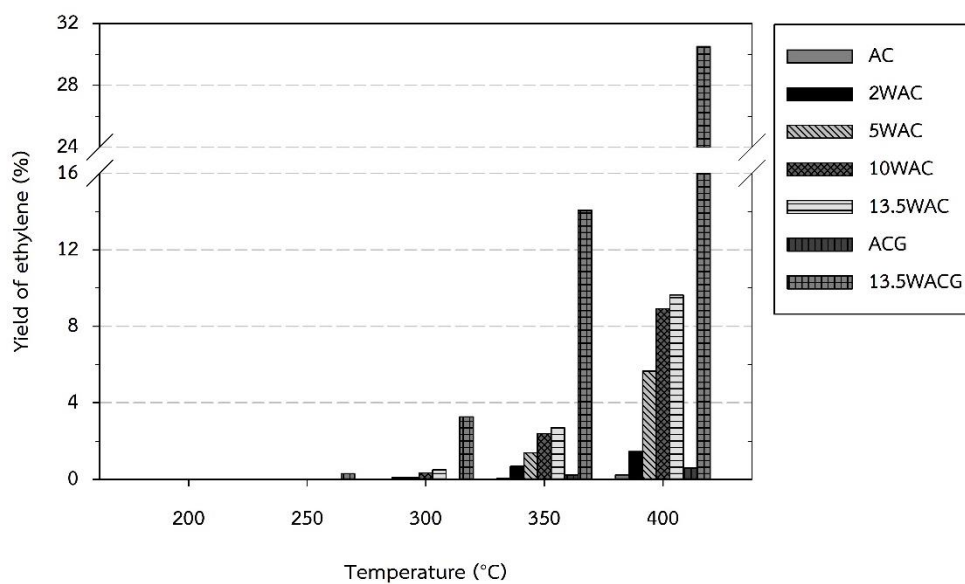


Figure C.11 Ethylene yield of various W supported on AC catalysts for ethanol dehydration at various operating temperature (WHSV=11.44 $\text{g}_{\text{ethanol}} \cdot \text{g}_{\text{cat}}^{-1} \cdot \text{h}^{-1}$)

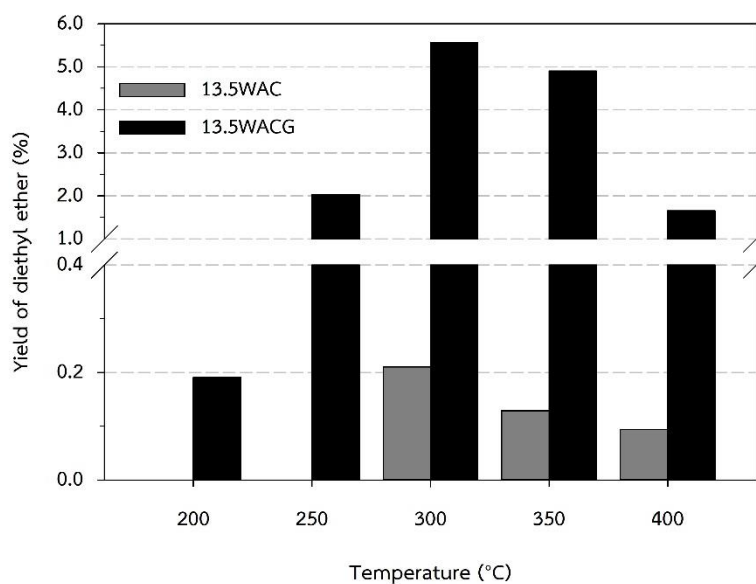


Figure C.12 Diethyl ether yield of various W supported on AC catalysts for ethanol dehydration at various operating temperature (WHSV=11.44 $\text{g}_{\text{ethanol}} \cdot \text{g}_{\text{cat}}^{-1} \cdot \text{h}^{-1}$)

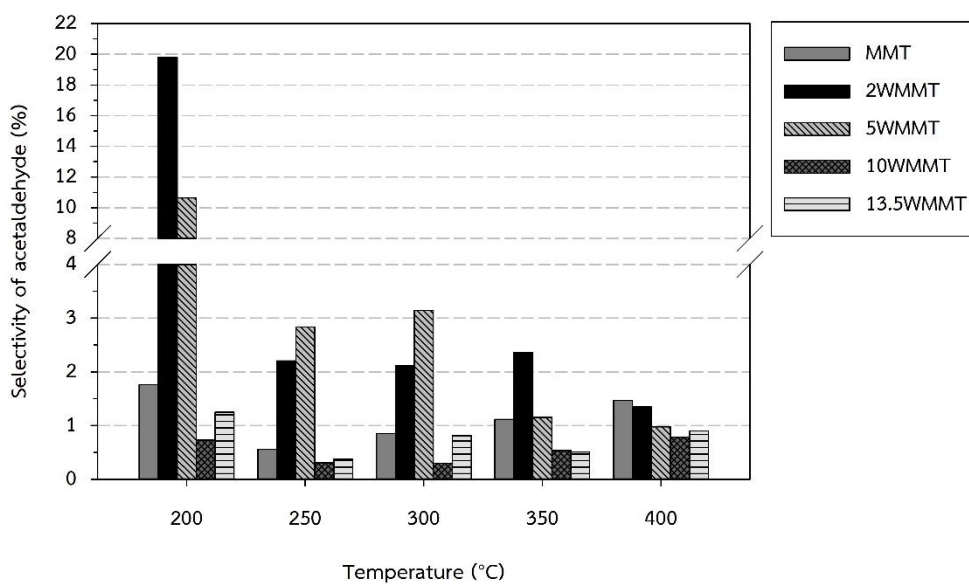


Figure C.13 Acetaldehyde selectivity of various W supported on MMT catalysts for ethanol dehydration at various operating temperature (WHSV=11.44 $\text{g}_{\text{ethanol}} \cdot \text{g}_{\text{cat}}^{-1} \cdot \text{h}^{-1}$)

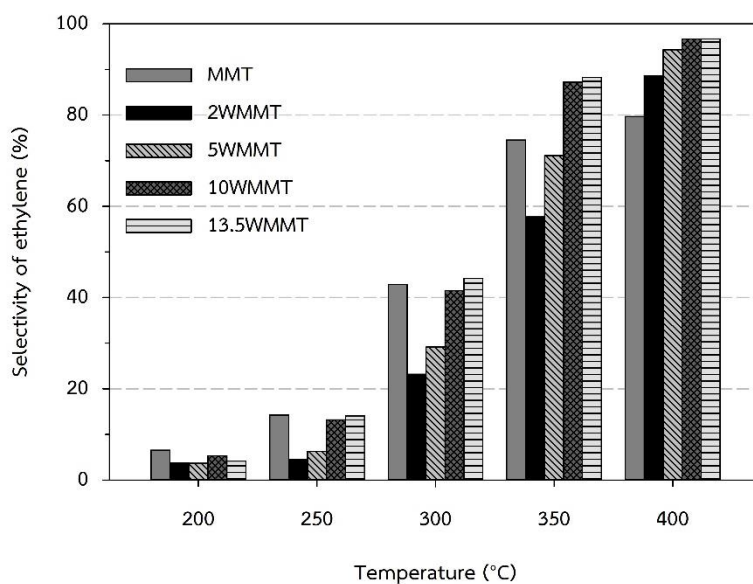


Figure C.14 Ethylene selectivity of various W supported on MMT catalysts for ethanol dehydration at various operating temperature (WHSV=11.44 $\text{g}_{\text{ethanol}} \cdot \text{g}_{\text{cat}}^{-1} \cdot \text{h}^{-1}$)

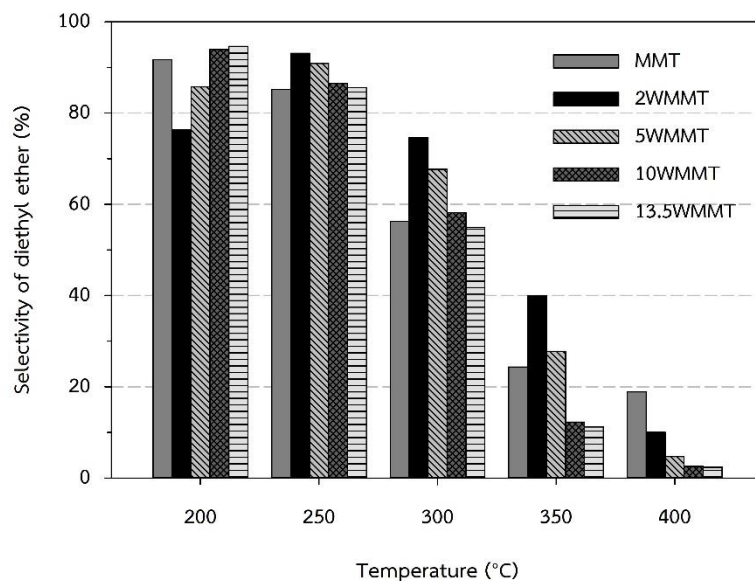


Figure C.15 Diethyl ether selectivity of various W supported on MMT catalysts for ethanol dehydration at various operating temperature ($WHSV=11.44 \text{ g}_{\text{ethanol}} \cdot \text{g}_{\text{cat}}^{-1} \cdot \text{h}^{-1}$)

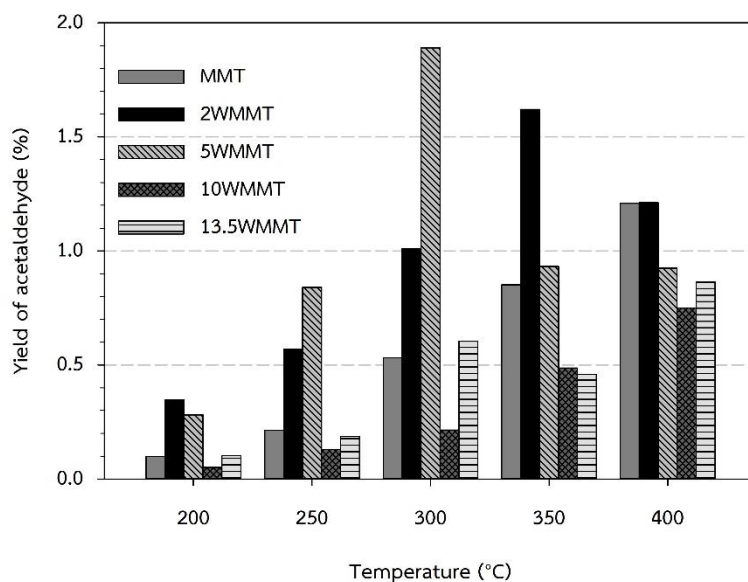


Figure C.16 Acetaldehyde yield of various W supported on MMT catalysts for ethanol dehydration at various operating temperature ($WHSV=11.44 \text{ g}_{\text{ethanol}} \cdot \text{g}_{\text{cat}}^{-1} \cdot \text{h}^{-1}$)

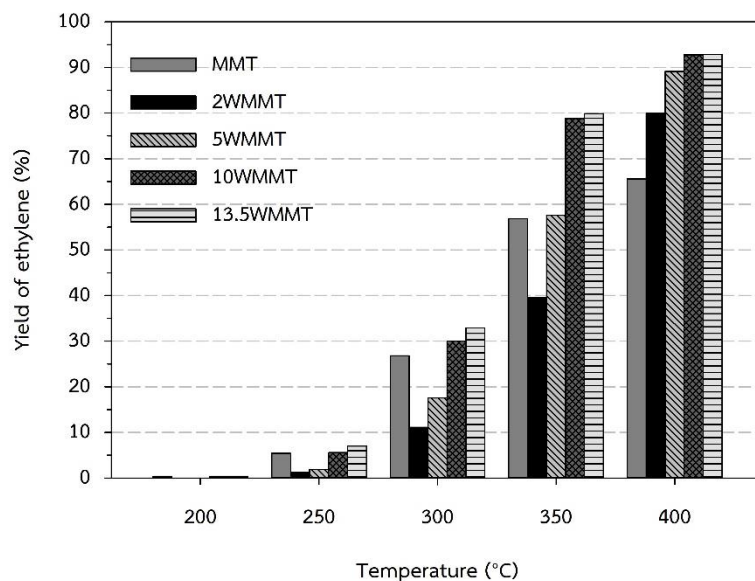


Figure C.17 Ethylene yield of various W supported on MMT catalysts for ethanol dehydration at various operating temperature (WHSV=11.44 $\text{g}_{\text{ethanol}} \cdot \text{g}_{\text{cat}}^{-1} \cdot \text{h}^{-1}$)

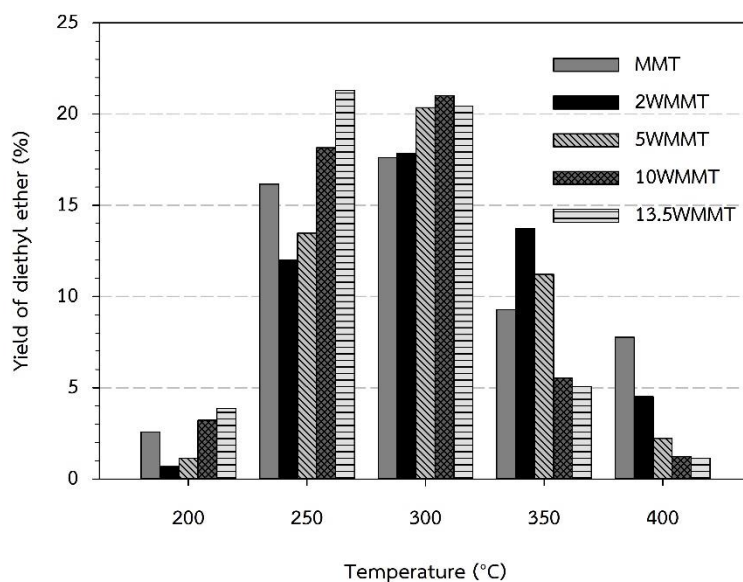


Figure C.18 Diethyl ether yield of various W supported on MMT catalysts for ethanol dehydration at various operating temperature (WHSV=11.44 $\text{g}_{\text{ethanol}} \cdot \text{g}_{\text{cat}}^{-1} \cdot \text{h}^{-1}$)

Table C.1 The catalytic activity and product distribution for activated carbon groups
(the reaction condition: T=200-400°C and WHSV=3.13 g_{Ethanol}·g_{Cat}⁻¹·h⁻¹)

Catalyst	Temp. (°C)	Conversion (%)	Selectivity (%)				Yield (%)				Rate of reaction ($\mu\text{mol}\cdot\text{s}^{-1}\cdot\text{g}_{\text{cat}}^{-1}$)				
			Ethylene	Acetaldehyde	Diethyl ether	Ethyl acetate	Ethylene	Acetaldehyde	Diethyl ether	Ethyl acetate	Ethylene	Acetaldehyde	Diethyl ether	Ethyl acetate	total
AC	200	1.6	100				1.6				0.30				
	250	5.0	100				5.0				0.95				
	300	7.4	100				7.4				1.41				
	350	13.4	2.8	97.2			0.4	13.0			0.07	2.46			2.53
	400	20.9	4.4	95.6			0.9	19.9			0.17	3.77			3.94
2WAC	200	2.0	100				2.0				0.39				
	250	7.5	100				7.5				1.42				
	300	16.2	1.4	98.6			0.2	16.0			0.04	3.02			3.07
	350	20.5	7.4	91.7	1.0		1.5	18.8	0.1		0.29	3.56	0.02		3.86
	400	29.1	14.6	85.4			4.2	24.9			0.80	4.70			5.50
5WAC	200	1.4	100				1.4				0.26				
	250	5.0	100				5.0				0.94				
	300	10.1	3.1	93.8	3.1		0.3	9.5	0.2		0.06	1.80	0.03		1.89
	350	19.7	20.6	77.4	1.9		4.1	15.3	0.2		0.77	2.89	0.04		3.69
	400	38.7	40.6	58.7	0.7		15.7	22.7	0.1		2.97	4.30	0.02		7.29
10WAC	200	0.7	100				0.7				0.13				
	250	2.1	100				2.1				0.40				
	300	8.8	8.3	86.8	4.9		0.73	7.67	0.22		0.14	1.45	0.04		1.63
	350	21.0	33.4	63.8	2.8		7.0	13.4	0.3		1.33	2.54	0.06		3.92
	400	38.1	52.5	46.6	0.9		20.0	17.8	0.2		3.78	3.35	0.03		7.16
13.5WAC	200	0.6	100				0.6				0.11				
	250	2.0	100				2.05				0.39				
	300	9.3	15.9	81.3	2.8		1.48	7.57	0.13		0.28	1.43	0.02		1.74
	350	23.1	42.6	56.1	1.3		9.8	12.9	0.1		1.86	2.44	0.03		4.33
	400	37.8	59.0	40.1	0.9		22.3	15.1	0.2		4.21	2.86	0.03		7.10
ACG	200	1.4	100				1.4				0.27				
	250	4.2	100				4.2				0.80				
	300	10.5	100				10.5				1.98				
	350	18.9	2.5	94.3	3.2		0.5	17.8	0.3		0.09	3.36	0.06		3.51
	400	30.1	7.4	91.5	1.1		2.2	27.5	0.2		0.42	5.20	0.03		5.65
13.5WACG	200	13.7	0.8	9.6	89.6		0.1	1.3	6.1		0.02	0.25	1.16		1.43
	250	25.9	8.4	16.4	73.2		2.2	4.3	9.5		0.41	0.80	1.79		3.05
	300	50.7	38.5	16.7	44.0		19.5	8.4	11.1		3.68	1.59	2.10		7.42
	350	81.8	76.7	12.1	10.7		62.8	9.9	4.4		11.86	1.87	0.82		14.59
	400	90.5	85.1	11.2	3.4		77.0	10.1	1.6		14.54	1.91	0.29		16.77

Table C.2 The catalytic activity and product distribution for activated carbon groups
(the reaction condition: T=200-400°C and WHSV=11.44 g_{ethanol}·g_{cat}⁻¹·h⁻¹)

Catalyst	Temp. (°C)	Conversion (%)	Selectivity (%)				Yield (%)				Rate of reaction ($\mu\text{mol}\cdot\text{s}^{-1}\cdot\text{g}_{\text{cat}}^{-1}$)				
			Ethylene	Acetaldehyde	Diethyl ether	Ethyl acetate	Ethylene	Acetaldehyde	Diethyl ether	Ethyl acetate	Ethylene	Acetaldehyde	Diethyl ether	Ethyl acetate	total
AC	200	0.5	100				0.45				0.31				
	250	0.7	96.0				0.70				0.48				
	300	1.1	0.8	92.8	6.4		0.01	1.04	0.04		0.01	0.71	0.02		0.75
	350	1.8	3.7	89.7	6.6		0.07	1.62	0.06		0.05	1.12	0.04		1.20
	400	3.2	7.3	88.4	4.3		0.23	2.82	0.07		0.16	1.94	0.05		2.15
2WAC	200	0.8	97.0				0.76				0.52				
	250	1.3	93.2				1.25				0.86				
	300	1.9	5.1	90.2	4.7		0.10	1.75	0.05		0.07	1.21	0.03		1.31
	350	3.2	21.4	76.0	2.5		0.68	2.40	0.04		0.47	1.66	0.03		2.15
	400	4.9	29.4	68.7	1.9		1.44	3.37	0.05		1.00	2.33	0.03		3.35
5WAC	200	0.5	96.4				0.47				0.32				
	250	0.9	94.6				0.90				0.62				
	300	1.2	8.5	87.6	3.9		0.10	1.05	0.02		0.07	0.73	0.02		0.81
	350	3.0	46.3	52.2	1.5		1.38	1.56	0.02		0.95	1.07	0.02		2.04
	400	9.2	61.3	38.2	0.5		5.65	3.52	0.02		3.90	2.43	0.02		6.34
10WAC	200	0.8	97.3				0.74				0.51				
	250	0.8	97.5				0.80				0.55				
	300	1.5	23.3	73.9	2.8		0.34	1.08	0.02		0.23	0.74	0.01		0.99
	350	3.8	62.6	36.3	1.1		2.39	1.39	0.02		1.65	0.96	0.01		2.62
	400	12.5	71.5	28.0	0.4		8.92	3.50	0.03		6.15	2.41	0.02		8.58
13.5WAC	200	0.1	100				0.13				0.09				
	250	0.3	9.3	90.7			0.02	0.23			0.02	0.16			0.18
	300	1.4	36.0	31.9	31.0	1.2	0.49	0.43	0.21	0.01	0.34	0.30	0.15	0.01	0.79
	350	3.9	68.7	24.1	6.6	0.6	2.69	0.94	0.13	0.01	1.85	0.65	0.09	0.01	2.60
	400	12.1	79.4	18.7	1.5	0.4	9.63	2.27	0.09	0.02	6.64	1.57	0.06	0.02	8.29
ACG	200	0.2	100				0.22				0.15				
	250	0.5	100				0.51				0.35				
	300	0.8	2.4	97.6			0.02	0.82			0.01	0.56			0.58
	350	1.8	12.0	88.0			0.21	1.56			0.15	1.08			1.22
	400	4.1	14.4	85.6			0.60	3.54			0.41	2.44			2.85
13.5WACG	200	0.5	1.5	27.6	70.8		0.01	0.15	0.19		0.01	0.10	0.13		0.24
	250	4.6	6.5	5.4	88.2		0.30	0.25	2.03		0.20	0.17	1.40		1.77
	300	14.8	22.1	2.7	75.2	0.1	3.27	0.39	5.56	0.01	2.26	0.27	3.84	0.00	6.37
	350	25.3	55.7	5.4	38.8	0.1	14.06	1.36	4.90	0.01	9.70	0.94	3.38	0.01	14.03
	400	38.3	79.7	11.4	8.6	0.2	30.51	4.37	1.66	0.04	21.05	3.02	1.14	0.03	25.23

Table C.3 The catalytic activity and product distribution for montmorillonite groups
(the reaction condition: T=200-400°C and WHSV=11.44 g_{ethanol}·g_{cat}⁻¹·h⁻¹)

Catalyst	Temp. (°C)	Conversion (%)	Selectivity (%)			Yield (%)			Rate of reaction ($\mu\text{mol}\cdot\text{s}^{-1}\cdot\text{g}_{\text{cat}}^{-1}$)			
			Ethylene	Acetaldehyde	Diethyl ether	Ethylene	Acetaldehyde	Diethyl ether	Ethylene	Acetaldehyde	Diethyl ether	total
MMT	200	5.6	6.5	1.8	91.7	0.37	0.10	2.57	0.25	0.07	1.77	2.09
	250	37.9	14.2	0.6	85.2	5.39	0.21	16.16	3.72	0.15	11.15	15.01
	300	62.5	42.8	0.8	56.3	26.78	0.53	17.60	18.47	0.37	12.14	30.98
	350	76.2	74.6	1.1	24.3	56.81	0.85	9.27	39.19	0.59	6.39	46.17
	400	82.3	79.7	1.5	18.8	65.55	1.21	7.75	45.21	0.83	5.35	51.39
2WMMT	200	1.8	3.8	19.8	76.4	0.07	0.35	0.67	0.05	0.24	0.46	0.75
	250	25.8	4.5	2.2	93.1	1.17	0.57	12.02	0.81	0.39	8.29	9.50
	300	47.9	23.2	2.1	74.6	11.09	1.01	17.86	7.65	0.70	12.32	20.68
	350	68.6	57.7	2.4	40.0	39.59	1.62	13.72	27.31	1.12	9.46	37.89
	400	90.2	88.7	1.3	10.0	79.96	1.21	4.51	55.16	0.84	3.11	59.10
5WMMT	200	2.6	3.6	10.6	85.7	0.10	0.28	1.13	0.07	0.19	0.78	1.04
	250	29.6	6.3	2.8	90.9	1.86	0.84	13.47	1.28	0.58	9.29	11.15
	300	60.2	29.1	3.1	67.7	17.52	1.89	20.36	12.09	1.30	14.04	27.45
	350	81.0	71.1	1.2	27.7	57.59	0.93	11.22	39.73	0.64	7.74	48.11
	400	94.5	94.3	1.0	4.7	89.14	0.92	2.22	61.49	0.64	1.53	63.66
10WMMT	200	6.8	5.3	0.7	94.0	0.36	0.05	3.21	0.25	0.03	2.21	2.50
	250	42.0	13.2	0.3	86.5	5.54	0.13	18.15	3.82	0.09	12.52	16.43
	300	72.2	41.5	0.3	58.2	29.98	0.21	21.01	20.68	0.15	14.49	35.32
	350	90.4	87.2	0.5	12.2	78.85	0.49	5.53	54.39	0.34	3.81	58.54
	400	96.0	96.7	0.8	2.6	92.75	0.75	1.23	63.98	0.52	0.85	65.34
13.5WMMT	200	8.2	4.1	1.2	94.6	0.34	0.10	3.87	0.23	0.07	2.67	2.97
	250	49.8	14.0	0.4	85.6	6.98	0.19	21.30	4.82	0.13	14.70	19.64
	300	74.4	44.2	0.8	55.0	32.89	0.60	20.44	22.69	0.42	14.10	37.21
	350	90.5	88.3	0.5	11.2	79.91	0.46	5.06	55.12	0.32	3.49	58.93
	400	96.0	96.7	0.9	2.4	92.88	0.86	1.14	64.07	0.60	0.78	65.45

VITA

NAME Jirayu Liewchalermwong

DATE OF BIRTH 13 jun 1993

PLACE OF BIRTH Rayong

INSTITUTIONS ATTENDED finished high school from Triam Udom Suksa School in 2011.
Graduated in bachelor's degree from Faculty of Engineering in Chemical Engineering, Chulalongkorn University in 2015.

HOME ADDRESS 468/147 Baan Klang Krung Siam-Pathumwan, Phetchaburi Rd., Ratchathewi, Bangkok 10400, Thailand



จุฬาลงกรณ์มหาวิทยาลัย
CHULALONGKORN UNIVERSITY